THE EXTRAGALACTIC DISTANCE SCALE KEY PROJECT

III. THE DISCOVERY OF CEPHEIDS AND A NEW DISTANCE TO M101 USING THE *HUBBLE SPACE TELESCOPE*

Daniel D. Kelson, Lick Observatory

Barry Madore, IPAC/California Institute of Technology/Jet Propulsion Laboratory

Abstract

We report on the discovery of 29 Cepheid variables in the galaxy M1 01 after using the original Wide Field Camera (WFC 1) and the new Wide Field and Planetary Camera (WFPC 2) on the *Hubble Space Telescope (11 S7'),* to observe a field in Ml 01 at 14 independent epochs in F555W. We found Cepheids with periods ranging from 10 to 60 days. The data have been calibrated using the Medium-Deep Survey (MDS) WFC 1 photometric zero-points, the preliminary WFPC 2 Status Report photometric calibration, and ground-based secondary standards in V and I. We have constructed V, I, and B period-luminosity (PL) relations and have derived apparent distance moduli using an assumed Large Magellanic Cloud (LMC) distance modulus of $\mu_0 = 18{,}50$ mag and LMC reddening of $E(B-V) = 0.10$ msg. Using a Galactic extinction law to fit the apparent V and I distance moduli, we found a mean reddening for the Ml 01 sample of $E(B-V) = 0.02$ msg. The true distance modulus to Ml 01 was found to be 29.383:0.18 mag, corresponding to a distance of 7.523:0.68 Mpc.

The distance to Ml 01 is one of three distance determination from the HST Key Project on the Extragalactic Distance Scale. These data, taken in a field 7!9 from the center of Ml 01 will be used in conjunction with Cepheid search results in a field 1!7 from the center, with nearly a factor of seven increase in metal abundance, in order to empirically calibrate the abundance effects on the Cepheid PI, relationship. The goal of the Key Project is to provide a value of the Hubble Constant to 1 O% accuracy.

Subject headings: galaxies: individual (Ml 01) - galaxies: distances - stars: Cepheids

1. Introduction

Much of the controversy over the Hubble Constant (H_0) arises from disagreement over distance indicator zero-points (see, for example, Sandage 1993, Jacoby *et al.* 1992, Fukugita, Hogan, and Peebles 1991, and other reviews). The goal of the *Hubble Space Telescope* Extragalactic Distance Scale Key Project is to define zero-points for a number of independent secondary distance indicators: the Tully-Fisher relation, planetary nebulae luminosity functions, surface brightness fluctuations, and supernovae methods. By calibrating these distance indicators, and understanding their systematic differences, the Key Project can then measure distances to the Hubble flow dominates over local velocity perturbations, with the goal of providing a value of the Hubble Constant accurate to 10%. The more distant galaxies in the *HST* Key Project sample were deferred due to the primary mirror's spherical aberration, Results from the first galaxy, M81, have already been published (Freedman *et al.* 1994 and Hughes *et al.* 1994). Ml 01 was the second and final galaxy to be observed with the WFC 1.

M101 is located at $\alpha_{2000} = 14^h03^m$, $\delta_{2000} = 54021'$, ($l = 102°$, $b = 60°$). It is a large, luminous Sc spiral with morphological type SAB(rs)cd (de Vaucouleurs *et al.* 1991). As a face-on, grand-design spiral, M1OI has been widely used for the study of spiral structure (Elmegreen at al 1992 and others). It also has a substantial metallicity gradient (see Shields and Searle 1978, and Zaritsky *et al.* 1 994), Two fields have been observed in Ml 01, one at a radius of 1.'7 using WFPC 2, and the one presented here, 7.'9 from the center, with the goal of establishing the effects of metallicity on the P-L relationship. Only the outer field was observed before the *HST* refurbishment mission, because crowding and the poor WFC1 point-spread function (PSF) would have prevented adequate photometry in the inner field.

Previously reported distances to M101 range from roughly 5.2 to 8 Mpc, though these estimates largely fall into two groups. Sand age and Tammann (1974) determined a distance modulus of 29.3 msg. Since then, others have derived distance moduli around 28.5 mag (see de Vaucouleurs 1993 for a brief review of distances to many nearby galaxies, including Ml 01). Cook *et al. (1986)* discovered two Cepheids with R-band CCD images. They found a relative Ml 01-LMC distance modulus of 10.8 mag. Citing the debate over the LMC true distance modulus, they argued that a reasonable range for the M101 distance modulus is 29,0 $\lesssim$ (m – M) $\lesssim$ 29.5 msg. The Type II SN 1970G has received surprisingly little attention in this context. Recently, however, Schmidt, Kirshner and Eastman (1992) reported a distance of $7.6^{+1.0}_{-2.2}$ Mpc or $(m - M) \approx$ 29.4 msg. Fesen (1993) recovered the SN 1970G remnant and derived a distance of 7 Mpc, or $(m - M) =$ 29.2 (with no error estimate). Eastman, Schmidt and Kirshner (1994) have re-analyzed the data and Schmidt *et al.*(1994) reported a revised distance of $7.4^{+1.0}_{-1.5}$ Mpc, or (m – M) $\approx$ 29.3 msg. Pierce (1994). reported a mean BRI Tully-Fisher distance modulus of 29.2 $\pm$ 0.5 mag in a recent comparison of Expanding-Photospheres Method (EPM) and luminosity -linewidth distances to local galaxies. These EPM distances seem to favour the long distance scale measurements of Sandage and Tammann 1974 and others which tended to (m – M) $\approx$ 29.2 msg.

Using the *Hubble Space Telescope (11 ST)*, *wc* have observed Ml 01 in 14 independent epochs in *V*, and 5 independent epochs in *I*. We have constructed *V* and *I* PL relations based on 29 Cepheids variables in the outer field, and have used the resulting *V* and *I* apparent distance moduli to derive a reddening-free distance estimate for M1OI.

In Section 2 we discuss the observations and pre-processing of the data. Section 3 covers the instrumental photometry and data reduction. In Section 4, wc detail the variable star search and period finding analysis. Section 5 briefly highlights the results from

the calibration (to be discussed in more detail in Appendix A). In Section 6 wc detail the procedures for finding reliable mean photometry. We derive apparent period-luminosity relations, as well as the reddening and distance to Ml 01 in Section 7 and discuss systematic effects arising from incompleteness, contamination, and flat-fielding. Appendix A details the calibration of the *HST* photometry. Appendix B contains the tabulation of magnitudes and positions of the Cepheids for every epoch used in the distance analysis, Lastly, Appendix C lists several apparently variable stars which could not easily be classified.

2. The Observations

The outer field is shown in Figure 1, which was taken from an image of Ml 01 obtained at the Canada-France-Hawaii Telescope (CFHT).

The field in M1 01 ($r=7\farcm9$) was observed with the WFC 1 at 13 independent epochs with the F555W filter ($\sim V$) and at 1 epoch with the F785LP filter ($\sim I$). Most of the WFC 1 observations were cosmic-ray (cr) split (i.e. a pair of exposures taken onc immediately after the other to facilitate the identification, and removal, of cosmic ray events). I? ffective exposure times of 3800 seconds in the spring, and 4200 seconds in the summer and fall. As a consequence of telescope scheduling constraints, the WFC 1 observations were made in roughly three rounds: spring, summer, and late fall, each observation at a different roll angle, with the exception of the summer observations, which were at constant roll angle with small pixel offsets. These observations spanned 260 days, beginning on 2 March 1993,

With the WFPC 2, onc F555W observation, 4 independent F814W observations and onc cr-split F439W observation were made, Most of the individual WFPC 2 exposure times were about 1200 seconds. The first WFPC 2 observation was made on 21 February

1994 and the last on *4* April 1994. The final F555W epoch was takenon *18* March 1994. Therefore, the total baseline for the Cepheid period search is 381 days.

The WFC 1 observations were processed by the pipeline system at the Space Telescope Science Institute. Lauer (1989) described the pipeline calibration process in detail. Four calibration steps were performed, namely correction of small A/D errors, bias subtraction, dark subtraction, and fiat-field division. The flat-fields used were made from observations of the bright Earth. Corrections using the Medium-Deep Survey (MDS) correction fiats (Phillips et al 1994) were applied *after* the photometry reduction. Epoch-to-epoch magnitude offsets were applied to register all photometry to the first epoch, taken about half-way between two decontamination (August 1992 and August 1993).

The WFPC 2 observations were processed by the pipeline as outlined in the WFPC 2 status report (Holtzman *et al.* 1994), and involved correction of small A/D errors, bias subtraction, superbias subtraction, superdark subtraction, and flat-field division. The flat-fields before mid-March were constructed from the thermal-vacuum (TV) flat-fields and a model for the on-orbit illumination pattern. All of the WFPC 2 data was taken at an operating temperature of $-76°$C. At this operating temperature, the detectors suffered from enhanced charge transfer inefficiency; observed magnitudes correlated with position on a chip. Counts were suppressed with increasing distance from read-out. We did not correct the charge transfer effect before photometering the data. Corrections for this problem were looked at during analysis of the photometry.

3. Instrumental Photometry

Most of the independent epochs were cosmic-ray split, facilitating recognition of genuine stars in each frame. Coordinate transformations between each of the observations were derived from comparison of preliminary object lists from each image (discussed below), instead of treating the data in 4 distinct sets (as in the case of M81), the large relative rotations of our frames required us to place all images onto a single coordinate system. Using these coordinate transformations on the cr-split exposures, all 108 WFC 1 800 x 800 images (100 in F555W, 8 in F785LP) were reduced simultaneously using ALLFRAME (Stetson 1994a). Without loss of precision, the pixel values were multiplied by four and stored as short integers, to reduce disk usage. Using the data quality files, we replaced bad pixels in the observations with values of 32767. DAOPHOT and ALLFRAME treat these pixels as null valued, and exclude them from the least-squares fitting.

ALLFRAME was the primary software package used; it simultaneously solves for the magnitudes and positions of all of the stars in all of the frames. The WFC1 point-spread functions (PSFs) were originally derived from WFC1 frames of the globular cluster NGC1 850 (see Stetson 1994a). The PSF features varied quadratically across each chip, as determined empirically from the stars in NGC 1850. As discussed in Freedman *et al.* (1 994), the ALLFRAME magnitudes are representative of stellar core magnitudes. Mischaracterization of the features in the outer parts of the PSF do not directly affect the measurement of the core photometry. While the profile fitting was restricted to a radius of 2.5 pixels, the derived magnitudes (—2,5 log DN) were determined over the entire PSF radius of 25 pixels.

The large WFC 1 star list input to ALLFRAME was generated in several steps. First, individual epoch star lists were generated from averages of the cr-split paired images. The

STSDAS package was used to reject cosmic-rays in the averaging process. This procedure was used only for generating star lists, not for carrying out the stellar photometry. A master star list was generated from the individual lists by comparing star positions in the coordinate transformation derivation. Any object found in a single image was included in the master list. ALLFRAME discarded many objects as spurious, but kept more than 23000 stars by the final iteration. This post-ALLFRAME star list was used in the WFPC 2 ALLFRAME run as well.

After the WFPC 2 exposures were taken, coordinate transformations were derived to incorporate the new data into the WFC 1 dataset. ALLFRAME was run on the 32 new 800 x 800 images (4 in F555W, 20 in F814W, and 8 in F439W), combined with one WFC 1 exposure (4 images in F555W) to facilitate incorporation of the new data into the WFC 1 coordinate system. The WFPC 2 PSFs were derived from public-domain observations of ω Cen (Stetson 1994b). Corrections to the WFC 1 ALLFRAME photometry, based on the MDS correction-fiats (Phillips *et al.* 1994), were applied and the two different sets of PSF photometry were analyzed (uncorrected, and MDS-corrected, magnitudes).

4. Variable Star Search

Two search criteria were used to select variable star candidates in the ALLFRAME photometry. First, the Welch and Stetson (1993) variability test was ideally suited for the cosmic-ray split pairs, This technique relies on coherence in the magnitude deviations for pairs of images taken "simultaneously." For non-variable stars, the paired photometry errors of cr-split pairs should be uncorrelated. The variability index, a sum of the pairwise products of deviations from a star's mean magnitude, should tend to zero for these non-variables. For variable stars, the index should be some large positive value. The index is normalized so that most variables will have an index greater than one. Second, variable star

canal idates were also selected upon having a large dispersion in their measured magnitudes. Histograms of magnitude dispersion were generated for several magnitude bins. Light curves for stars in the large dispersion tails of the histograms were then inspected,

Real-time light curves for these initial candidates were inspected so we could eliminate spurious canal idates and, for real variables, eliminate spurious observations (due to, for example, cosmic rays or bad pixels). After Lagging potentially spurious observations for promising candidates, the data were searched for best-fitting periods, phased, and plotted. Periods were determined using a generalized Lafler and Kinman (1965) phase dispersion minimization method (PDM), as described by Stellingwerf (1978). The bin and cover structure, (N_b, N_c), was experimented with and typically $(N_p, 2)$ was most effective, where $N_b = N_p$ equals the number of independent observations for the relevant star, and $N_c = 2$. Two versions of the PDM algorithm were run simultaneously: one which weighted the individual points by their magnitude uncertainties, and another which did not. The listed potential periods were identical, but the estimated signal strengths would differ slightly because estimated total dispersions for trial periods would contain different, normalizations (the weights assigned to trial *phase* points arc what matters, even though these weights arc constant for any given epoch). The individual magnitudes within cosmic-ray split pairs were averaged prior to final period determinations.

The period search range was 2 to 400 days, in steps of 0.1 days. Potential periods were later refined for individual candidates. Anywhere from 4 to 10 periods were inspected for each candidate. In the final tests, V and I data were phased and plotted together to ensure that periods were consistent between the two bandpasses.

Two epochs were partially lost; the second epoch was a single on-target exposure and the third epoch contained a short exposure member in the pair. These epochs have noisy

photometry because of shortened exposure times and so they frequently appeared as spurious points. These occasional gaps in the observations made our search more susceptible to aliasing in the period determinations. The single 1200 second WFPC 2 F555W observation was not cosmic-ray split and typically did little to refine derived periods. The WFC 1 observations, over a 260 day baseline, already strongly constrained the periods for the Cepheids. 1 Iowever, the follow-up WFPC 2 observation did help to single out potential long-period variables (1. PVs).

A parallel effort for photometry and detection of variable stars was done using a variant of the DoPHOT program (Schechter *et al.* 1993). The essentials of the variant, it's rationale, and details of the procedure to obtain photometry are described in Saha *et al.* (1994). A list of variable stars was thus generated independently, and cross compared with the objects obtained from the ALLFRAME reductions. Variables that were found in common (about 75%) were further examined for period agreement from these 2 independent methods for photometry. Variables found by only onc of the methods were further scrutinized to see if they were specious detections. The final list of definite Cepheids and other possible variables was made after this cross comparison. DoPHOT photometry was not calibrated to the correct zero-point. The reported numbers in this paper are all derived from ALLFRAME.

The variable star and period search was carried out by several people, including both the DoPhot and ALLFRAME photometry, Agreement, in most cases, was quite good, with occasional alternate period disagreements between DoPhot and A LLFRAME photometry. Discrepancies between *period* determinations generally arose from differences over which spurious observations had been rejected in the initial analysis. The disagreements generally could be resolved by close inspection of discrepant observations, and by simultaneously

inspecting the phased V and I observations, as a check of the consistency between the two band passes.

The relatively high number of spurious magnitudes in the dataset, combined with the non-optimum scheduling of the observations, led to substantial incompleteness in what would normally be considered a rich field for Cepheids. Figure 2 shows a Monte Carlo estimate of the sampling incompleteness for the a period range of 5 to 80 days. The simulation included our observing schedule and effectively sampled a random distribution of phases and periods, with an ad hoc threshold for period detection, Incompleteness due to luminosity selection criteria have not been included, Given the slope and intrinsic width of the period-luminosity relation, there would naturally be greater incompleteness at faint magnitudes (short periods). Based on the differences in the derived relative distance moduli in V and I (derived below, and shown to be ~ 0.2 mag) for the short and long period Cepheids, and the intrinsic width of the PL relations, our luminosity completeness is likely to be about 2/3. If the mean phase-detection completeness is about 2/3, as can is seen in Figure 2, then our sample is about 50% incomplete. The short-period incompleteness is discussed later, in tandem with the systematic effects of different Cepheid subsets on the PL relations.

The two Cepheids of Cook *et al.* (1986) were recovered. V1(=C9) was recovered with a revised period of 38 days (compared to the original determination of 37 days) and V2(=C5) " was recovered with a revised period of 47.1 days (compared to 47 days).

Finder charts for the Cepheids arc shown in Figure 3(a-d), with magnified image sub-sections shown in Figure 4. Applicable positions are listed in Table 1. Some candidates remained unclassified but are clearly variable; these arc discussed in Appendix C.

5. Calibration

The magnitude zero-point, calibration is a crucial step in establishing the distance modulus. Fortunately, three independent sources of calibration were used to calibrate the F555W data, two sources for the F814W data, and one for the F439W. The full details of these independent sources of the calibration are discussed in Appendix A and summarized below.

The simplest calibration of the WFC 1 F555W ALLFRAME magnitudes was derived from the Phillips *et al.* (1 994) WFC 1 photometric zero-points. Using these zero-points, removing the intrinsic ALLFRAME photometric zero-point, adding small aperture corrections (for light outside the effective aperture defined by the PSF radius), and adding the reference frame exposure time correction, wc were able to internally calibrate the WFC 1 photometry. These magnitude offsets are listed specifically in Table A1 and are discussed in Appendix A. The single epoch in F785LP was calibrated in the same fashion, but a mean colour term between F785l P and 17814W was added to the Cepheids prior to the final Cepheid photometry analysis. The F814 W-F785LP colour term is described in Appendix A as well.

The second calibration was based on WFPC 2 secondary standards. Our single F555W observation with WFPC 2, when calibrated using the WFPC 2 Status Report (Holtzman *et al.* 1994), contained several thousand potential secondary standards. To calibrate the WFPC 2 ALLFRAME magnitudes, we added the components listed in Table A2 to the WFPC 2 F555W A LLFRA ME magnitudes, We followed the same procedures to calibrate the F814 W and F439W photometry. Now that we had F555W, F814W, and F439W total apparent magnitudes in the WFPC 2 filter system, we needed to transform

these magnitudes to the WFPC 1 system, for comparison with the WFC 1 ALLFRAME photometry,

The WFPC 2 Status Report (Holtzman *et al* 1994) lists the transformation to the WFPC1 filter system. Using the 3 colour photometry, we were able to exploit the full status report transformations. These photometric transformations were applied to *all* stars whose reported WFPC 2 A LLFRAME photometry errors were less than 0.3 magnitudes, to bring the F555W, 1"814W, and F439W magnitudes on to the WFPC 1 system.

For the F555W WFPC 2 calibration of the WFC 1 ALLFRAME magnitudes, we used 1 8 secondary standards in the PC chip, plus 25, 32, and 27 secondary standards in the three WF chips. The difference in the *mean* offsets for the MDS-corrected and uncorrected WFC 1 photometry was small ($\lesssim 0.01$ mag), indicating that flat-fielding errors would not be a serious issue as a systematic effect in the calibration.

The Phillips *et al.* (1994) and WFPC 2 secondary standard F555W calibrations agree remarkably well. The mean offset for the four CCD's derived from Phillips *et al.* (1 994) is nearly identical to that derived from the WFPC 2 secondary standards. The difference is significantly less than 0.01 msg. Using the mean calibrating offset, from these secondary standards, and applying the expected chip-to-chip deviations (from Phillips *et al.* 1 994), therefore results in an identical calibration.

The third calibration of the F555W observations utilized ground-based KPNO 4-m V observat ions. The crowding prevented accurate ground-based photometry, but with many *groups* of stars used as secondary standards, wc found a mean 0.05 mag difference between the WFC 1 (or WFPC 2) calibration and the ground-based calibration. An additional colour term 0.02 mag is applicable for the mean $(B - V)$ colours of Cepheids, so the systematic effect of 0.03 mag is likely to be negligible. The detailed usc of groups as

secondary standards is explained in Appendix A.3. Briefly, the *HST* star list comprised a nearly complete list of stars for groups that were unresolved in the ground-based CCD images. Using an approximation to ground-based seeing effects, we were able to combine the counts from stars by summing their ALLFRAME-measured intensities, artificially convolved with an effective seeing profile. Because many secondary standards were used, the effects of random errors, incurred by such an approximation, were minimized.

The lack of good WFC1F785LP photometry did not allow for adequate comparison with F814W secondary standards. However, since most of our Cepheid sample's *I* photometry would be derived from the WFPC 2 F814W observations, wc used the Phillips *et al.* zero-points to calibrate the single F785LP epoch, in the same manner as the F555W observations. An additional, mean (F814W – F785LP) colour term was applied to this epoch, leaving a potential random error of up to ±0.07 mag in that single epoch's calibration. As most of our Cepheid's have several F814W observations, the systematic effect of the single F785LP epoch is minimal.

Ground-based *I* secondary standard magnitudes were converted to WFPC1 F814W magnitudes (1 Iarris *et al. 1991)* so no additional colour term is expected for the (Ground – ALLFRAME) magnitude off'sets. 1 Iowever, since the original WFC1 star list was used in the WFPC 2 ALLFRAME run, the 1"814W photometry lists, and hence, group membership lists, were not as complete as the increase in instrument resolution required, The systematic effect of this is to decrease the (Ground -- ALLFRAME) magnitude offsets because the ALLFRAME secondary standards will not reflect full stellar group membership. 1 n the comparison of the WFPC 2 self-calibration offsets and the ground-based secondary standard offsets, the individual differences could be partially attributable to group incompleteness (on top of the random errors present in this calibration tcchniquc).

Using an intercomparison of the calibration methods, we have recalculated WFPC 2 Instrument photometric zero-points for F555W and F814W. Using the deviations from the WFPC2 calibration, and averaging over the four CCD's (because the fiat-fields for each CCD have been normalized to consistent photometric zero-points), we found extremely good agreement with the zero-points listed in the status report. Table 2 lists the newly derived photometric zero-points, based on weighted and unweighted means of the individual chip photometric zero-points. The results agree "well with those found by Gilliland (1994) in M67 and Freedman *et al.* (1994) in M1 00.

6. Light Curves and Mean Magnitudes

The Cepheid F555W and 1"814W magnitudes and (x, y) positions for each exposure are tabulated in Tables B1 and B2, in Appendix B.

Each cosmic-ray split pair samples a single phase point in the light curve of a Cepheid. Therefore, the pairs were averaged prior to generating the light curves and computing final mean magnitudes. The phase-wrapped light curves for the Cepheids are shown in Figure 5.

6.1 Mean F555W Magnitudes

The temporal sampling in F555W was very uniform, as these light curves clearly indicate. in calculating mean V magnitudes for these Cepheids, we computed mean intensit, ies for all the data points not rejected by light curve analysis as spurious. Unweighted, weighted (by the reported ALLFRAME uncertainties), and phase-weighted mean intensity magnitudes were computed and used in separate 1'1, analyses to assess the differences in

the way the light curves were sampled for different Cepheids. Phase-weighted mean photometry is defined by the mean intensity, as integrated over an entire phase ($0 \leq \phi \leq 1$), such that

$$\langle m \rangle \equiv -2.5 \log \sum_{i}^{N} 0.5(\phi_{i+1} - \phi_{i-1}) 10^{0.4 m_i}$$

6.2 Mean F814W Magnitudes

The much small number of F814W epochs meant that we did not sample the light variation as uniformly as in F555W and needed to determine our I magnitudes quite carefully. By incorporating Cepheids whose I data satisfy various constraints (based on the quality of the data), we can probe the effects of the sampling, and hence the derivation of the mean I magnitudes, on the final distance estimates.

The first constraint is based solely on the uncertainties reported by ALLFRAME. The poor sampling of the light curve makes it difficult to detect outlyers and subtly discrepant points, in a statistically meaningful way. Only F814W observations with uncertainties ($\sigma_{i,\mathrm{ALLFRAME}}$) *less than some* value were used in the computation. These uncertainty constraints were chosen to be $\sigma_{i,\,\mathrm{ALLFRAME}} < 0{,}4$ mag, 0.3 mag, and 0.2 mag, for all $i = \{1, N_{\mathrm{F814W\ \ observations}}\}$.

The second quality constraint was based on an overall ability of ALLFRAME to photometer a given star. To continue computing a Cepheid's mean I photometry, the reported error of the *least* uncertain observation was required to be smaller than some value (we used $\sigma_{min,\mathrm{ALLFRAME}} < 0.4$ mag, 0.2 mag, and 0.1 mag). Since the Cepheids also had to satisfy the first constraint, we grouped the constraints and discuss these grouped restrictions below.

The third, and most important constraint, was related to the required number of I frames a Cepheid had to be found in. Therefore for each Cepheid, we counted the number of F814W observations *with* associated F555W phase points (where the phase difference, $\Delta\phi \leq 0.1$) that had F814 W magnitude uncertainties less than the previously defined tolerance levels. Strong constraints would require nearly all (at least 4) I observations to satisfy the criteria, Weak constraints (allowing Cepheids with a single observation) would allow many more Cepheids to be included in the PL analysis. We chose two extremes for this constraint. Requiring at least 4 observations imposes a strong selection effect. including Cepheids with only a single I detection (that still satisfies that previous two restrictions) allows us to study the faint-end population of the PL in more detail.

These restrictions arc clearly flux-dependent. Resulting flux-dependent systematic effects are easily seen by comparing the slopes of the PL relations derived by varying these constraints. No simple, standard set of restrictions should be assumed so that these systematic effects can be analyzed. Three sets of these three constraints were used: strong restrictions (0.2, 0.1, 4), moderate restrictions (0.3, 0.2, 4), and weak restrictions (0.4, 0.4, 1) in generating unweighed, weighted, and phase-weighted mean intensity magnitudes.

Since the 1“814W epochs form a poorly sampled subset of the light curve, mean I magnitudes were computed by utilizing V and I empirical light curve correlations. For a given period, the closest F555W *phase points* to those observed in F814 W (or the old F785LP) were used to calculate a correction to the computed I magnitude. Only F555W phase points within $\Delta\phi \leq 0.1$ were used. Any F814W observation without an associated F555W phase point was excluded. For a given Cepheid, we used the $\langle$F555W$\rangle$ subset to compute a subset mean $\langle$F555W$\rangle$ magnitude. Then we used its offset from the mean using all F555W epochs, scaled by the I to V amplitude ratio (0.5:1) reported in Freedman

(1988) to correct the computed mean ⟨F814W⟩ magnitude. This procedure is similar to the procedure used for M81.

Overall, the results were encouraging. For all three mean photometry sets, the average correct ion was close to zero, reducing the impact of systematic effects. The *mean* correction to the unweighted mean (F814 W) magnitudes was 0.001 msg. The *rms* correction was 0.070 mag, with corrections ranging from –O. 18 to 0.19 msg. The *mean* correction to the weighted mean (F814W) magnitudes was 0.005 msg. The *rms* correction was 0.074 mag, with corrections ranging from –0.21 to 0.17 msg. The *mean* correction to the phase-weighted mean (F814W) magnitudes was 0,000 msg. The *rms* correction was 0.083 mag, with corrections ranging from –0.23 to 0.25 msg. In all three mean photometry sets, the extreme corrections were typically found in cases of the weakest ⟨F814W⟩ photometry restrictions. However, typical I light curve amplitudes and random sampling cannot preclude large mean magnitude corrections; they arc expected when there arc few observations.

The mean F555W and F814W Cepheid magnitudes were transformed to Johnson V and I as prescribed by Harris *et al. (1991):*

$$V = \text{F555W} - 0.0768(11 - V) + 0.0254(B - V)^2$$

$$I = \text{F814W} - 0.0575(V - I) + 0.0271\,(V - I)^2$$

A mean $(B - V) = 0.66$ was used to transform F555W to V. For a single Cepheid, the largest incurred errors in V will be ±0.02 msg. Over the entire PL, wc expect no detectable systematic bias.

For the 22 Cepheids with F439W magnitude uncertainties less than 0.8 mag, only 7 had associated V phase-points, and so mean magnitude corrections could not be derived for the bulk of our sample, The mean F439W uncertainty was also 0.4 msg. Therefore,

we used the mean V photometry to transform the single F439W phase points to B with the transformation from Harris *et al.* (1991):

$$B = \text{F439W} + 0.0915(B - \text{v}) - 0.0168(B - \text{v})?$$

As evidence for the consistency of the calibration, we note that the Cepheid sample spans a range of $(V - I)$ colours of 0.5 to 1.6, appropriate for our range of periods. There are two blueish outlyers, C27 and C2, with periods of 17.2 and 18.2 days. A colour-magnitude diagram is shown in Figure *6.* The Cepheids are marked with closed circles, where C27 and C2 arc the shown as the bluest Cepheids. Only those stars with V errors $\leq \pm 0.2$ mag, and I errors $\leq \pm 0.3$ mag are plotted in the CM diagram (about 20% of the total). The mean $(B - V)$ derived for the 22 Cepheids with both B and V photometry is discussed below, with the derivation of the apparent period-luminosity relations.

Tables 3(a-c) list the Cepheid periods with unweighed, weighted, and phase-weighted mean V and I photometry, respectively. Table 4 lists the single B observation for each Cepheids.

7. The Distance to M1 01

7.1 Period-I. uminosity Relations and Apparent Distance Moduli

The *V and I* period-luminosity relations arc shown in Figure 7(a,b), where the Ml 01 outer field Cepheids are displayed as filled circles. The 1,MC Cepheid PI, data from Madore (1985) are superimposed as open circles. The solid lines arc least-squares (unweighed) fits to the combined LMC and Ml 01 data. The LMC sample shown and used here is a sample of 22 Cepheids with both V and I photometry and periods in the same range as the Ml 01 outer field Cepheids ($1.0 < \log P < 1.8$).

As was the case for M81 (Freedman *et al.* 1994), we adopted a true distance modulus to the LMC of 18.50 mag (Feast and Walker 1987). However, we adopted a mean reddening for the LMC Cepheids of $E(B-V) = 0.10$ mag (see Bessel 1991) and discuss this choice below. We derived the following apparent PI, relations in V and I for the combined PL of 22 LMC Cepheids and 29 V (23 I, from the moderate restrictions) M1OI outer field Cepheids, using weighted intensity mean photometry:

$$(V) = -2.80\,(\pm 0.23)(\log P - 1.4) + 24.27\ (\pm 0.05)\ [0.33]$$

$$\langle I \rangle = -3.10\,(\pm 0.20)(\log P - 1.4) + 23.44\ (\pm 0.04)\,[0.24].$$

Using unweighed intensity mean magnitudes, we found:

$$(V) = -2.80\,(\pm 0.22)(\log P - 1.4) + 24.23\ (\pm 0.04)\,[0.32]$$

$$\langle I \rangle = -3.11\,(\pm 0.20)(\log P - 1.4) + 23.39\ (3,0.04)\,[0.25].$$

Using phase-weighted intensity mean magnitudes, we found:

$$(V) = -2.85\,(\pm 0.23)(\log P - 1.4) + 24.21\ (\pm 0.04)\,[0.32]$$

$$\langle I \rangle = -3.08\,(\pm 0.20)(\log P - 1.4) + 23.40\ (\pm 0.04)\,[0.25].$$

The *rms* scatter about these relations is given in brackets on the right. These values agree well with the 0.29 mag and 0.26 mag, reported in Madore and Freedman (1991).

in calculating the apparent distance moduli for Ml 01, we used a method of sliding PLs, where one shifts the LMC data in magnitude steps (Ml 01 -LMC distance modulus offsets), fits new relations to the combined PI, relations of the two galaxies, and finds the minima in the residuals to deduce the appropriate apparent relative distance moduli. By fitting separate 1'1, relations to the 'two galaxies and simply comparing mm-points, onc cannot enforce consistent slopes between the two populations, in Cepheid discovery programs, selection effects alter the 1'1, relation's slope. By sliding the LMC PL relation(s), one comes closer to fitting an appropriate slope to a potentially incomplete sample, assuming the LMC sample is relatively complete over the period range of interest,

Using the unweighed intensity mean magnitudes, apparent distance moduli were μ_V = 29.45 and μ_I = 29.41 mag (wc have adopted μ_0 = 18.50 and $E(B-V)$ = *0.10* for the I,MC, $A_V/E(B-V)$ = 3.30 and the Galactic extinction law of Cardelli, Clayton and Mathis 1989).

Using the single phase-point observations in F439W, and the derived mean *(V)* photometry (for the Harris transformation to give B magnitudes), we constructed a B band 1'1. relation. For most of the Cepheids, there were no closely associated *V* phase points, so corrections to determine mean B photometry could not be made. The constructed B PL relation reflects the intrinsic width of the B PI, (*rms* dispersion of 0.4 mag, Madore and Freedman 1991), *and* the random sampling of the $\sim$ 1 mag amplitude of the light curve, The unweighted fit, enforcing the Madore and Freedman (1991) slope of –2.53 PL for the single phase-point B PL relation, was

$$B = -2.53(\log P - 1.4) + 25.07(\pm 0.90).$$

Comparison of the B and *V* zero-points, supplies a mean colour of $(B - V) \approx 0.7$, in reasonable agreement with typical mean Cepheid colours. Using the B zero-point from Madorc and Freedman (1991), the above fit translates to a B apparent distance modulus of 29.53 msg. Within the PI, zero-point errors, this distance modulus is in reasonable agreement with the *V* and *I* moduli, and the reddening curve discussed below.

7.2 Interstellar Extinction and the True Distance Modulus

7.2.1 Reddening

One might expect our results to depend crucially on the adopted LMC distance and reddening since we used the LMC Cepheid population *with* its intrinsic reddening. The

derived *apparent* distance moduli do depend strongly on the assumed reddening, but by fitting a Galactic extinction law to the apparent distance moduli, we have removed the adopted LMC reddening, and have dereddened the M 101 Cepheids at the same time.

Our approach involves finding the *relative* Ml 01-LMC distance moduli, adding the adopted LMC dist ante and V and I extinctions to the derived relative moduli, and solving for a Galactic extinction law (Cardelli, Clayton, and Mathis 1989) at V ($\lambda^{-1} = 1.82\mu m^{-1}$) and I ($\lambda^{-1} = 1.11\mu m^{-1}$) to deduce the *difference* in reddening between the LMC and M101 Cepheid populations. Typically one would usc B as well, but the lack of good photometry in B, and the greater *potential* impact of abundance effects in B (Madore and Freedman 1991), led us to derive the reddening based on V and I. The B data do provide a consistency check, as we shall see.

The Cardelli, Clayton, and Mathis (1989) Galactic extinction law defines $A_I/A_V \equiv (0.68 - 0.6239/R_V)$. If the apparent V and I distance moduli arc μ_V and μ_I then $\mu_{M101} = (\mu_V - A_v)$ and $\mu_{M101} = (\mu_I - A_I)$. 'J'here are two equations with two unknowns, the true distance modulus, μ_{M101}, and the visual extinction, A_v. In this process, the adopted LMC extinctions are removed along with the mean Ml 01 extinctions. Again, this technique is insensitive to changes in the adopted LMC reddening, as long as the derived Galactic extinction law is appropriate for *both* galaxies. For the two moduli listed above wc found $E(B-V)_{LMC} - E(B-V)_{M101} = 0.08$, and since wc adopted $E(B-V)_{LMC} = 0.10$, $E(B-V) = 0.02$ for the M1OI Cepheids. The unwcightcd V and I apparent distance moduli have been plotted in Figure 8, with the implied extinction law. The B apparent modulus has been plotted ($\lambda^{-1} = 2.27pm^{-1}$) as a large "plus" sign to show the consistency in t hc reddening curve. and arises from the excess scatter in the random The reddening-free distance modulus we derive from the outer field Cepheids is 29.38+ 0,18 mag, or a distance of 7.52 ± 0.68 Mpc (the error budget is discussed below).

Without other constraints on the internal reddening, this approach gives distances that are relatively independent of reddening effects. For example, let us assume $E(B-V) = 0.17$ for the LMC Cepheids. In solving for a Galactic extinction law, the M101 reddening becomes E(D – *V)* = 0.09 and the resulting distance modulus *remains* unaffected. Only if independent estimates of the reddening can be made can one be insured of internal consistency. However, the colours of this Cepheid sample suggest that the reddening in Ml 01 is small, and probably $E(B-V) \lesssim 0.05$. As for sensitivity to the assumed LMC distance, any changes in the LMC distance modulus can easily be added as zero point offsets to the derived true distance to Ml 01. This method has been used on Cepheids in 1 C 1613 (Freedman 1988), M33 (Freedman, Wilson, and Mad ore 1991), M31 (Freedman and Mad ore 1990), NGC 300 (Freedman *et al.* 1992), and M81 (Freedman *et al. 1994).* The results suggest that this approach is reasonable at this time.

7.2.2 Galactic Extinction

The ext nction for the outer field of Ml 01 was expected to be quite low. Burstein and Heiles (1984) reported Galactic foreground reddening of $E(B-V) = -0.03$ (i.e. $E(B-V) \equiv 0$). Even casual examination of the images shows several distant background galaxies and groups. The low, even zero extinction from Burstein and Heiles (1984) suggests any reddening is internal to Ml 01. However, wc caution against making such an interpretation with the current uncertainties in the reddening determination.

The outer field is extremely patchy in its distribution of stars and gas and one should not assume that localized transparency indicates uniformly low dust content. Most of our Cepheids though, were found in relatively uncrowded regions similar to the areas with distant background galaxies. Therefore, wc expected the reddening, internal to M101 and due to the Galaxy, to be quite low. This circularity prevents us from arguing that the

deduced reddening is solely internal to M1OJ since we selected objects for which it is likely to be small. Recall that our distance estimate remains *unaffected* by the assumed value of the LMC reddening (because we measure the differen in reddening, not the absolute reddening),

Our Ml 01 data, however, can possible contribute to the debate over the reddening to the LMC Cepheids. If we had adopted $E(B-V) = 0.17$ for the LMC, the derived Ml 01 reddening would have been $E(B-V) = 0.09$. Such a value might be considered high for a region plainly transparent to distant groups of galaxies, We recognize that this argument is weak at this level because of the patchy nature of the region, the observed colour distribution of the Cepheids, and the difficulty in measuring accurate reddening. Even the well-studied sample of the LMC Cepheids has a debated reddening estimate!

7.2.3 Systematic Effects -- Biases

Wc searched for systematic biases in the derived relative distance moduli. By using only those LMC Cepheids with *both* V and I photometry, our primary concern is with systematic effects arising within the Ml 01 Cepheid data. One approach to adopt us to select subsets of the Ml 01 Cepheids to see if they return similar distance moduli. Tables 5(a-c) list derived PL slopes, relative distance moduli, reddening, and reddening-independent distance moduli, for the different subsets and mean photometry sets. We used the subset of M101 Cepheids containing *both* V and I photometry. We also varied the restrictive criteria defining usable I photometry (see Section 6.2). Period-groupings of the Cepheids were also fit. These subsets for different period ranges, offered the largest changes in *relative* distance moduli. The fainter, short-period subset clearly shows evidence for a Malmquist-like bias. The resulting *true* distance modulus, however, remained essentially unaffected (since the reddening changed to compensate -- without an independent check on the reddening,

this is expected, though, as noted, the Cepheids themselves provide upper limits to the reddening). It is unlikely that our short period Cepheids were systematically oscillating in the first harmonic (see Bohm-Vitense 1994) since our shortest period is 13 days, while the oscillatory mode transition period is said to be about 9 days.

The effects of incompleteness were tested and these effects can be seen explicitly in Tables 3(a-c) and 5(a-c). The Cepheid search was carried out in V and the sample is intrinsicly incomplete at the faint end. This effect shows up in the 0.21 mag difference between short and long period *relative* V distance moduli. For I, effect of incompleteness is spread across the broad colour distribution. As the different subsets, selected on the basis of I photometry errors and observations, arc used, wc sec that they lead to changes in the PL relation. In comparing PL relations derived from using tight limits on the I photometry quality, wc sec a much steeper slope in the I PL relation than the slope derived from the subset with less stringent limits on the I photometry quality.

At the short-period end, wc must clearly be missing some faint Cepheids in the distribution. By merely comparing the short and long-period subsets, the effect is not as easily seen because the incompleteness in V has been smeared by the intrinsic $(V - I)$ colour distribution. Upon casual examination of the Cepheid subsets and I photometry requirements, one plainly sees that the Ml 01 sample suffers from magnitude selection effects. Despite the sample selection effects, the derived true distance modulus remains fairly constant across subset and I photometry restrictions. Note that some subsets lead to unreasonable estimates of the reddening. Negative values of the reddening can imply that wc have adopted an unreasonably low value for the LMC reddening. However, since most of the subsets give low, positive values for the reddening, the potentially unphysical values can at least be considered outlyers and given lower weight.

To test the effects of magnitude selection biases on the PL fitting, we also fit log $P = f(m)$. By fitting the periods as functions of magnitude, one can minimize the magnitude selection effects on the combined PL relation. In refitting PL relations for *all* Cepheid subsets, the resulting true distance moduli remained constant to $\lesssim 0.01$ msg. The relative moduli generally shifted by $\lesssim 0.02$ mag, with V and I relative moduli moving together in near lockstep ($\Delta\mu_V / \Delta\mu_I \approx 2$), Therefore, the least-squares fitting of the PI, relations is essentially unaffected by the presence magnitude selection biases.

7.2.4 Systematic Effects — Contamination

We searched for systematic effects from contamination by neighboring stars. Contamination from unresolved neighbours can decrease observed light curve amplitudes, if the neighbour is of comparable luminosity to the Cepheid. We searched for systematic errors due to undetected contamination by generating distance moduli for subsets selected by the amplitude of their light curves. The results from these subsets arc also listed in Tables 5(a-c). One normally expects that the subset most susceptible to contamination would be low-amplitude, faint variables, though unusually low-amplitude bright ones could also be contaminated. These would appear unusually bright and therefore would lead to a short distance modulus. The small-amplitude subset should contain both intrinsically small-amplitude Cepheids, and the contaminated large-amplitude Cepheids. The large-amplitude subset should be mostly uncontaminated by neighbours. In *V,* the relative modulus between the small and large-amplitude subsets differed by 0.1 msg. Contamination effects in the small-amplitude subset should lead to a *shorter* distance estimate, because the Cepheids should be artificially brighter in the mean. However, the small-amplitude subset gave rise to a *longer* distance! The change in V PL relation slope was most likely the cause of the modulus difference, rather than contamination. The use of

different *I* samples also obscured the systematic effects of contamination. The inclusion of many Cepheids, for the samples that included those with large *I* errors, improved agreement of the slope and relative modulus with that derived from the complete sample. However, even with these weak restrictions, the small-amplitude subset's *I* relative modulus was 0.1 mag *fainter* than the relative modulus of the large-amplitude subset, again in the wrong direction! The derived true distance moduli for the two subsets, using the weighted and phase-weighted mean photometry, agreed well (with the *I* subset that allowed large magnitude errors). Disagreement between the subsets' relative moduli appear to primarily com c from incompleteness in subset samples, and the resulting slope differences. Since the amplitude-based subsets have led to counterintuitive changes in the distance, it appears that contamination effects are probably minimal in the overall Cepheid sample.

7.2.5 Systematic Effects --- **Flat-Fielding**

Systematic effects from flat-fielding errors were also considered, Onc can imagine if the Cepheids resided on one part of a single chip, then a relative distance modulus based solely on those Cepheids would systematically be ofi'set by any large-scale flat-fielding error. 1 lowever, two features of this particular dataset naturally work against such a systematic effect. First, there arc four distinct chips. Any systematic bias arising from preferential chip location would need to be repeated in the other four, in locations consistent with the same flat-fielding errors, for some large fraction of our Cepheid sample, Second, and more importantly, our data was obtained at several different roll angles. This proved to be a useful feature of the distribution of roll angles (but the only one!). The first set of observations had rotations of up to 20°. Any PL based on observations consistently in a large depression or enhancement in the flat-field, could indeed contain fla.t-fielding *systematic errors* arising from the flat-field structure consistent with the largest rotation

angle. However, the second set of observations had, a consistent roll angle around 90° from the first epoch. For example, from the early observations, CCD ##1 objects were placed in CCD #2 in the next set of observations. Mean ccd-to-ccd zero-point offsets come from stars all across the ccd's. Any star with a flat-fielding error of 0.1 mag in the first set observations would have an uncorrelated flat-fielding error in the second set of observations. Figure 6 of Phillips *et al.* (1994) shows that the flat-fielding errors for a given position are fairly uncorrelated from one chip to the next. The third set of roll angle offsets ranged from 0° to $\sim$ 45°, leading to further decorrelation of flat-fielding errors.

The F555W calibration, discussed in detail in Appendix A, was consistent for both the Medium-Deep Survey flat-field corrected and uncorrected ALLFRAME photometry. The largest zero-point difference was 0.02 msg. As an *extreme* example, one Cepheid had *individual* datapoints with typical flat-field corrections of $\pm$0.08 msg. However, its *mean* magnitude changed by less than 0,01 msg. Again, the distribution of rotations helped alleviate flat-fielding errors.

Since the rotation between the first epoch and second round of observations was $\sim$ 90°, one might naively wish to, for example, use the WFPC 2 chip 2 to calibrate the first round WFC 1 chip 2 *and* second round chip 3 (and so forth) zero-points, From the discussion above, where even large flat-field corrections have been applied, mean magnitudes derived from the full set of images show little change when the flat-field corrections were applied (the *rms* offset was 0,016 mag). For the chips with no distinct localization of secondary standards, the flat-fielding errors arc a source of scatter in the individual observations of a single star. The distribution of roll angles helped minimize any systematic effects caused by errors in flat-fielding, not merely in the mean for the entire population of stars, but even *in the mean* for *individual* stars.

7.2.6 The Error Budget of the True Distance Modulus

Table 6 lists the factors in our error budget. An estimate of the final error can be seen by comparing the distance moduli from the different sets of mean photometry. Between the unweighed and weighted mean photometry, the distance moduli differ by 0.05 msg. There were also a couple of Cepheid subsets which showed more extreme distance moduli (short and long, by $\lesssim 0.2$ mag). The mean ALLFRAME photometry error, was estimated at ± 0.05 mag, arising from comparison of the raw and MDS-corrected photometry, and the consistency of the WFPC 2 and WFC 1 ALLFRAME photometry, The epoch rotations, PSF changes, and instrument changes showed consistency, in the mean, to better than ± 0.02 mag, as shown by the differences in calibration from the two instruments, for both the flat-field corrected and uncorrected photometry. Extinction and transformation errors were estimated to be ± 0.03 msg. The zero-point calibration uncertainty was estimated at ± 0.05 msg. Errors in the mean PL relations were estimated by $\sigma/\sqrt{N-1}$. Uncertainty in the LMC reddening and absorption were estimated at ± 0.1 mag (again, see Bessel 1991). The error in the true LMC distance modulus was assumed to be about ± 0.1 mag (see Feast and Walker 1987). The LMC and Ml 01 outer field metallicities are fairly similar (see Zaritsky *et al.* 1994), so the uncertainty duc to abundance effects was estimated to be small, at ± 0.03 msg. Taking all these together, the total error in the true distance modulus amounted to +0.18 mag, or a 9% error in the distance.

8. Conclusions

De Vaucouleurs (1993) has emphasized the pivotal role that M101 plays in the extra-galactic distance scale debate. Past distance estimates have clearly not converged to a value consistent with the typical quoted errors. Table 7 shows some previously reported distance estimates for Ml 01, To illustrate the full range of distances reported over the last

20 years, Table 10 of de Vaucouleurs (1993) shows distance moduli for M101 from 1973 to 1986, with the range of distance moduli extending from 28.56 mag (Jaakkola and Le Denmat 1976) to 29.5 mag (the upper limit of the Cook *et al.* 1986 result), equivalent to a range of 5.2 to 8 Mpc in distance.

After finding 29 Cepheid variables, we derived a reddening-independent distance modulus of 29.383:0.18 mag, corresponding to a distance of 7.523:0.68 Mpc. We derived a mean reddening of $E(B-V) = 0.02$ mag for the Cepheid population, adopting a reddening of $E(B-V)_{\rm LMC} = 0.10$ mag for the LMC Cepheids. The colour distribution of our Cepheid sample indicates that, despite any choice of $E(B-V)_{\rm LMC}$, the *mean* reddening of the M101 Cepheids should probably $E(B-V) \lesssim 0.05$ msg.

Previously derived, shorter distances tended to come from brightest supergiant techniques coupled with large (relative) internal reddening. Past distances in closer agreement to our Cepheid-based distance were derived, in part, from brightest supergiant methods coupled with low internal reddening. The new Cepheid distance clearly agrees with the distances reported by Sandage (1983) and Sandage and Tammann (1974).

The Tully-Fisher distances favoured the longer distance, but were extremely uncertain be.cause of Ml 01's inclination. The recent Tully-Fisher distance modulus of 29.2+ 0.5 from Pierce (1 993), while extremely uncertain, agrees with our Cepheid distance. Since Ml 01 is nearly face-on, it is not directly useful as a Tully-Fisher calibrator. Ml 01's utility, with regards to the Tully-Fisher relation, is as a distance calibrator for the Ml 01 group (Fisher and Tully 1975), containing the calibrating galaxies DDO 169, 185 (Ho IV), 186 (NGC 5477), and 194. They all have galactocentric recession velocities around 350 km/s (except DDO 185, at about 250 km/s), The original Tully-Fisher linewidth analysis assumed

the Sandage and Tammann (1974) distance to the group (7.2 Mpc). Our Cepheid-based distance corresponds to a 0.1 mag correction.

Often neglected, the Expanding-Photospheres distance determinations to M101, based on SN 1970G have favoured a longer distance estimate, with $D_{\rm EPM} = 7.4^{+1.0}_{-1.5}$ Mpc (Schmidt *et al.* 1994).

Cook *et al.* (1986) found a relative M101-LMC modulus of 10.8 with two Cepheids from KPNO 40-m CCD R-band images. Using an LMC distance of $\mu_0 = 18.50$, $E(B-V)_{\rm LMC} = 0.10$, and $A_R/A_v = (0.8686 - 0{,}3660/RR)$ (Cardelli, Clayton, and Mathis 1989), the *apparent* R distance modulus of 29.55 mag leads to a true distance modulus of 29.50 msg. By adopting a true LMC distance modulus of 18.5 mag *and* including our reddening estimate, the Cook *et al.* (1986) R band photometry is consistent with our new distance. Given the intrinsic width of the Cepheid period-luminosity relationship, the previous Cepheid distance agrees surprisingly well with the onc presented here.

This new distance to M101 combined with the inner field analysis will finally determine the abundance dependence of the PL relations. Table 1 of Zaritsky *et al.* (1994) list an [O/H] gradient of -0.14 dex/ρ_s. The Ml 01 outer field's metal abundance is $z/z_{\rm LMC} = 0.7$ while the inner field's abundance is $z/z_{\rm LMC} = 4{,}7$. The factor of 7 change in abundance between the two fields will enable the Key l'reject to calibrate any effect, if present. Past studies, such as in M31, have been inconclusive (see Madorc and Freedman 1991).

M101 is clearly a large galaxy. At a distance of 7.52 Mpc, the disk scale length of 2'.11 corresponds to 4,6 kpc. M101's isophotal radius of 14'.42 (de Vaucouleurs *et al.* 1991) corresponds to 31.5 kpc. Sandage (1 993) attempted to usc the isophotal dia.meters of Sc galaxies as standard rods to derive H_0. The Freedman *et al.* (1994) distance to Ml 00, an Sc galaxy in the Virgo cluster, however, implies a scale ratio of isophotal diameters

of about $D_{25,\mathrm{M101}}/D_{25,\mathrm{M100}} \approx 2$. Ml 00's size discrepency could have resulted from gas stripping in the Virgo cluster (see Giovanelli and Haynes 1983, Bosma 1985, or Warmels 1985). However, in the Giovanelli and Haynes (1983) study of HI deficiency in Virgo cluster spirals, M1 00's measured deficiency appears to be similar to the empirically fit deficiencies in a sample of "isolated" galaxies.

The Ml 01 outer field dataset contains data from two *HST* instruments, the WFC1 and WFPC 2. The WFC 1 and WFPC 2 calibrations (Phillips et al 1994; Holtzman *et al.* 1994) arc clearly consistent to better than 2%. Freedman *et al.* (1994) also show that the WFPC 2 calibration is consistent with their ground-based calibration. Using our WFC 1 observations of the M1OI outer field, wc have derived a WFPC 2 F555W photometric zero-point of 21.72 ± 0.02 mag (≡ 1DN/s at gain=1 4), compared with the WFPC Status Report value of 21 .7183= 0.012 msg. The ground-based *I* observations do not provide as a good a constraint. Wc derived an F814W zero-poilit of 20.923:0.06 mag compared to a reported 20.9153:0.012 msg.

M101's heliocentric radial velocity is roughly 240 km/s, which corresponds to a galactocentric radial velocity of about 340 km/s. If H_0 is large, as the distance to M1OO might suggest (Freedman *et al.* 1994, Mould *et al.* 1994), then M1OI's peculiar velocity is on the order of 200 km/s. Taken by itself, M1OI's radial velocity suggests a low H_0. We caution at this time that any determination of the Hubble Constant from such isolated systems is extremely dangerous. The ultimate goal behind the Key Project's Cepheid distance measurements is to define the zero-points for secondary distance indicators which allow us to sample the Hubble Flow directly.

1 Despite the many problems intrinsic to the dataset (crowding, epoch-to-epoch rotations, aliasing), 29 Cepheids have been found, including the two previously discovered by

Cook *et al.* (1986), The new distance is consistent with the previous Cepheid distance estimate, EPM distance estimates, and even a recent Tully-Fisher reanalysis.

The continued use of *HST* to measure Cepheid distances to roughly 20 galaxies will allow us to set accurate zero-points for these and other secondary distance indicators. Currently, the independent secondary distance indicators suffer from systematic differences that arc poorly understood. New Cepheid-based distances will finally solve many of the discrepancies between the different techniques. The Key Project's continued usc of WFPC 2, with its secure calibration, insures that the Key l'reject's goal of H_0 to 10% is within reach.

References

Bessel, M.S. 1991, AA, 242 L17

Bohm-Vitense, 13.1994, AJ, 107, 673

Bosma, A. 1985, in ESO Workshop on The Virgo Cluster of Galaxies, held at Garching, 4-7 September 1984, ESO Conference and Workshop Proceedings No. 20, O.-G. Richter and 13. Binggeli, eds., p.425

Bottinelli, L., *et al.* 1985, A&A Sup, 59, 43

Cardelli, J. A., Clayton, G. C., & Mathis, J.S. 1989, ApJ, 345, 245

Cook, K.H., Aaronson, M., & Illingworth, G. 1986, ApJ, 301, L45

de Vaucouleurs, G., *et al.* 1991, *Third* Reference *Catalog of Bright Galaxies*, (New York: Springer-Verlag)

de Vaucouleurs, G. 1993, ApJ, 415, 10

Eastman, R.G. 1994, private communication

Elmegreen, B. G., Elmegreen, D. M., & Montenegro, L. 1992, ApJS, 79, 37

Feast, M., &, Walker, A.R. 1987, ARA&A, 25, 345

Fesen, R.A. 1993, ApJ, 413, 1,109

Freedman, W. L. 1988, ApJ, 326, 691

Freedman, W.L., & Madore, B.F. 1990, ApJ, 365, 186

Freedman, W.L., Wilson, C. D., & Madore, B.F. 1991, ApJ, 372, 455

Freedman, W.J.,, *et al.* 1992, ApJ, 396, 80

Freedman, W.L., *et al.* 1994, ApJ, 427, 628

Fukugita, M., Hogan, C. J., Peebles, P.J.E. 1993 Nature 366, 309

Gilliland, R.L 1994, Submitted to ApJ Lett

Giovanelli, R., & Haynes, M.P. 1983, AJ, 88, 881

Grillmair, C. 1994, private communication

Harris, H. C., Baum, W. A., Hunter, D. A., & Kreidl, T.J. 1991 AJ, 101,677

Hughes, S. M., *et al.* 1994, ApJ, 428, 143

Holtzman, J. A., *et al.* 1994 *WFPC 2 Status Report*

Jacoby, G. I-I., *et al.* 1992, PASP, 104, 599

Jaakkola, T.,& Le Denmat, G., 1976 MNRAS, 176, 307

Lafler, J. & Kinman, T.D. 1965, ApJS, 11, 216

Landolt, A. 1992, AJ, 104, 340

Lauer, T.R. 1989, PASP, 101, 445

MacKenty, *et al.* 1992 *WF/PC instrument Handbook*

Madore, B.F. 1985, in IAU Colloquium 82, *Cepheids: Theory and Observations,* ed. B.F. Madore (Cambridge: Cambridge University Press), p. 166

Madore, B.F., & Freedman, W.L. 1991, PASP, 103, 933

Phillips, A.C., *et al.* 1994, AJ, 107, 1904

Pierce, M.R. 1994, ApJ, 430, 53

Saha, A., Labhardt, 1,., Schwengeler, H., ., Macchetto, F. D., Panagia, N., Sandage, A., & Tammann, G. A. 1994, ApJ, 425, 14

Sandage, A A., & Tammann, G.A A. 1974, ApJ, 194, 223

Sandage, A. R., & Tammann, G.A. 1976, ApJ, 210, 7

Sandage, A.R. 1983, AJ, 88, 1569

Sandage, A.R., & Bedke, J. 1988, *Atlas of Galaxies: Useful jor Measuring the Cosmological Distance Scale,* (Washington, DC)

Sandage, A.R. 1993, ApJ, 402, 3

Schechter, 1'. 1,., Mateo, M. & Saha, A. 1993, J'ASI', 105, 1342

Schmidt, B. P., Kirshner, R. P., & Eastman, R.G. 1992 ApJ, 395, 366

Schmidt, B.P., *et al.*, 1994 Submitted to ApJ

Stellingwerf, R.F., 1978 ApJ, 224, 953

Stetson, P.B. 1987, PASP, 99, 101

Stetson, P.B. 1990, PASP, 102, 932.

Stetson, P.B. 1994a, PASP, 106, 250.

Stetson, P.B. 1994b, private communication.

Stetson, P.B. 1991, in 3rd ESO/ST-ECF Data Analysis Workshop, held at Garching, 22-23 April 1991, ESO Conference and Workshop Proceedings No. 38, P.J. Grosbol and R.H. Warmels, eds., p.187

Warmels, R.H. 1985, in ESO Workshop on The Virgo Cluster of Galaxies, held at Garching, 4-7 September 1984, ESO Conference and Workshop Proceedings No. 20, O.-G. Richter and B. Binggeli, eds., p.51

Welch, D.L. & Stetson, P.B. 1993 AJ, 105, 1813

Zaritsky, D., Kennicut, R. ., & Huchra, J.F. 1994 ApJ, 42087

Table 1, Finder Chart Coordinates

ID	P (days)	CCD	x	y
c l	58.54	2	82.1	133.9
C5	47.10	3	712.0	233.5
C6	45.80	3	179.3	271.9
C7	43.00	3	329.1	670.1
C19	43.00	1	517.3	783,3
C20	42.50	1	148,4	205.9
C8	41.00	3	284,0	211.7
C9	38.00	3	326.8	72.4
C10	37.60	3	302.0	754.3
C21	33.50	1	272.5	727.9
C12	33.50	4	343.9	235.6
C13	32.00	4	205.0	497,7
C22	27.30	1	300.2	469,7
C23	25.60	1	178.0	509.4
C14	25.00	4	619.3	451.3
C11	23.70	3	389.1	202,2
C24	23.50	1	81.1	242,1
C15	23.40	4	306.5	218.8
C16	22.80	4	710.4	662.8
C25	19.35	1	294.4	517.6
C2	18.20	2	194.2	334.2
C26	17.70	1	35.6	300.3
C27	17.20	1	454.5	62.2
C28	16.70	1	519.1	604,0
C3	16.67	2	327.7	457.5
C17	16.45	4	371.5	302.3
C4	14.27	2	411.8	134.9
C29	14.00	1	73.8	182.6
C18	13.00	4	69.7	141.7

Note:
Locations applicable for epochs shown in finder charts.

Table 2. WFPC 2 Calibration

WFPC 2 Photometric Zero-Points					
	WFC (straight)	WFC (weighted)	Ground (straight)	Ground (weighted)	Status Report
F555W	21.721 ± 0.027	21.712 ± 0.013	21.68 ± 0.05	21.67 ± 0.04	21.718 ± 0.012
F814W			20.92 ± 0.06	20.96 ± 0.06	20.915 ± 0.012

Notes:
Zero-points listed for high gain (gain= 14) state.
F555W ground-based zero-points were derived from *V*-F555W comparison.
F814W ground-based zero-points were derived after *I* transformed to F814W. (Harris *et al.* 1991)

Figure Captions

Figure 1. An image of Ml 01 taken at the Canada-France-Hawaii Telescope. The WFPC 2 field of view is shown. North is to the top and East is to the right.'

Figure 2. The phase-detection incompleteness function for a Monte Carlo simulation based on the M101 outer field observation dates. No other selection effects have been modeled for this plot.

Figure 3(a-d). Finder charts made from median images of the summer M101 Outer Field observations, rotated and aligned with chip 3 so that North is approxiametly towards the top of the page. The original (x, y) axes of arc rotated with the images. The outer field Cepheids are circled and labelled. Each 800 x 800 image is 80" across.

Figure 4. Magnified finder chart subsections $10''$ across, with the M101 outer field Cepheids circled.

Figure **5.** Phase-wrapped V light curves for the M101 outer field Cepheids.

Figure **6.** A Colour-Magnitude Diagram for the outer field of M1OI showing V *vs.* $(V-I)$.

Figure **7(a,b).** Combined LMC and M101 V and I apparent period-luminosity relations.

Figure 8. Galactic extinction law shown passing through V and I apparent distance moduli. Apparent B distance modulus shown for consistency,

Completeness Function

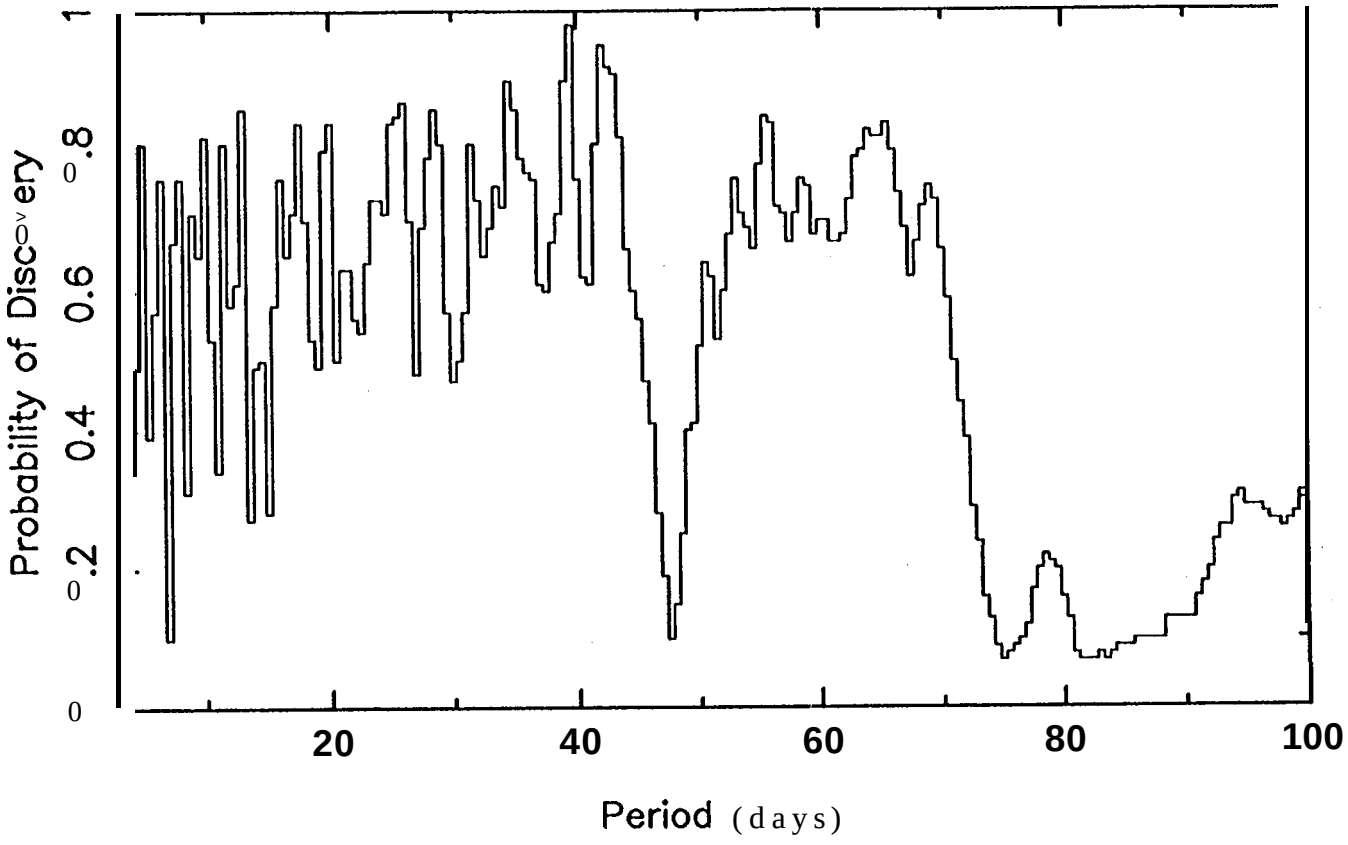

M101 Outer Field WFC Chip 1

Median of JD 2449131 through JD 2449163

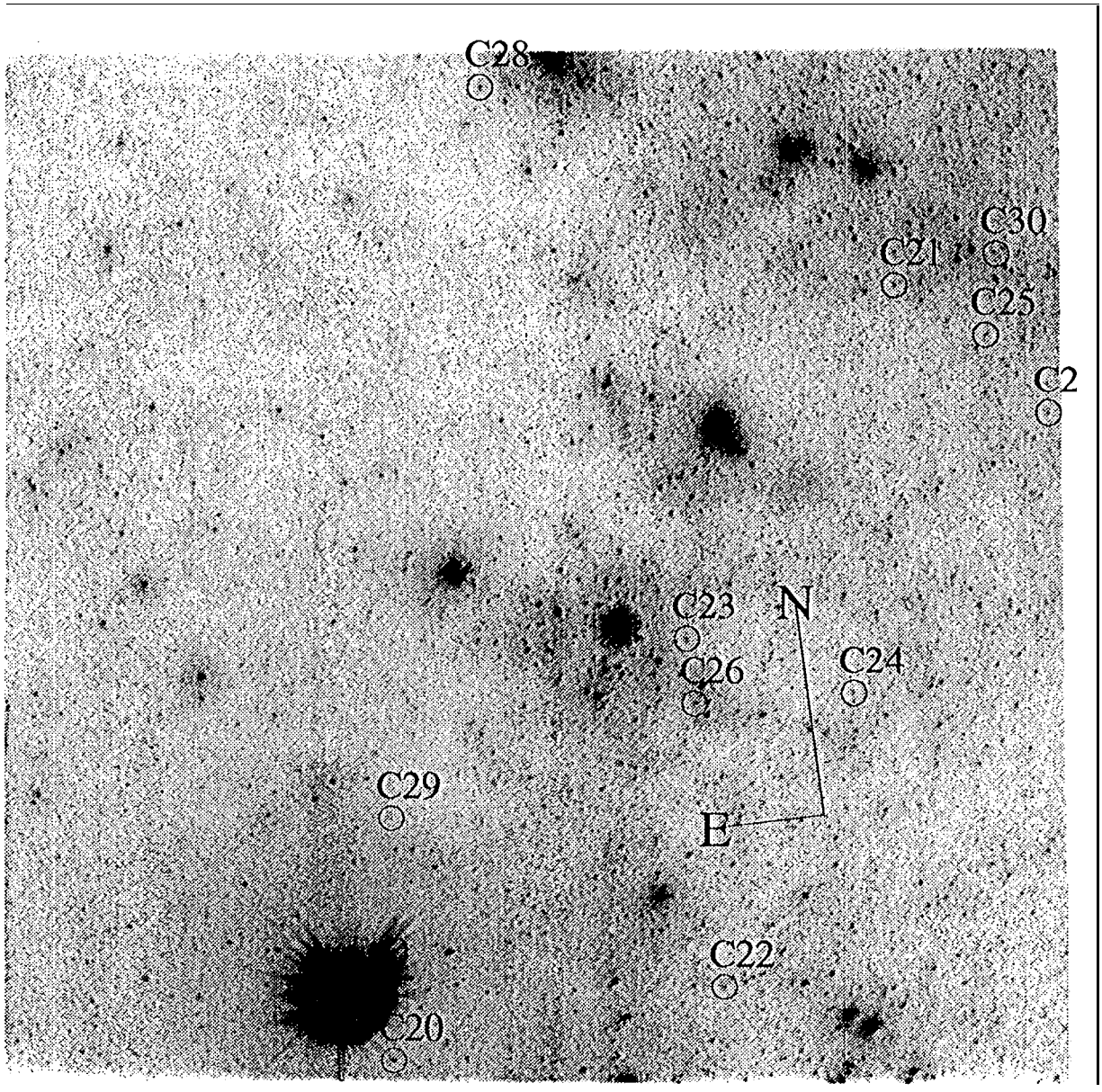

M101 Outer Field WFC Chip 2

Median of JD 2449131 through JD 2449163

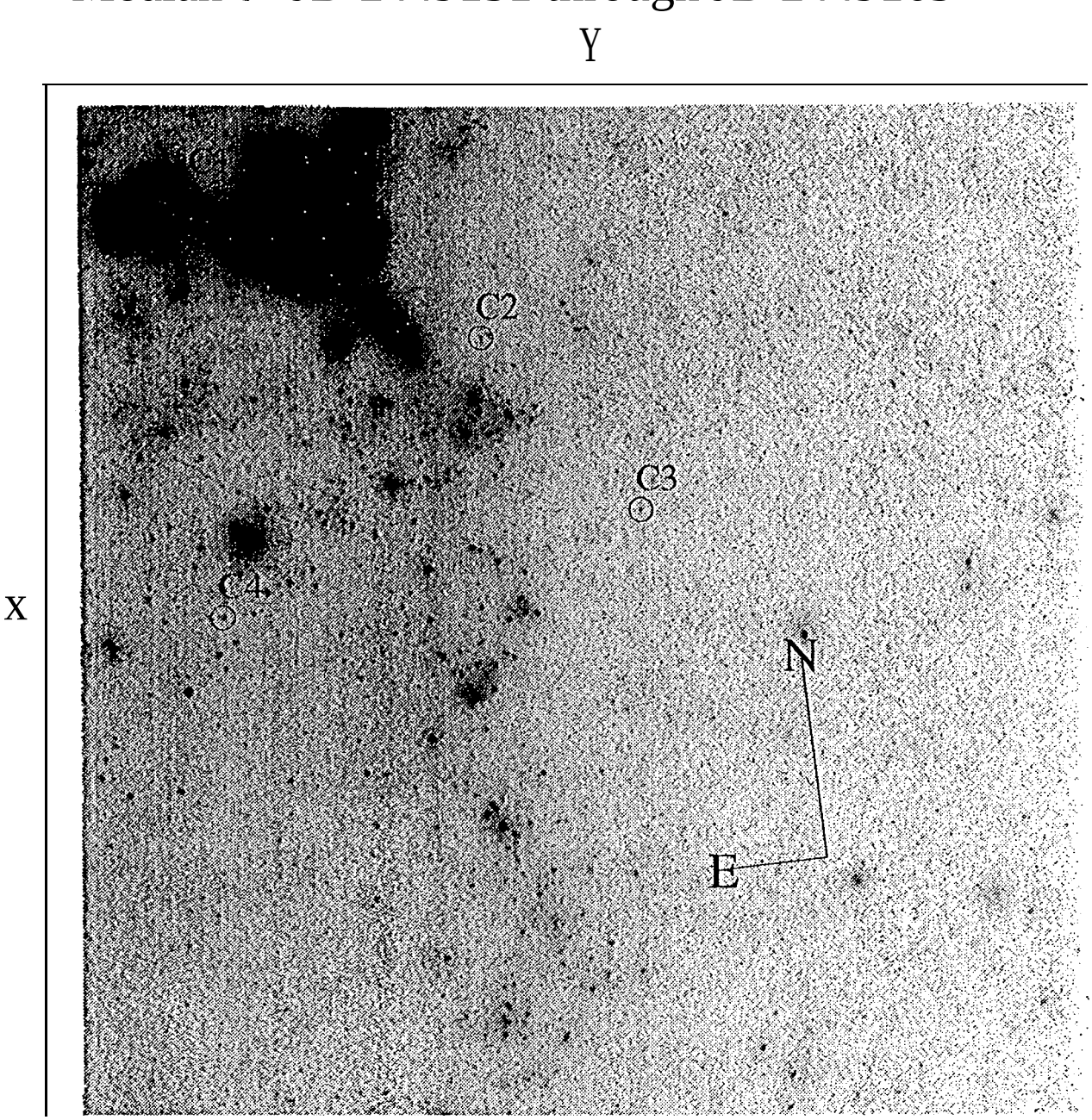

M101 Outer Field WFC Chip 3

Median of JD 2449131 through JD 2449163

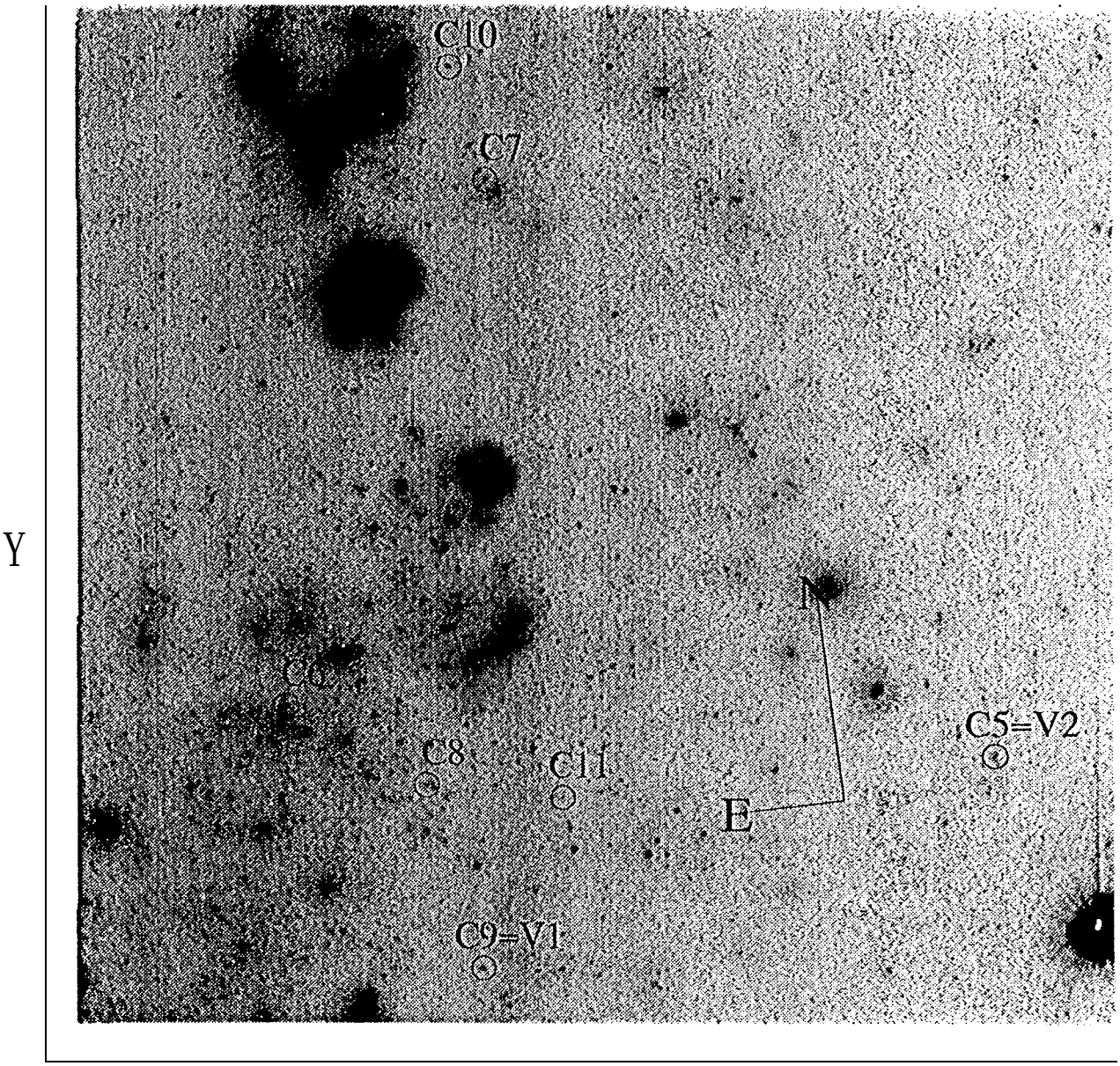

M101 Outer Field WFC Chip 4

Median of JD 2449131 through JD 2449163

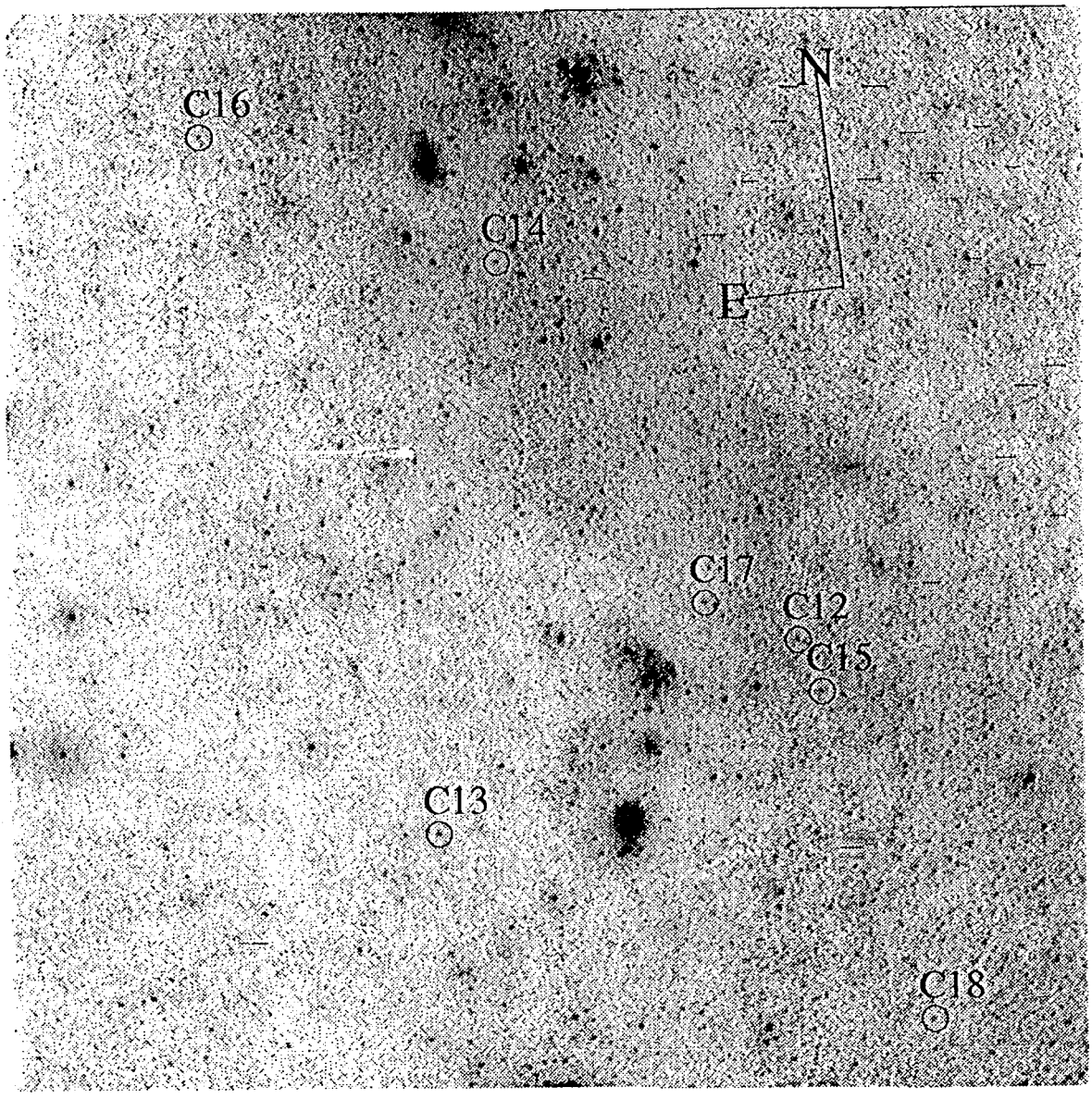

Ml 01 Outer Field and LMC Cepheids

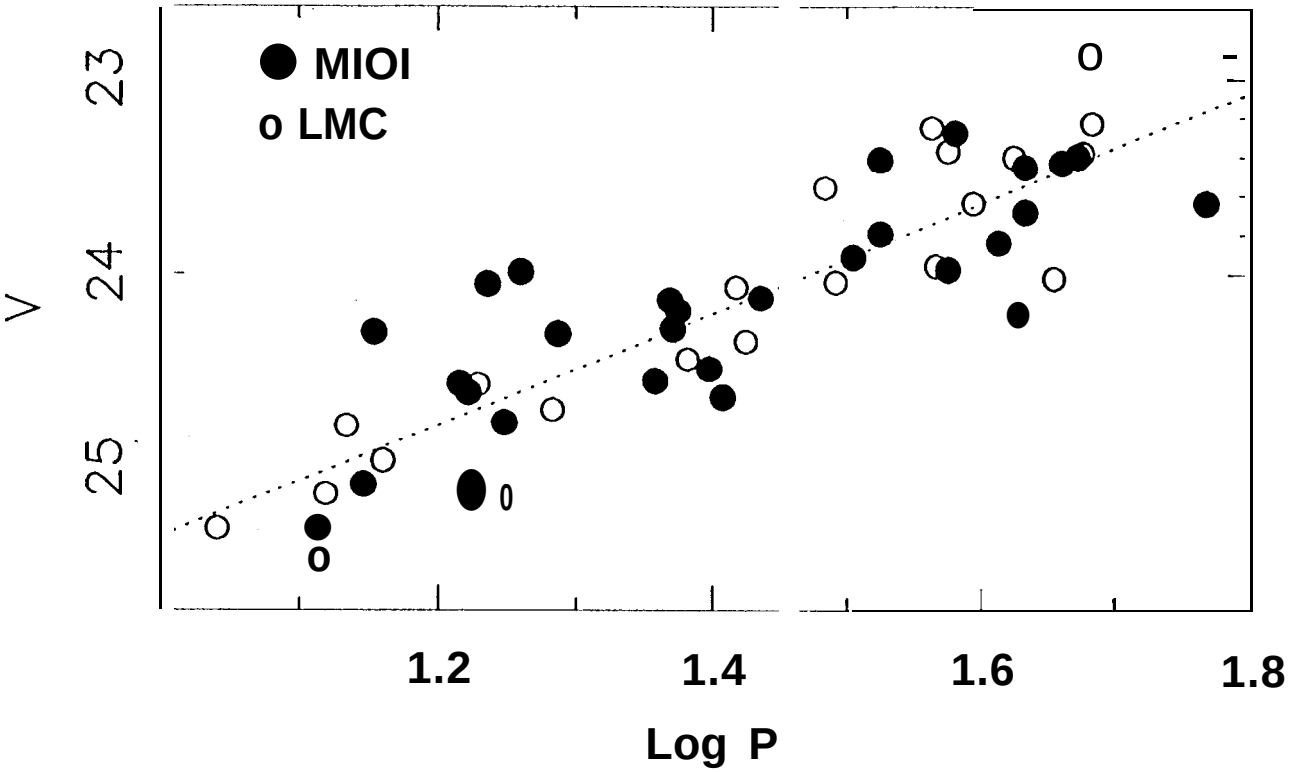

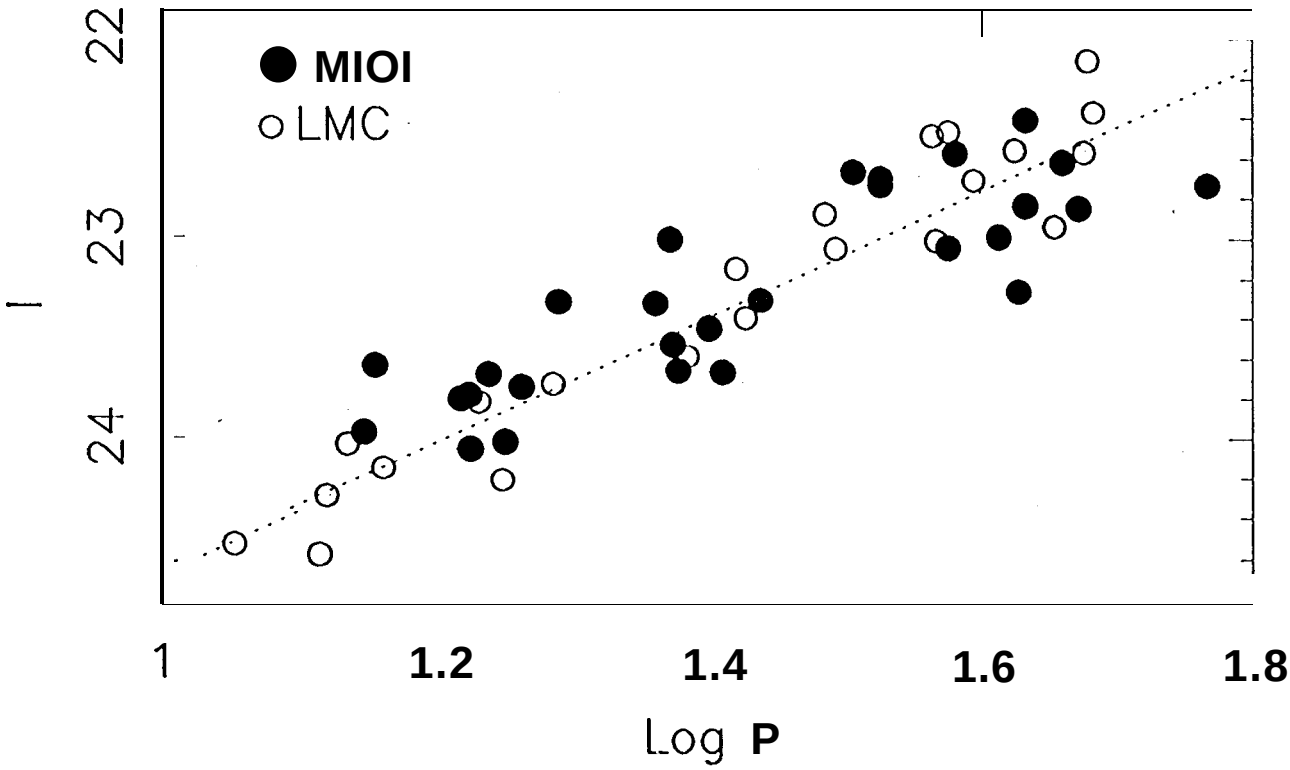

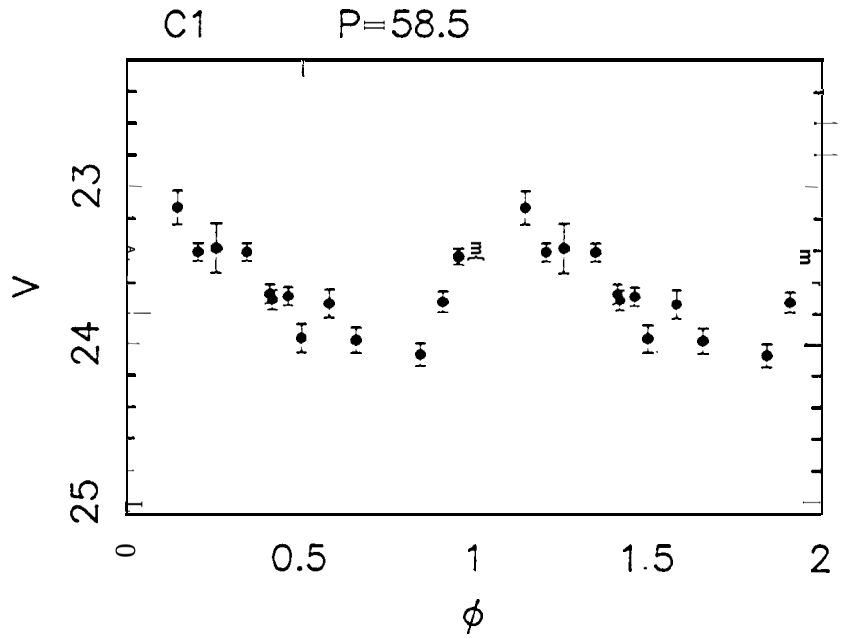
C1
P=58.5
V
23
24
25
0
0.5
1
1.5
2
ϕ

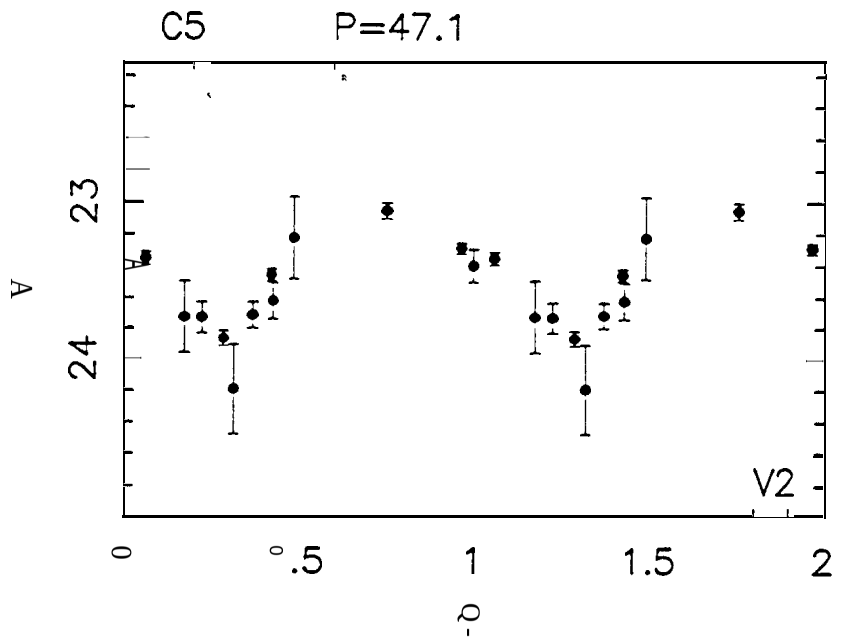
C5
P=47.1
V
23
24
0
0.5
1
1.5
2
V2

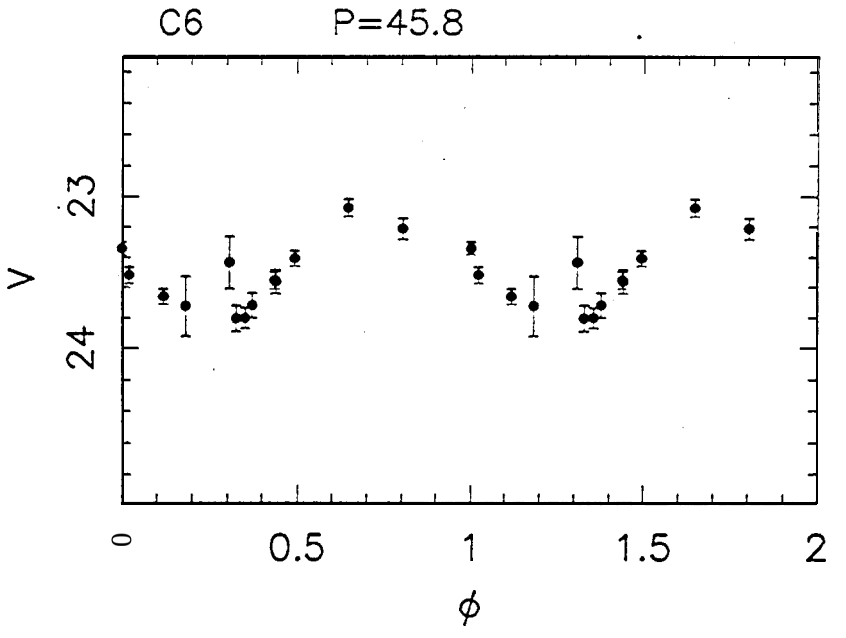
C6
P=45.8
V
23
24
0
0.5
1
1.5
2
ϕ

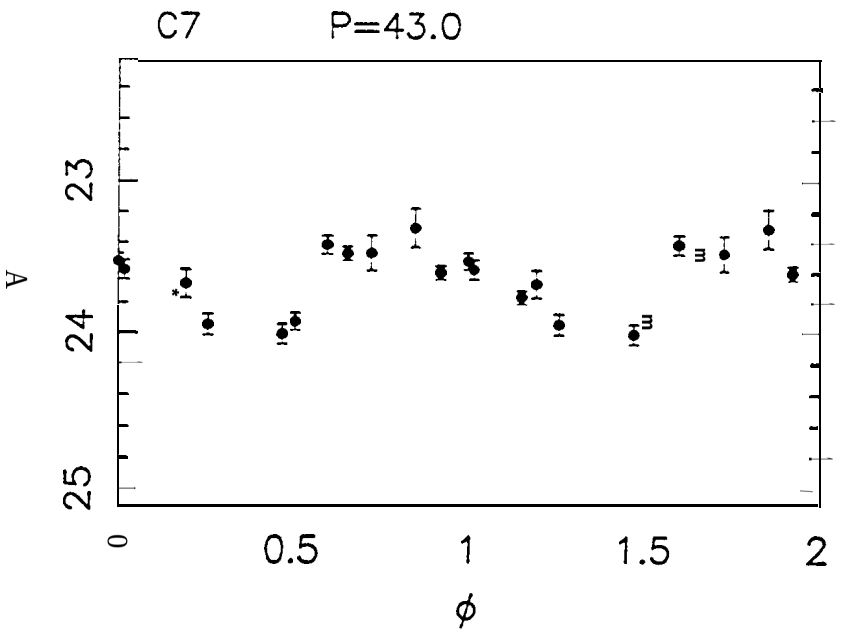
C7
P=43.0
V
23
24
25
0
0.5
1
1.5
2
ϕ

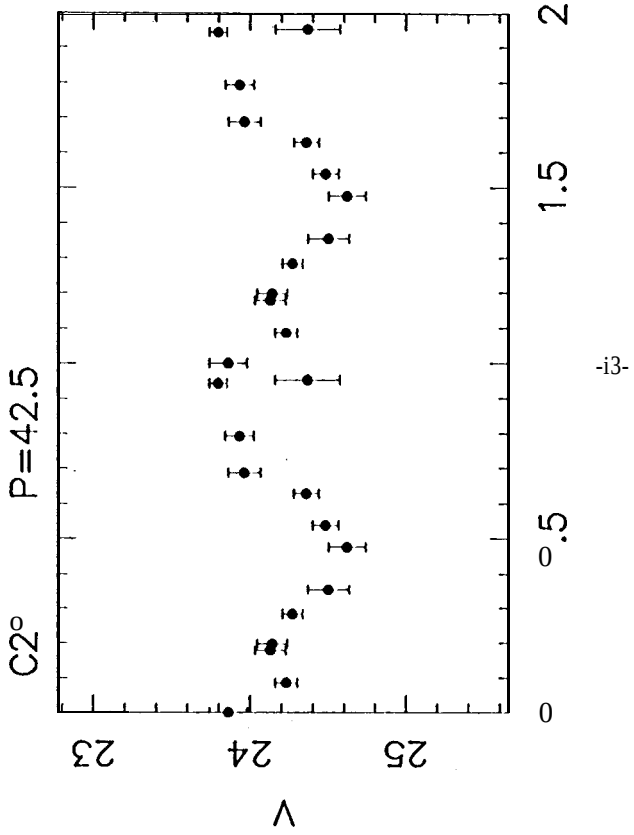
C2°
P=42.5
V
A
25
24
23
0
0.5
1
1.5
2
φ

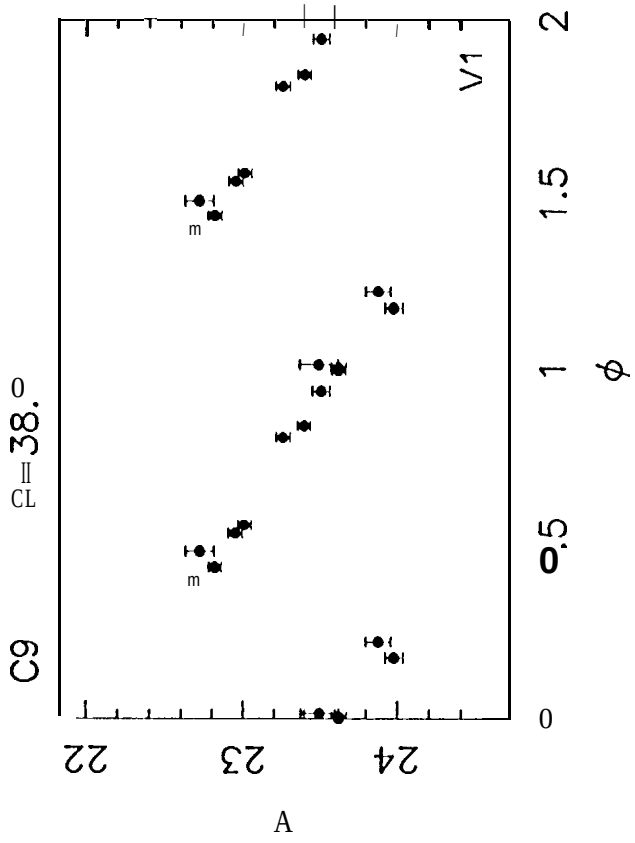
C9
CL
38.
V1
m
m
A
24
23
22
0
0.5
1
1.5
2
φ

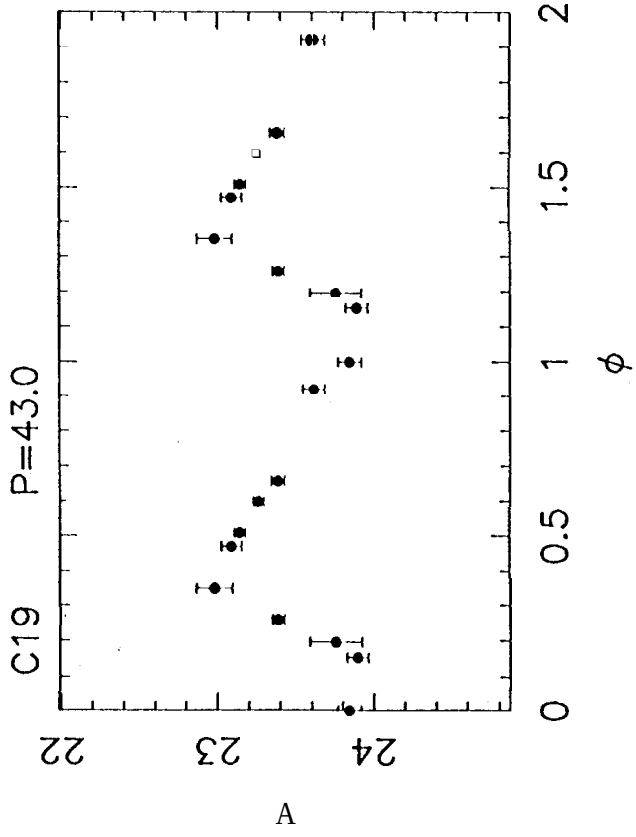
C19
P=43.0
A
24
23
22
0
0.5
1
1.5
2
φ

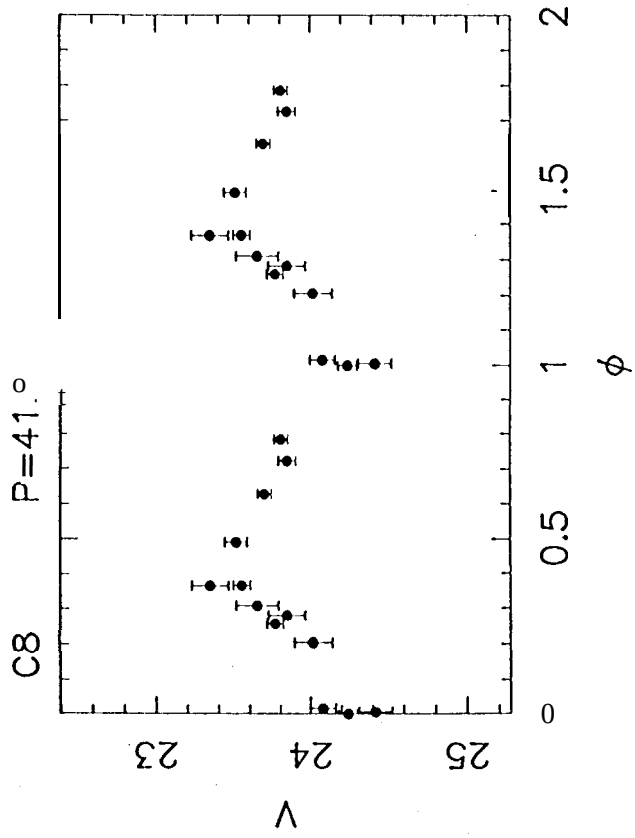
C8
P=41.°
V
25
24
23
0
0.5
1
1.5
2
φ

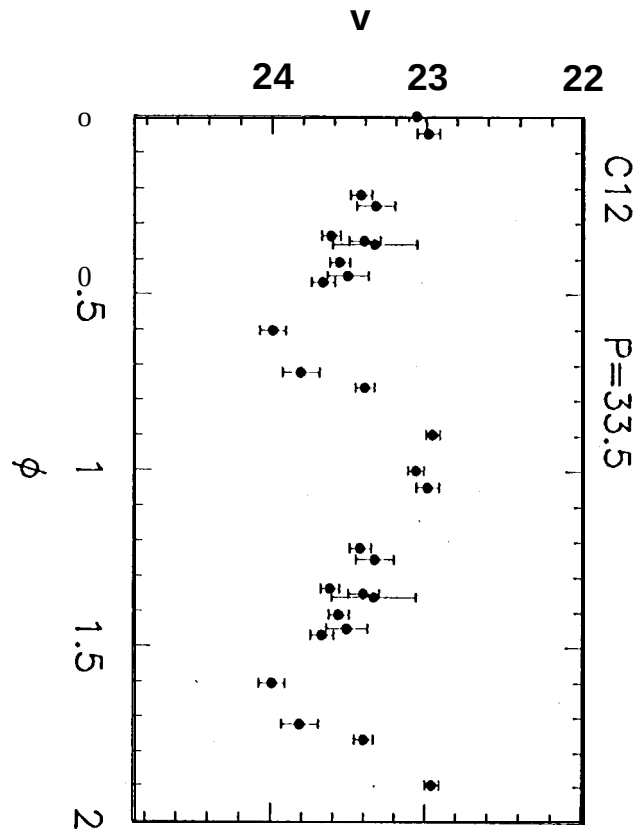
V
24
23
22
0
0.5
1
1.5
2
φ
C12
P=33.5

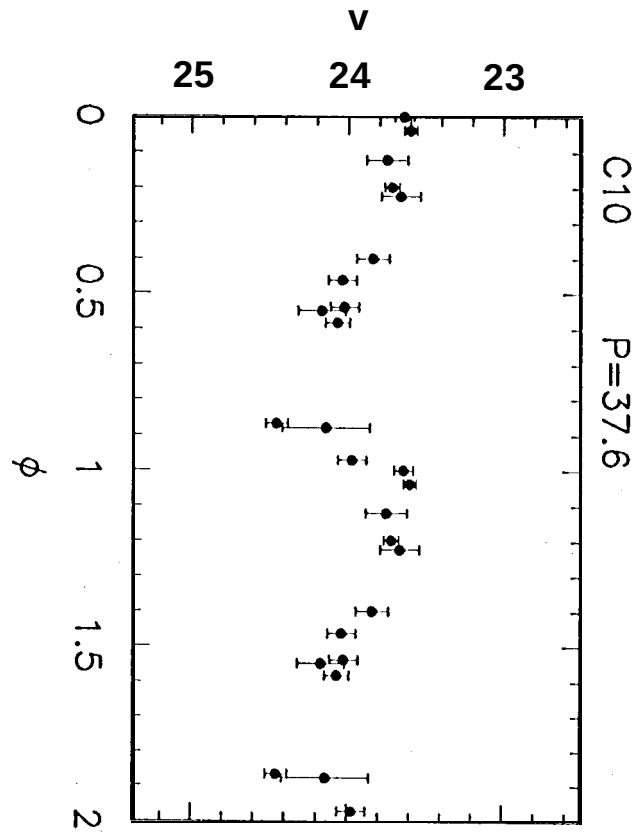
V
25
24
23
0
0.5
1
1.5
2
φ
C10
P=37.6

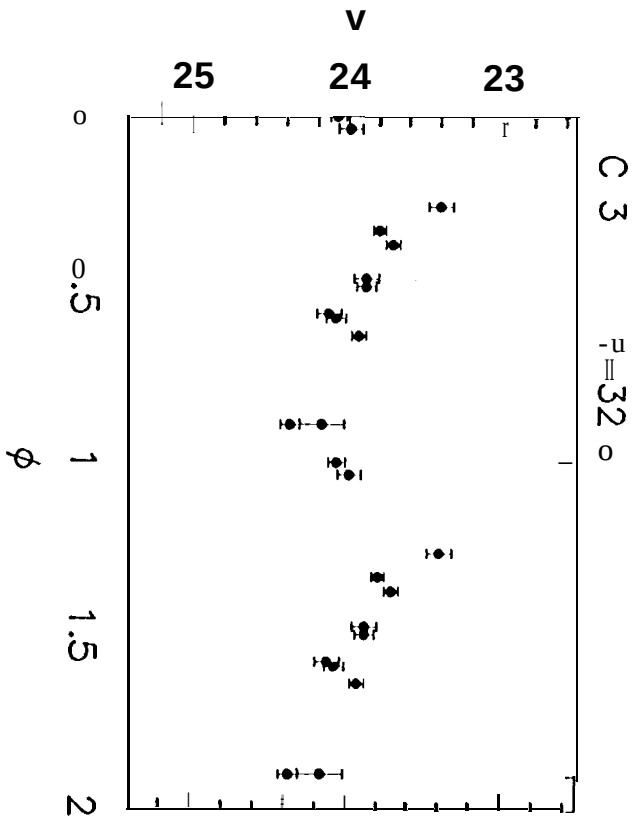
V
25
24
23
0
0.5
1
1.5
2
φ
C 3

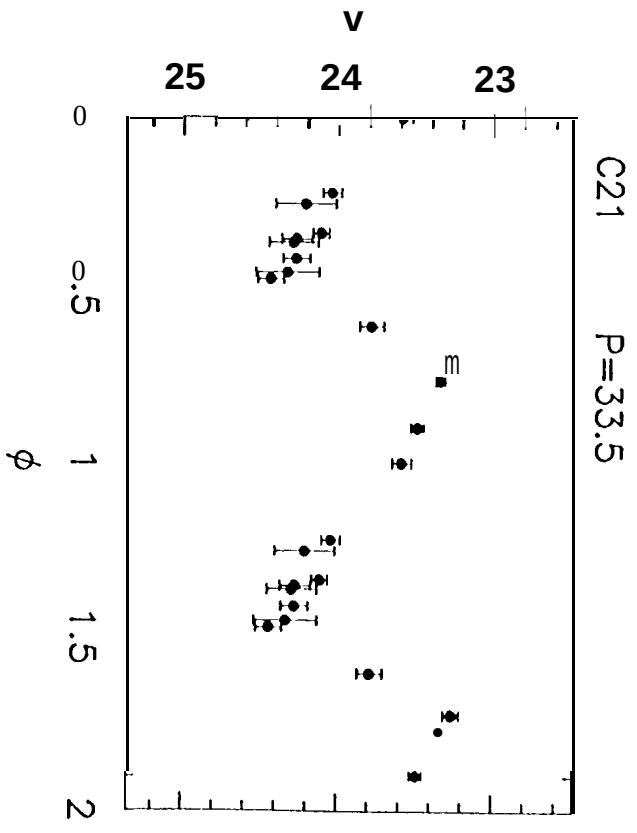
V
25
24
23
0
0.5
1
1.5
2
φ
C21
P=33.5

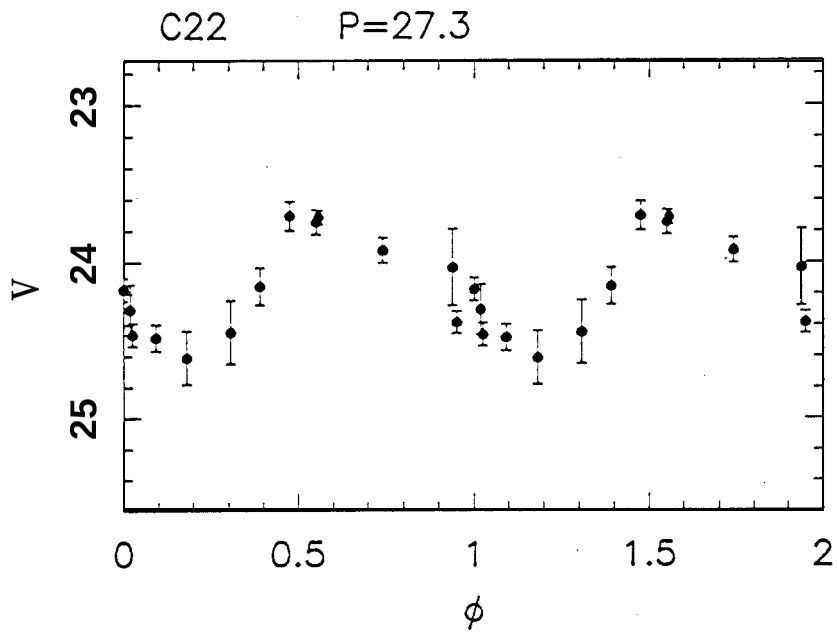
C22
P=27.3
V
23
24
25
0
0.5
1
1.5
2
φ

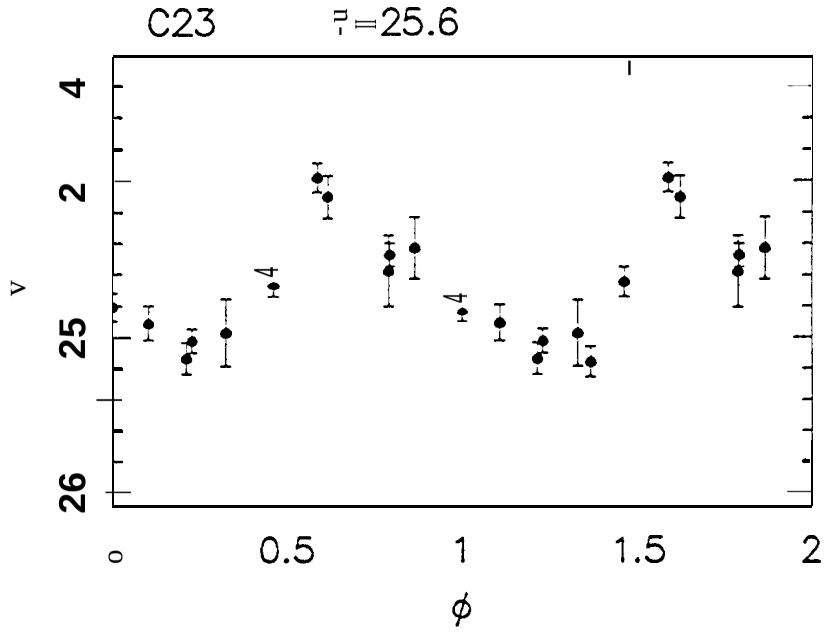
C23
P=25.6
V
2
25
26
0
0.5
1
1.5
2
φ

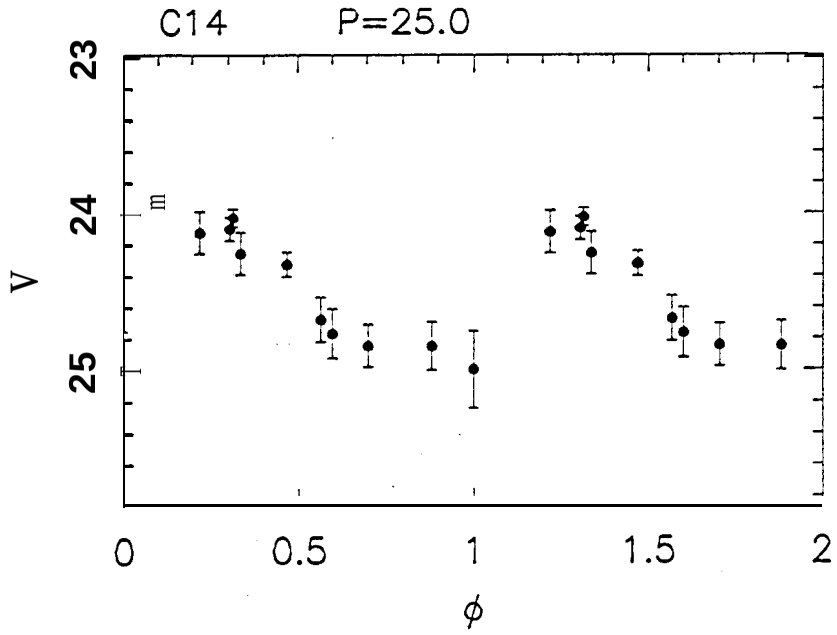
C14
P=25.0
V
23
24
25
0
0.5
1
1.5
2
φ

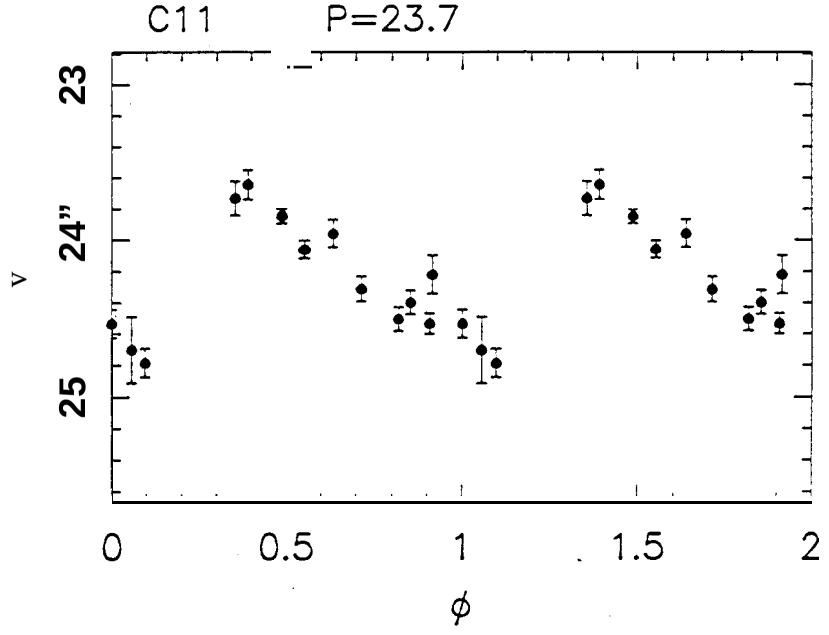
C11
P=23.7
V
23
24"
25
0
0.5
1
1.5
2
φ

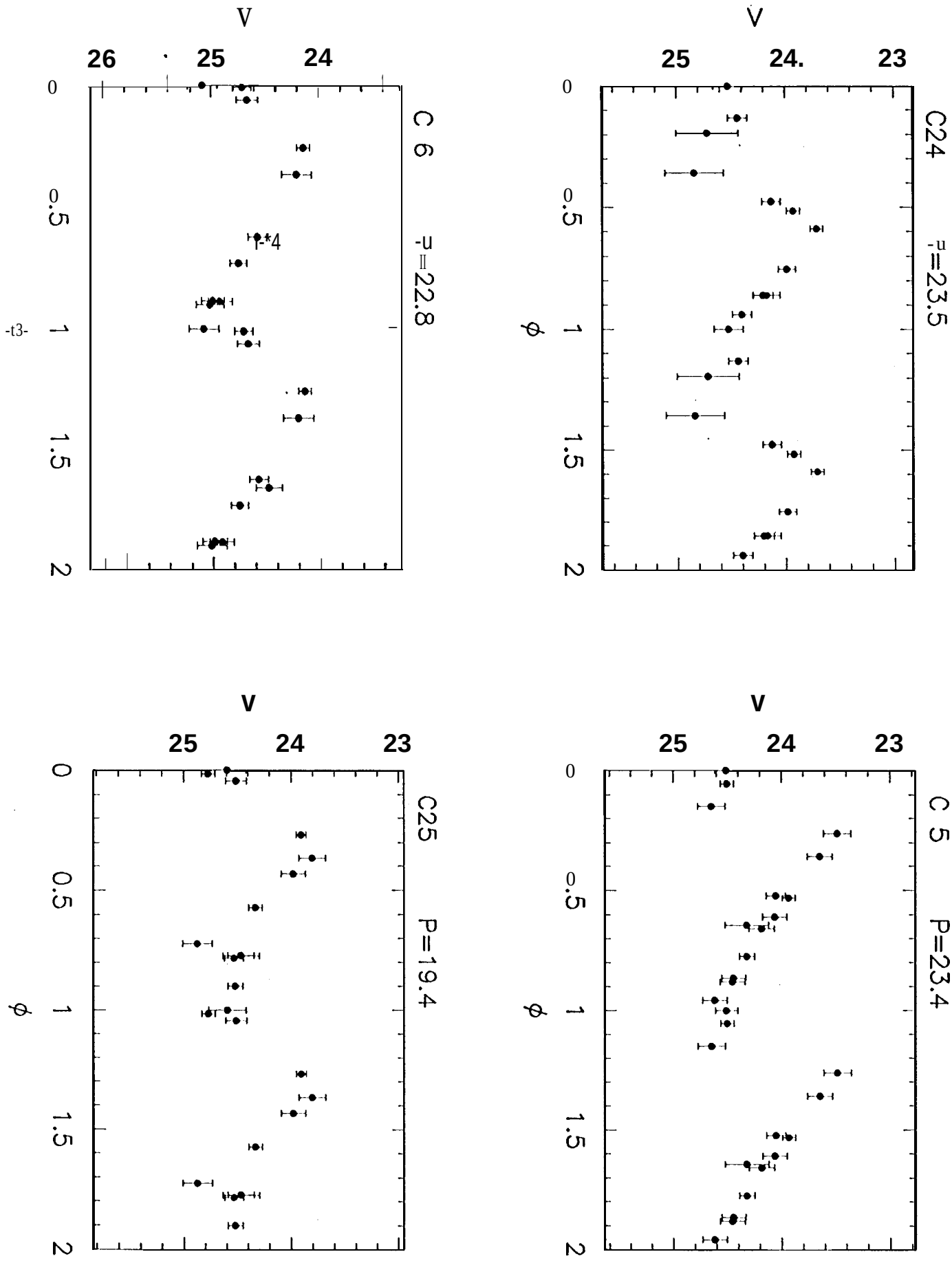
V
26
25
24
0
0.5
1
1.5
2
C 6
P=22.8
V
25
24.
23
C24
P=23.5
V
25
24
23
C25
P=19.4
V
25
24
23
C 5
P=23.4
φ

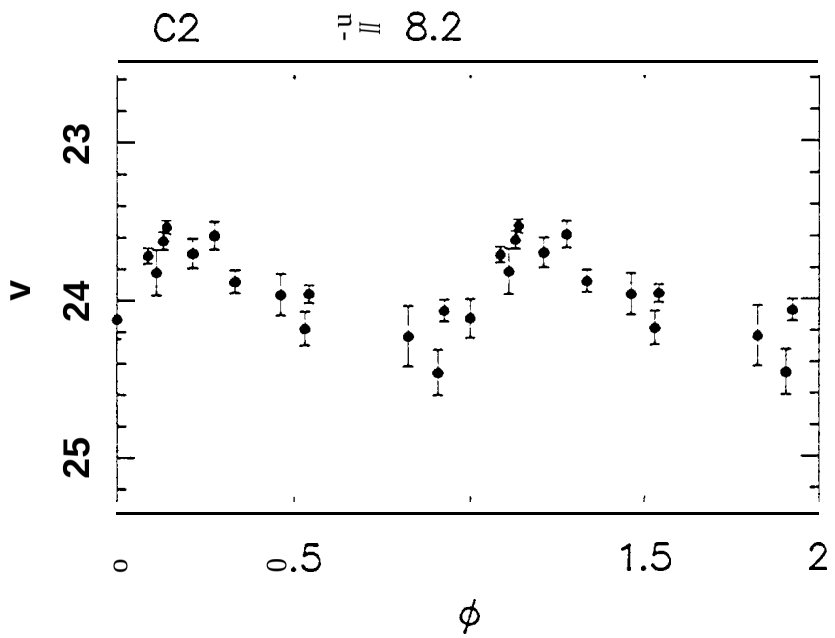
C2
P=8.2
V
23
24
25
0
0.5
1.5
2
φ

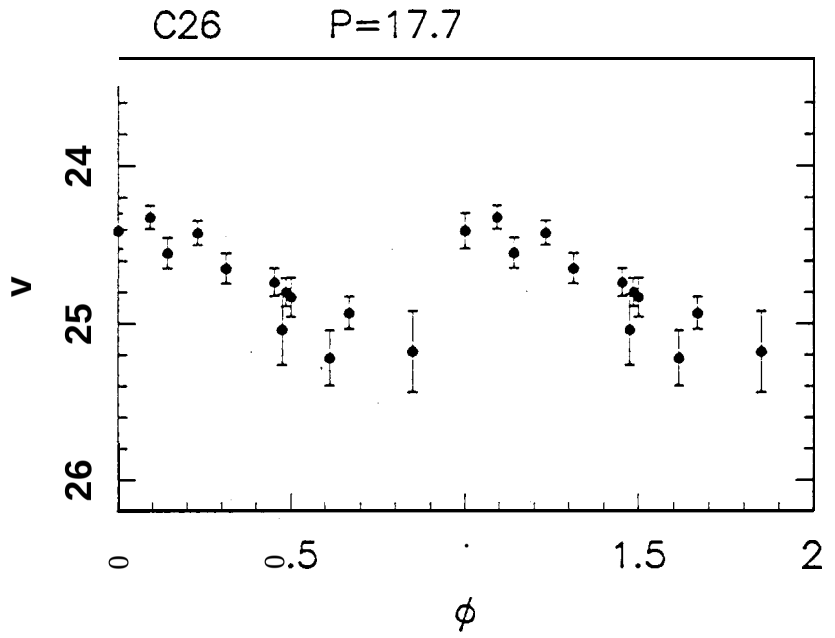
C26
P=17.7
V
24
25
26
0
0.5
1.5
2
φ

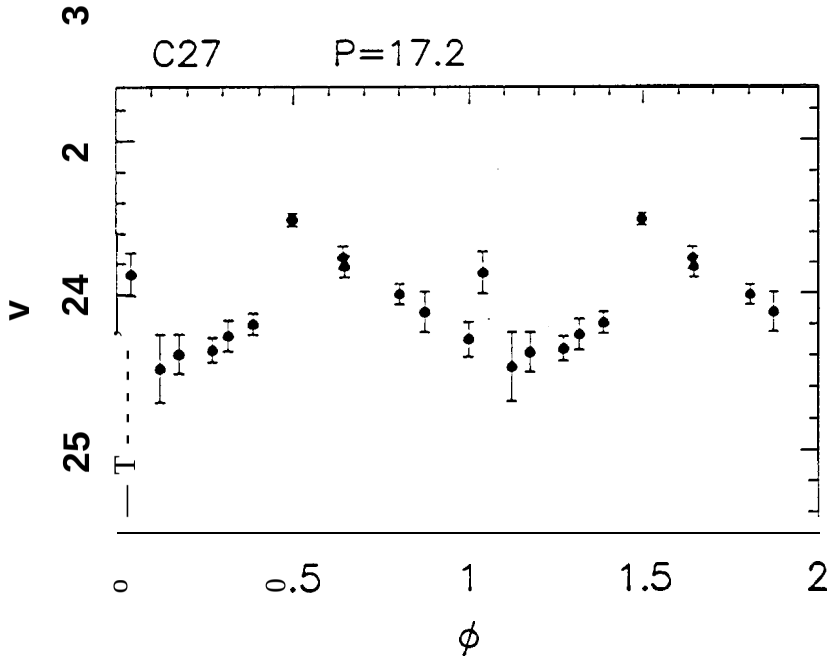
C27
P=17.2
V
2
3
24
25
0
0.5
1
1.5
2
φ

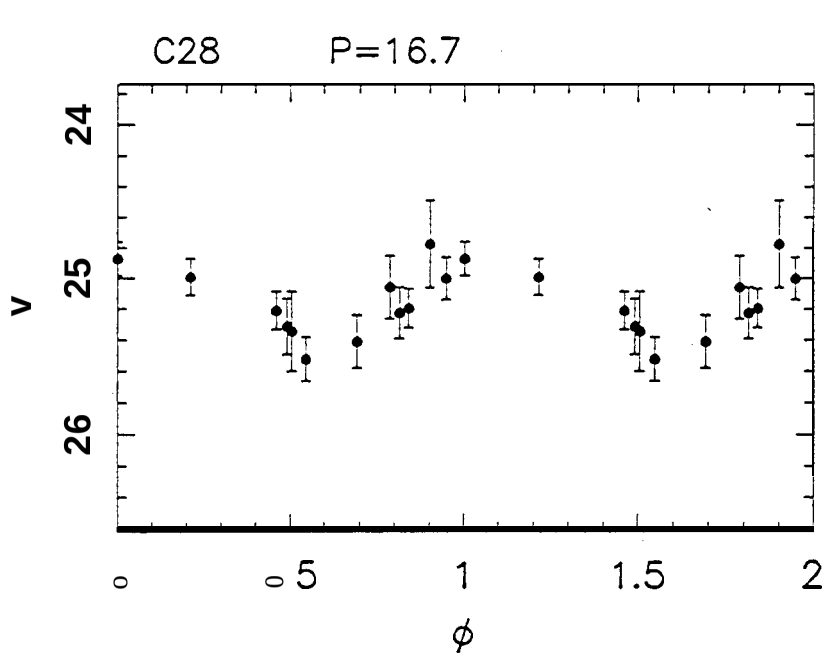
C28
P=16.7
V
24
25
26
0
0.5
1
1.5
2
φ

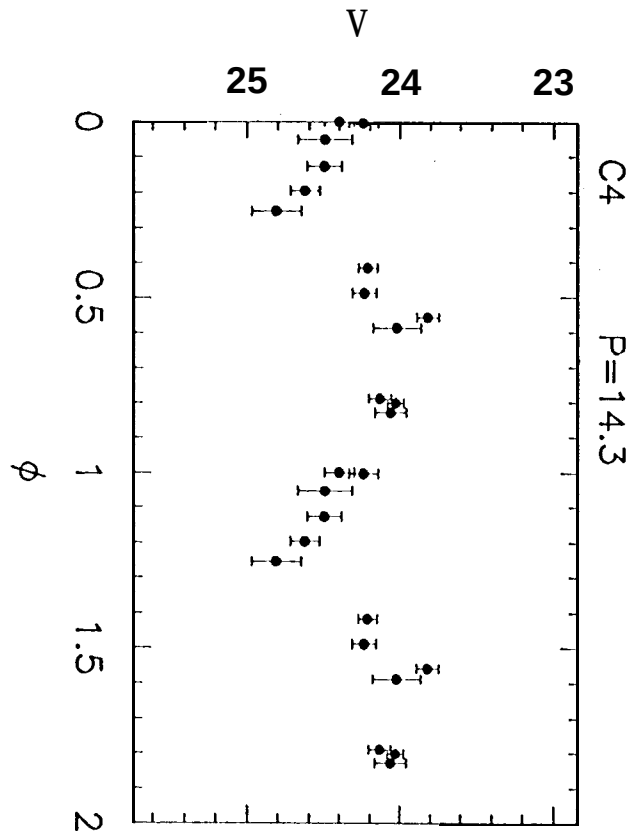
V
25
24
23
0
0.5
1
1.5
2
φ
C4
P=14.3

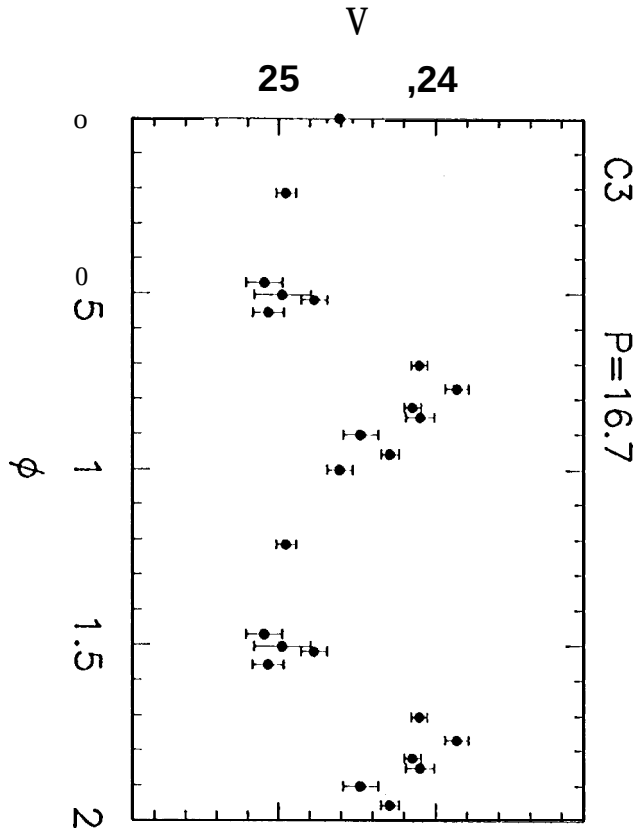
V
25
,24
0
0.5
1
1.5
2
φ
C3
P=16.7

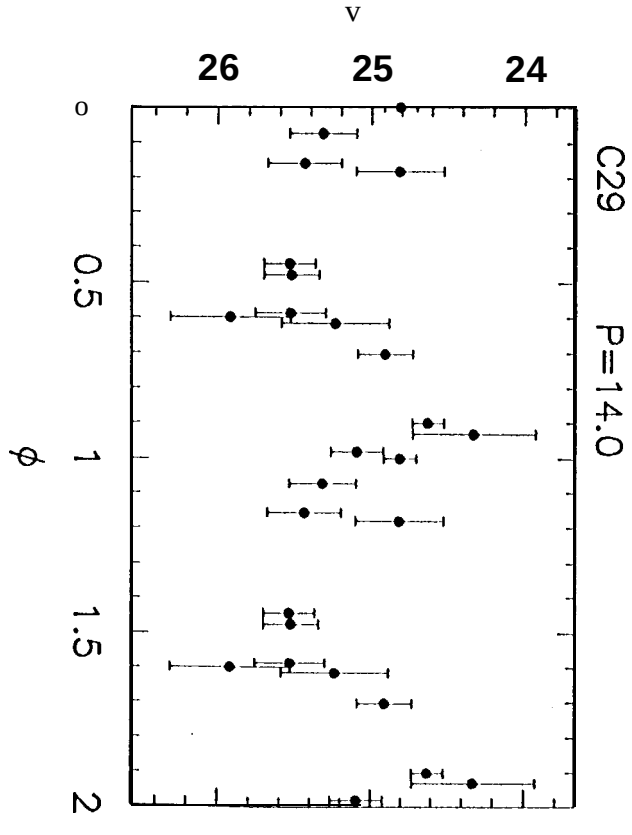
v
26
25
24
0
0.5
1
1.5
2
φ
C29
P=14.0

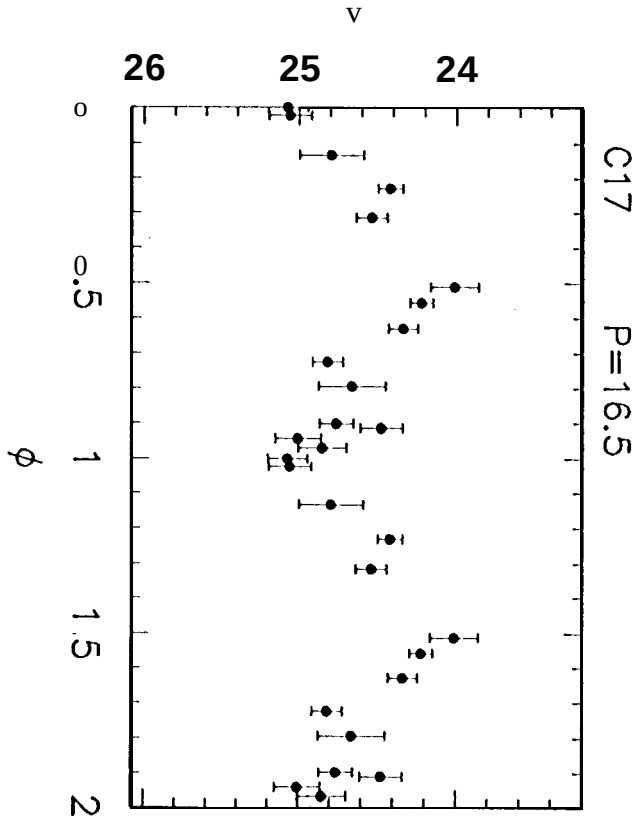
v
26
25
24
0
0.5
1
1.5
2
φ
C17
P=16.5

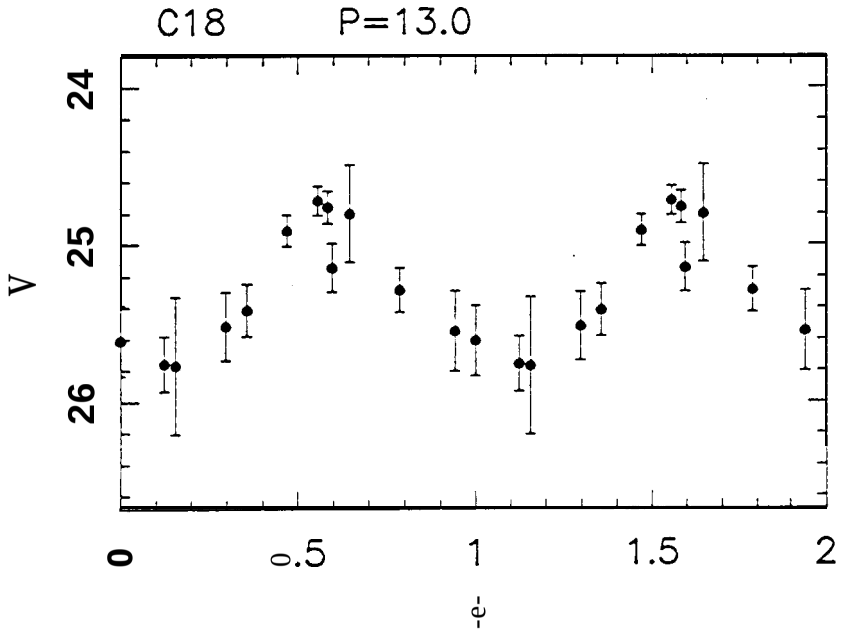
C18
P=13.0
V
24
25
26
0
0.5
1
1.5
2
-e-

MIOI Outer Field

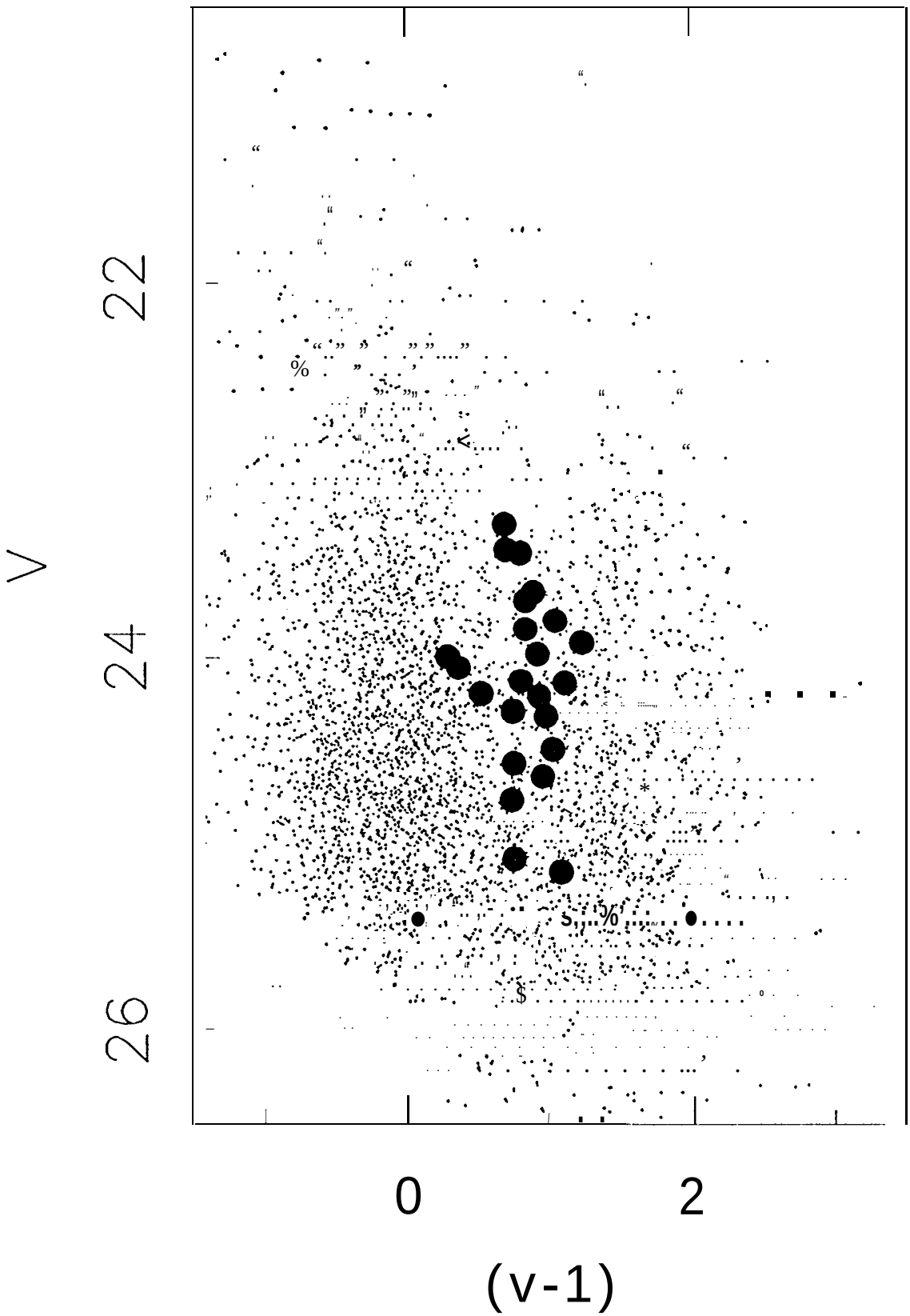

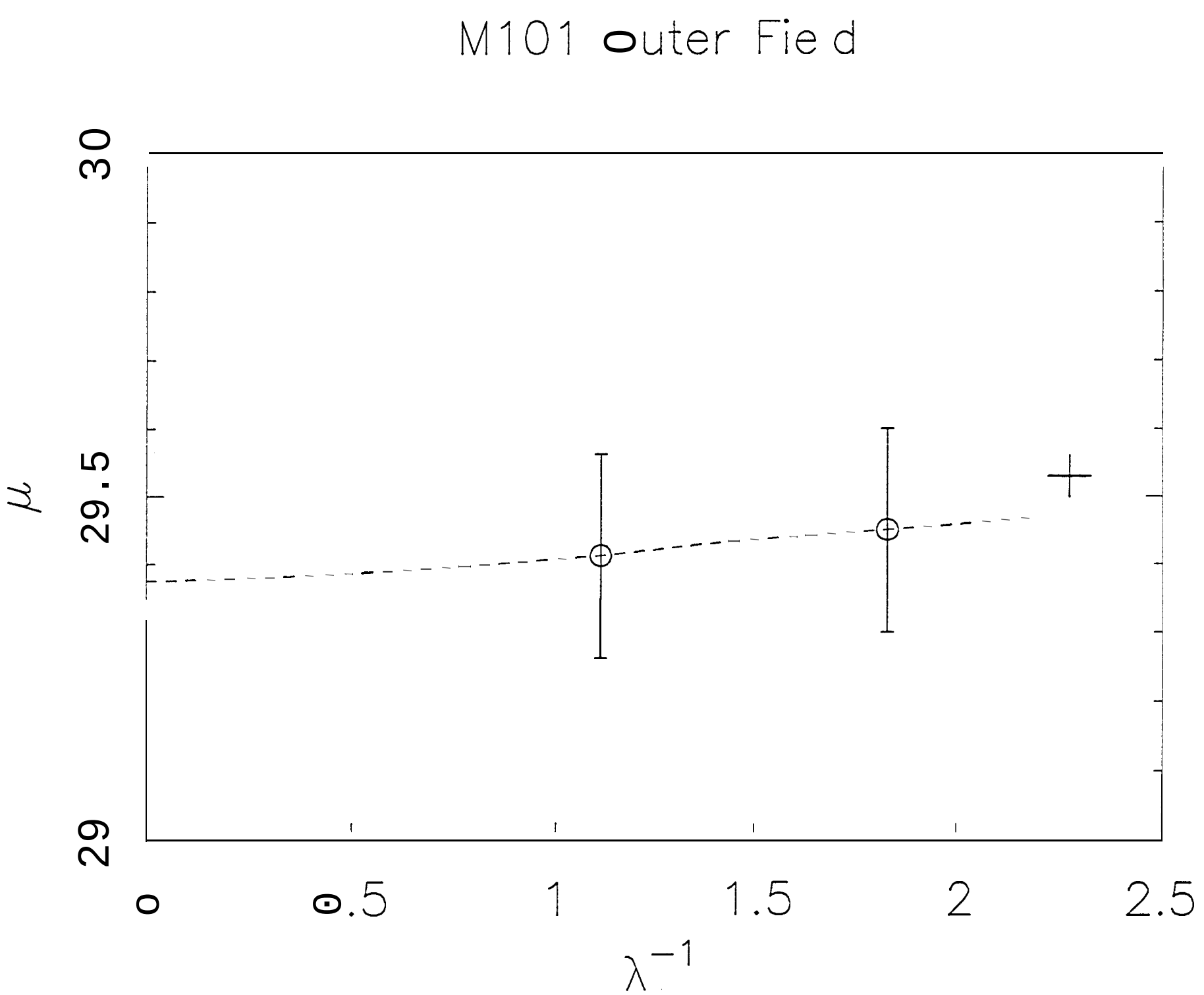
M101 Outer Field
30
29.5
29
μ
0
0.5
1
1.5
2
2.5
λ^-1

Table 3a. Unweighed Mean Photometry of M1OI Outer Field Cepheids

ID	P (days)	(v)	σ_V	(1)[1]	σ_I	$\langle I\rangle^2$	σ_I	$\langle I\rangle^3$	σ_I	$\Delta\langle I\rangle^3$
c l	*58.54*	23.63	0.07	*22.72*	0,10	*22.72*	0.10	*22.72*	0,10	0.04
C5	*47.10*	23,55	0,09					*22.92*	0.04	0.10
C6	*45.80*	*23.54*	0.06	*22.64*	0.14	*22.64*	0.14	*22.64*	0.14	−0.08
C7	*43.00*	*23.66*	0.07	*22.81*	0.08	*22.81*	0.08	22.81	0.08	−0.01
C19	*43.00*	*23.43*	0.10					*22.40*	0.04	−0.07
C20	*42.50*	*24.21*	0.07	23.19	0,10	*23.24*	0.09	*23.24*	0.09	0.11
C8	*41.00*	*23.83*	0.08	22.92	*0.08*	*22.92*	0.08	*22,92*	0.08	−0.02
C9	*38.00*	*23.27*	0.12	22.63	0.10	*22.63*	0.10	*22.63*	0.10	−0.01
C10	*37.60*	*23.94*	0.07	*23.03*	0.12	*23.03*	0.12	*23.03*	0.12	−0.01
C21	*33.50*	23.92	0.12	*22.78*	0,21	*22.78*	0.21	*22.78*	0.21	0.06
C12	*33.50*	*23.44*	0.08	*22.66*	0.02	*22.65*	0.02	*22.65*	0.02	0.01
C13	*32.00*	*23.96*	0.07	*22.65*	0.14	*22.65*	0.14	*22,65*	0.14	0.01
C22	*27.30*	*24,16*	0.09	*23.30*	0,07	*23.25*	0.07	*23.25*	0.07	0.03
C23	*25.60*	*24.66*	0.11	*23.72*	0.09	*23.64*	0.10	*23.64*	0.10	0.03
C14	*25.00*	*24.42*	0.12	*23.23*	0.10	23.39	0.14	*23.39*	0.14	−0.03
C11	*23.70*	*24.23*	0.10	*23.61*	0.16	*23.61*	0.16	*23.61*	0.16	0.06
C24	*23.50*	*24.27*	0.10	*23.48*	0.31	*23.57*	0.13	*23,57*	0.13	0.10
C15	*23.40*	*24.21*	0.10	*22,89*	0.19	*22.99*	0.18	*22.99*	0.18	−0.02
C16	*22.80*	*24.68*	0.10					*23.39*	0.13	0.19
C25	*19.35*	*24.39*	0.10			*23.32*	0.10	*23.32*	0.10	0.00
C2	*18.20*	*23.93*	0.07	23.61	0.14	*23.61*	0.14	*23.67*	0.12	0.02
C26	*17.70*	*24.76*	0.09			*24,03*	0.14	*24.03*	0.14	−0.01
C27	*17.20*	*24.09*	0.09			*23.71*	0.17	*23.71*	0.17	0.02
C28	*16.70*	*25.18*	0.07	*24.07*	0.03	*24.07*	0.03	*24.07*	0.03	−0.07
C3	*16.67*	*24.50*	0.13					*23.73*	0.16	−0.18
C17	*16.45*	*24.64*	0.09			23.85	0,14	*23.85*	0.14	−0.06
C4	*14.27*	*24.28*	0.08					*23.63*	0.10	−0.09
C29	14.00	*25.11*	0.13			24.31	0.49	*23.98*	0.40	0.06
C18	*13.00*	*25.24*	0.12							

Notes:
[1] Using strong F814W magnitude uncertainty restrictions (0.2,0.1,4) (see Section 6.2).
[2] Using moderate F814W magnitude uncertainty restrictions (0.3,0.2,4) (see Section 6.2).
[3] Using weak F814 W magnitude uncertainty restrictions (0.4,0.4,1) (SCC Section 6.2).

Table 3b. Weighted Mean Photometry of MIOl Outer Field Cepheids

ID	P (days)	(v)	σ_V	(I)"	σ_I	$\langle I\rangle^2$	σ_I	$\langle I\rangle^3$	σ_I	$\Delta\langle I\rangle^3$
c l	58.54	23.68	0.07	22.70	0.10	22.70	0.10	22,70	0.10	0.08
C5	47.10	23.54	0.09					22.92	0.04	0.11
C6	45.80	23.56	0.06	22.75	0.14	22.75	0.14	22.75	0.14	–0.08
C7	43.00	23.72	0.07	22.79	0.08	22.79	0.08	22.79	0.08	0.00
C19	43.00	23.46	0.10					22.41	0.04	–0.08
C20	42.50	24.25	0.07	23.23	0.10	23.26	0.09	23.26	0.09	0.08
C8	41.00	23.89	0.08	23.00	0.08	23.00	0.08	23.00	0.08	–0.05
C9	38.00	23.40	0.12	22,65	0.10	22.65	0.10	22.65	0.10	–0.01
C10	37.60	23.96	0.07	23.07	0.12	23.07	0.12	23,07	0.12	0.01
C21	33.50	23.91	0.12	23,02	0.22	23.02	0.22	23.02	0.22	0.06
C12	33.50	23.48	0.08	22.65	0.02	22.65	0.02	22.65	0.02	0.02
C13	32.00	24.00	0.07	22,76	0.14	22.76	0.14	22.76	0.14	–0.03
C22	27.30	24.19	0.09	23.29	0.07	23.27	0.07	23.27	0.07	0.04
C23	25.60	24.80	0.11	23.73	0.09	23.70	0.10	23.70	0.10	0.03
C14	25.00	24.40	0.12	23.22	0.10	23.36	0.14	23.36	0.14	0.00
c l]	23,70	24.31	0.10	23.66	0.16	23.66	0.16	23.66	0.16	0.05
C24	23.50	24.23	0.11	23.51	0.31	23.57	0.13	23.57	0.13	0.09
C15	23.40	24.31	0.10	22.94	0.19	23.02	0.18	23.02	0.18	0.01.
C16	22,80	24.72	0.10					23.41	0.13	0.17
C25	19.35	24.45	0.10			23.35	0.11	23.35	0,11	0.02
C2	18.20	23.91	0.07	23.68	0.14	23.68	0.14	23.70	0.12	0.01
C26	17.70	24.75	0.09			24.08	0.14	24.08	0.14	–0.02
C27	17.20	24.08	0.09			23.80	0.17	23.80	0.17	–0.04
C28	16,70	25.22	0.07	24.08	0.03	24.08	0.03	24.08	0.03	–0.08
C3	16.67	24.57	0.13					23.76	0.16	–0.21
C17	16.45	24.69	0.09			23.96	0.14	23,96	0.14	–0.08
C4	14.27	24.30	0.08					23.64	0.10	–0.10
C29	14.00	25.22	0.12			24.30	0,48	24.37	0.38	0.12
C18	13,00	25.26	0.11							

Notes:

[1] Using strong F814W magnitude uncertainty restrictions (0.2,0.1,4) (see Section 6.2).

[2] Using moderate F814W magnitude uncertainty restrictions (0.3,0.2,4) (see Section ,6.2).

[3] Using weak F814W magnitude uncertainty restrictions (0.4,0.4,1) (see Section 6.2).

Table *3c.* Phase-Weighted Mean Photometry of M101 Outer Field Cepheids

ID	P (days)	(v)	σ_V	$\langle I\rangle^1$	σ_I	$\langle I\rangle^2$	σ_I	$\langle I\rangle^3$	σ_I	$\Delta\langle I\rangle^3$
cl	*58.54*	*23.64*	0.07	22.73	0.10	22.73	0.10	22.73	0.10	0.00
C5	*47.10*	*23,40*	0,11					22.85	0.56	0.18
C6	*45.80*	*23.43*	0.07	22.62	0.14	22.62	0.14	22.62	0.14	–0.04
C7	*43.00*	*23.68*	0.07	22.84	0.08	22.84	0.08	22.84	0.08	–0.03
C19	*43.00*	*23,45*	0.10					22.41	0.33	–0.08
C20	*42.50*	*24.21*	0.07	23.19	0.10	23.26	0.09	23.26	0.09	0.10
C8	*41.00*	*23.84*	0.08	22.99	0.08	22.99	0.08	22.99	0.08	–0.02
C9	*38.00*	*23.28*	0.12	22.58	0.11	22.58	0.1J	22,58	0.11	–0.01
C10	*37.60*	*23.98*	0.07	23.04	0.12	23.04	0.12	23.04	0.12	–0.01
C21	*33.50*	*23.79*	0.13	22,73	0,21	22,73	0.21	22.73	0.21	0.04
C12	*33.50*	*23.41*	0.08	22.71	0.03	22.70	0.02	22.70	0.02	–0.02
C13	*32.00*	*23.92*	0.08	22.67	0.14	22.67	0.14	22.67	0.14	0.03
C22	*27.30*	*24.12*	0,09	23.45	0.08	23.31	0.07	23.31	0.07	–0.04
C23	*25.60*	*24.64*	0.11	23.71	0.09	23.67	0.10	23.67	0.10	0.05
C14	*25.00*	*24.49*	0.12	23.22	0.10	23.45	0.14	23.45	0.14	–0.02
c l]	*23.70*	*24.19*	0.11	23.66	0.16	23.66	0.16	23.66	0.16	0.01
C24	*23,50*	*24.28*	0.10	23.42	0.33	23.53	0.14	23.53	0.14	0.07
C15	*23.40*	*24,14*	0.10	22.92	0.19	23.01	0.18	23.01	0.18	0.01
C16	*22.80*	*24.55*	0.11					23.33	0.17	0.25
C25	*19.35*	*24.31*	0.10			23.32	0.11	23,32	0,11	–0.02
C2	*18.20*	*23.99*	0.07	23.70	0.14	23.70	0.14	23.74	0,12	–0.01
C26	17.70	*24.76*	0.09			24.02	0.14	24.02	0.14	0.00
C27	17,20	*24.05*	0.09			23.68	0.18	23.68	0.18	–0.02
C28	16.70	*25.15*	0.07	24.05	0.03	24.05	0.03	24.05	0.03	–0.06
C3	16.67	*24.61*	0.13					23.79	0.28	–0.23
C17	16,45	*24,57*	0.09			23.80	0.14	23.80	0.14	–0.04
C4	14,27	*24,30*	0.08					23.64	0.15	–0.10
C29	14.00	*25.08*	0.13			24.32	0.50	23.97	0.41	0.03
C18	13.00	*25.31*	0.11							

Notes:

[1]Using strong F814W magnitude uncertainty restrictions (0.2,0.1 ,4) (see Section 6.2).

[2]Using moderate I?814W magnitude uncertainty rest.rictions (0.3,0.2,4) (see Section 6.2).

[3]Using weak F814W magnitude uncertainty restrictions (0.4,0.4,1) (see Section 6.2).

Table 4. M101 Cepheid B Photometry

ID	P (days)	$B_{2449429.61}$	σ_B
c l	58.54	26,27	0.60
C5	47.10	25.02	0.35
C6	45.80	25.27	0.29
C7	43.00	24.26	0.18
C19	43.00	24,44	0.17
C20	42.50	26,11	0.66
C8	41.00	24.79	0.19
C9	38.00	25.16	0.23
C10	37.60	24.90	0.18
C21	33.50	26,01	0.27
C12	33.50	24.50	0.22
C13	32,00		
C22	27.30	25.47	0.24
C23	25.60	26.57	0.79
C14	25.00		
cl 1	23.70	26.19	0.36
C24	23.50	26.51	0.53
C15	23,40	24.14	0.16
C16	22.80		
C25	19.35	26.39	0.78
C2	18.20	25.59	0.24
C26	17.70	26.18	0.35
C27	17.20	26.77	0.59
C28	16.70		
C3	16.67		
C17	16.45		
C4	14.27		
C29	14,00	27.14	0.63
C18	13.00	25,82	0.41

Table 5. Comparison of Results from Different Cepheid Groupings

Table 5a. Strong I Photometry Restrictions (0.2,0.1,4)

Subset	N_V	N_I	Unweighted Photometry						Weighted Photometry						Phase-Weighted Photometry					
			$\frac{\partial V}{\partial \log P}$	$\frac{\partial I}{\partial \log P}$	μ_V	μ_I	$E(B-V)$	μ_0	$\frac{\partial V}{\partial \log P}$	$\frac{\partial I}{\partial \log P}$	μ_V	μ_I	$E(B-V)$	μ_0	$\frac{\partial V}{\partial \log P}$	$\frac{\partial I}{\partial \log P}$	μ_V	μ_I	E(B -V)	μ_0
Ml	29	18	-2.S2	-3.13	10.62	10.76	0.02	29.40	-2.S2	-3.13	10.66	10.S1	0.01	29.46	-2.S5	-3.14	10.61	10.78	*0.00*	29.44
Both VI	18	1s	-3.03	-3.13	10.70	10.76	0.06	29.32	-3.02	-3.13	10.74	10.S1	0.06	29.38	-3.04	-3.14	10.6S	10.7S	0.04	29-38
Chips 2,3,4	25	16	-3.11	-3.29	10.67	10.76	0.05	29.3.5	-3.11	-3.25	10.71	10.SO	0.05	29.39	-3.12	-3.28	10.64	10.77	0.02	29.40
Chips 1,3,4	22	12	-2.s5	-3.1S	10.62	10.SS	0.04	29.32	-2.86	-3.17	10.65	10.76	0.04	29.37	-2.SS	-3.1S	10.60	10.74	0.02	29.38
Chips 1,2,4	22	14	-2.76	-3.20	10.62	10.SS	-0.06	29.63	-2.76	-3.20	10.66	10.93	-0.06	29.69	-2.79	-3.29	10.60	10.90	-0.08	29.69
Chips 1,2,3	18	12	-2.s5	-3.11	10..57	10.70	0.02	29.33	-2.85	-3.12	10.62	10.74	0.03	29.36	-2.90	-3.13	10..56	10.72	0.01	29.37
chip 4	11	6	-3.13	-3.36	10.70	10.90	-0.02	29..59	-3.14	-3.33	10.73	10.9.5	-0.03	29.66	-3.12	-3.36	10.67	10.90	-0.04	29.62
Chip 2,3	14	10	-3.24	-3.27	10.66	10.68	0.09	29.20	-3.24	-3.26	10.71	10.72	0.09	29.23	-3.26	-3.28	10.63	10.70	0.06	29.27
$\log P > 1.3$	19	16	-3.16	-3.15	10.74	10.77	0.08	29.30	-3.17	-3.15	10.79	10.82	0.08	29.35	-3.15	-3.16	10.71	10.79	0.05	29.37
$\log P < 1.5$	17	8	-3.14	-3.41	10.54	10.70	0.01	29.35	-3.13	-3.41	10.5S	10.72	0.02	29.36	-3.17	-3.40	10.52	10.73	-0.03	29.43
Large Amp.	17	10	-3.08	-3.29	10..58	10.69	0.04	29.30	-3.09	-3.30	10.63	10.74	0.04	29.35	-3.12	-3.30	10.56	10.71	*0.01*	29.36
Small Amp.	12	8	-2.90	-3.24	10.69	10.88	-0.01	29..56	-2.88	-3.22	10.71	10.91	-0.02	29.60	-2.90	-3.23	10.68	10.89	-0.03	29.59

Note:
Derived reddening reflect assumed LMC $E(B-V)_{\rm LMC} = 0.10$. For $E(B-V)_{\rm LMC} = 0.17$, add 0.07 to the values above.

Table 5b. Moderate I Photometry- Restrictions (0.3,0.2,4)

Subset	N_V	N_I	Unweighed Photometry						Weighted Photometry						Phase-Weighted Photometry					
			$\frac{\partial V}{\partial \log P}$	$\frac{\partial I}{\partial \log P}$	μ_V	μ_I	$E(B-V)$	μ_0	$\frac{\partial V}{\partial \log P}$	$\frac{\partial I}{\partial \log P}$	μ_V	μ_I	$E(B-V)$	μ_0	$\frac{\partial V}{\partial \log P}$	$\frac{\partial I}{\partial \log P}$	μ_V	μ_I	$E(B-V)$	μ_0
All	29	23	-2.82	-3.09	10.62	10.75	0.02	29.38	-2.82	-3.09	10.66	10.80	0.02	29.44	-2.85	-3.08	10.61	10.77	0.01	29.42
Both VI	23	23	-2.90	-3.09	10.64	10.75	0.04	29.36	-2.89	-3.09	10.68	10.80	0.03	29.42	-2.89	-3.08	10.62	10.77	0.01	29.42
Chips 2,3,4	25	21	-3.11	-3.22	10.67	10.74	0.06	29.31	-3.11	-3.21	10.71	10.79	0.05	29.37	-3.12	-3.21	10.64	10.7.5	0.04	29.36
Chips 1,3,4	22	17	-2.85	-3.16	10.62	10.72	0.04	29.32	-2.86	-3.16	10.65	10.77	0.03	29.39	-2.S8	-3.14	10.60	10.73	0.02	29.36
Chips 1,2,4	22	18	-2.76	-3.10	10.62	10.83	-0.03	29.53	-2.76	-3.09	10.66	10.88	-0.03	29.59	-2.79	-3.10	10.60	10.84	-0.04	29.57
Chips 1,2,3	18	13	-2.85	-3.12	10.57	10.71	0.02	29.35	-2.85	-3.15	10.62	10.76	0.02	29.40	-2.90	-3.13	10.56	10.74	-0.01	29.41
Chip 4	11	10	-3.13	-3.27	10.70	10.80	0.04	29.40	-3.14	-3.24	10.73	10.8.5	0.03	29.47	-3.12	-3.26	10.67	10.80	0.02	29.43
Chip 2,3	14	11	-3.24	-3.27	10.66	10.69	0.08	29.22	-3.24	-3.28	10.71	10.74	0.08	29.27	-3.26	-3.27	10.63	10.71	0.05	29.29
$\log P > 1.3$	19	16	-3.16	-3.17	10.74	10.79	0.07	29.34	-3.17	-3.17	10.79	10.84	0.07	29.39	-3.15	-3.18	10.71	10.81	0.04	29.41
log P <1.5	17	13	-3.14	-3.39	10.54	10.69	0.01	29.34	-3.13	-3.40	10.58	10.72	0.02	29.36	-3.17	-3.37	10.52	10.70	-0.01	29.37
Large Amp.	17	13	-3.08	-3.29	10.58	10.69	0.04	29.30	-3.09	-3.30	10.63	10.74	0.04	29.35	-3.12	-3.29	10.56	10.69	0.02	29.32
Small Amp.	12	10	-2.90	-3.17	10.69	10.84	0.01	29.49	-2.88	-3.16	10.71	10.89	0.00	29.54	-2.90	-3.16	10.68	10.86	-0.01	29.53

Note:
Derived reddening reflect assumed LMC $E(B-V)_{\rm LMC} = 0.10$. For $E(B-V)_{\rm LMC} = 0.17$, add 0.07 to the values above.

Table 5. — Continued

Table 5c. Weak I Photometry Restrictions (0.4,0.4,1)

Subset	N_V	N_I	Unweighted Photometry						Weighted photometry						Phase-Weighted Photometry					
			$\frac{\partial V}{\partial \log P}$	$\frac{\partial I}{\partial \log P}$	μ_V	μ_I	$E(B-V)$	μ_0	$\frac{\partial V}{\partial \log P}$	$\frac{\partial I}{\partial \log P}$	μ_V	μ_I	$E(B-V)$	μ_0	$\frac{\partial V}{\partial \log P}$	$\frac{\partial I}{\partial \log P}$	μ_V	μ_I	$E(B-V)$	μ_0
All	29	2S	-2.92	-2.92	10.62	10.72	0.04	29.32	-2.82	-2.9S	10.66	10.77	0.04	29.3S	-2.85	-2.92	10.61	10.72	0.04	29.33
Both *VI*	28	2s	-2.7s	-2.92	10.62	10.'72	0.04	29.32	-2.78	-2.98	10.66	10.77	0.04	29.38	-2.80	-2.92	10.59	10.72	0.02	29.35
Chips 2,3,4	25	24	-3.11	-3.12	10.67	10.73	0.06	29.29	-3.11	-3.19	10.71	10.79	0.0.5	29.37	-3.12	-3.29	10.64	10.73	0.05	29.32
Chips 1,3,4	22	21	-2.s5	-3.06	10.62	10.66	0.0S	29.20	-2.86	-3.12	10.6.5	10.72	0.06	29.29	-2.SS	-3.0.5	10.60	10.67	0.06	29.24
Chips 1,2,4	22	22	-2.76	-2.92	10.62	10.77	0.01	29.42	-2.76	-2.9S	10.66	10.83	0.00	29.49	-2.79	-2.93	10.60	10.78	-0.01	29.4.5
Chips 1,2,3	18	17	-2.85	-2.94	10.57	10.69	0.03	29.31	-2.85	-2.95	10.62	10.72	0.04	29.32	-2.90	-2.95	10..56	10.70	0.02	29.34
chip 4	11	11	-3.13	-3.27	10.70	10.74	0.0S	29.2S	-3.14	-3.32	10.73	10.83	0.04	29.43	-3.12	-3.25	10.67	10.74	0.06	29.31
Chip 2,3	14	13	-3.24	-3.20	10.66	10.72	0.06	29.28	-3.24	-3.21	10.71	10.76	0.07	29.31	-3.26	-3.20	10.63	10.72	0.05	29.31
$\log P$ >1.3	19	19	-3.16	-3.13	10.74	10.78	0.08	29.32	-3.17	-3.13	10.79	10.82	0.0S	29.35	-3.15	-3.14	10.71	10.79	0.05	29.37
$\log P$ <1.5	17	16	-3.14	-3.2S	10..54	10.63	0.05	29.22	-3.13	-3.34	10.5S	10.6S	0.04	29.2S	-3.17	-3.25	10..52	10.65	0.02	29.2S
Large Amp.	17	16	-3.08	-3.14	10.58	10.68	0.04	29.28	-3.09	-3.24	10.63	10.7.5	0.03	29.37	-3.12	-3.15	10.56	10.68	0.03	29.30
Small Amp.	12	12	-2.90	-3.04	10.69	10.78	0.05	29.37	-2.88	-3.02	10.71	10.81	0.04	29.40	-2.90	-3.03	10.68	10.79	0.04	29.40

Note:
Derived reddening reflect assumed LMC $E(B-V)_{LMc} = 0.10$. For $E(B-V)_{LMc} = 0.17$, add 0.07 to the values above.

Table (i. ErrorBudget **for the True** Distance Modulus to **M101**

Error (mag)	Source
±0.05	Errors in ALLFRAME photometry; PSF uncertainty
±0.03	Extinction and transformation errors
±0.05	Calibration of ALLFRAME zero-point
±0.05	Error in mean of the M101 PL relation
±0.10	Uncertainty in LMC + M101 absorption
±0.05	Error in mean of the LMC PL relation
±0.10	Uncertainty in LMC true distance modulus
±0.03	Uncertainty due to metallicity
±0.18	Total Error in Ml 01 true distance modulus

Table 7. Comparison of Selected Distances to **M101**

Method	Distance Modulus	Distance (Mpc)	Reference
Group Membership	28.71	5.52	de Vaucouleurs (1973)
Group Membership	29.30 ± 0.3	7.24	Sandage & Tarnmann (1974)
Group Membership	29.08 ± 0.3	6.54	Sandage & Tammann (1976)
Revision of Above	28.56	5.15	Jaakkola & Le Denmat (1976)
Brightest Stars	29.2	&92	Sandage (1983)
B-Band Tully-Fisher	28.4	4.79	Bottinelli (1985)
R-Band Cepheids (2)	29.5	7.94	Cook et al (1986)
BRI-Band Tully-Fisher	29.2 ± 0.5	6.92	Pierce (1994)
EPM (SN 1970G)	29.35	$7.4^{+1.0}_{-1.5}$	Eastman et al (1994)
VI-Band Cepheids	29.40 ± 0.18	7.59	This Paper

Note: Cook et al (1986) value corrected for LMC distance modulus and reddening.

Appendix A. Calibration

A.1 Calibration Using the Medium-Deep Survey WFC 1 Zero-Points

Phillips *et al.* (1994) provided accurate zero-points and flat-field corrections for WFC 1 photometry, adding that relative photometry '(approaching 1% -270 is achievable with the WFC 1." While our dataset involved large relative rotations and required a single ALLFRAME reduction on the full set of CCD images, the photometry solution could still be analyzed in four distinct sets, based on the natural quadrants of the reference exposure (chosen by us to be the first exposure of the first epoch). For ALLFRAME photometry registered to the reference (first) exposure,

$$\mathrm{F555W} = \mathrm{F555W}_{\mathrm{ALLFRAME}} + \mathrm{offset},$$

where the components of the offset, for example exposure time correction (1900 seconds), photometric zero-point correction, aperture correction, and so forth, are listed in Table A 1. The ALLFRAME magnitudes arc defined as

$$m_{\mathrm{ALLFRAME}} \equiv -2.5 \log \mathrm{DN} + 25.0,$$

so the offsets must include the exposure time, intrinsic photometric zero-point of the instrument, removal of the ALLFRAME photometric zero-point (25 mag $\equiv$ 1 DN), and an aperture correction to convert the ALLFRAME magnitudes (with an effective aperture radius equal to the I) AOPHOT PSF radius) to total magnitudes (from a large enough aperture to effectively include *all* counts from a star). This aperture correction is small when the ALLFRAME point-spread function is a good fit to the observed point-spread function. If the actual PSF contains high signal features missing from the profile-fitting (when the DAOPHOT PSF does not match the observed point-spread function), then that "missing" light must be incorporated into this aperture correction. When the DAOPHOT PSF matches the observed stellar profiles well, then the largest component of this aperture

correction is the light unaccounted for outside the PSF radius. The PSF radius, or effective aperture of the photometry, was $2''.5$ so these offsets include an aperture correction of only -0.02 mag (the addition of light is a magnitude subtraction), as derived from the encircled energy curve shown in Figure 4.5 of the Wide Field and Planetary Camera Instrument Handbook (MacKenty *et al. 1992).*

There was no evidence of contamination features ("measles") in either the F555W or F785LP data. Figure 11,1(a) of the WF/PC 1 instrument Handbook suggests a small correction ($\sim$ –0.05 mag) based on the number of days since decontamination (August 1992) but we opted not to include this small effect because the typical scatter between epochs was much larger (typical *rms* scatter was 0.08 mag with the worst cases as large as 0.20 mag) than any contamination corrections. Epoch-to-epoch repeatability of the photometry was limited to these uncertainties because of the large relative rotations,

The calibration offsets derived from the additive terms discussed above, are listed under the column titled "MDS" in Table A3.

A.2 Calibration using WFPC 2 Observations and Zero-Points

The inclusion of WFPC 2 observations in the dataset also naturally provides a calibration of our photometric zero-point. While the WFPC 2 Status Report (Holtzman *et al.* 1 994) contains a preliminary calibration for the instrument, the uncertainty in using a calibration based on the current zero-points is quite small. Gilliland (1994) gives zero-points derived from comparison of WFPC 2 photometry with ground-based observations of M67. The zero-points he derived are consistent with the status report zero-points for F555W and F814W. The ground-based calibration for Ml 00 (Freedman *et al.* 1994) also confirms the WFPC 2 status report zero-points to ± 0.02 msg. Those zero-points were derived for the

higher temperature setting (–76°C), appropriate for our F555W and I?814W exposures (they were taken before the April 1994 decrease in operating temperature).

The WFPC 2 ALLFRAME reduction included a photometric zero-point of 25 mag (≡ 1 DN) and integrated magnitudes out to the PSF radius of 1″.0. We therefore treated the ALLFRAME magnitudes as equivalent to 1″.0 radius aperture photometry, with a zero-point of 25 mag ≡ 1 DN. To correct the ALLFRAME magnitudes to magnitudes derived from a large aperture radius (i.e. containing total counts), we needed to add an aperture correction:

$$-2.5 \log \int_{r=0}^{r=r_{\rm PSF}} \frac{d{\rm DN}}{dr} dr + \text{aperture correction} = -2,5 \log \lim_{x\to\infty} \int_{r=0}^{r=x} \frac{d{\rm DN}}{dr} dr .$$

Growth curve analysis on several isolated stars in a median image of the four 1200 sec F814W exposures was used to derive this aperture correction. Using DA OGROW (Stetson 1990) to extrapolate the model growth-curves, fit to those obtained in the median images, we found that aperture corrections of –0.036 40.001 mag and –0.031 ± 0.001 mag were derived from the PC and W F chips, respective y, to convert our effective 1 ″.0 radius aperture magnitudes to 2″.0 radius aperture magnitudes. The factor of ∼ 2.2x magnification of the PC image with respect to the WF images was taken into consideration to insure consistent aperture sizes for the PC and WF photometry.

DAOG ROW growth-curve analysis on grids of artificial stars for each chip in F555W, 1“814W, and F439W yielded aperture corrections of –0.02 msg. The encircled energy curves listed in the status report provided some confirmation of these aperture corrections, but could not be used to derive appropriate aperture corrections because we could not assume that our preliminarily defined PSF was perfectly well known, or was a perfect match to either the observations that comprised the status report encircled energy curves, or even *our* observations.

The $1'' \rightarrow 2''$ radius aperture correction that we used were the ones derived directly from the median I frames. In calibrating the total ALLFRAME magnitudes ($-2.5 \log$ DN) now valid for a $2''.0$ radius aperture, we used additive terms analogous to the WFC 1 calibration of Section Al. Calibration of the WFPC 2 F555W magnitudes included the additive terms shown in Table A2. Since the status report photometric zero-points are listed for the gain=14 setting, we needed to add 0.753 mag to convert to gain=7. For the WF chips, the appropriate aperture correction (given above) was applied. For the F814W, and F439W observations, the status report zero-points of 20.915 mag, and 20.117 mag ($\equiv 1$ DN/s at gain= 14) were used; the remainder of the additive terms did not change.

After adding the components listed in Table A2, this total offset, when added to the WFPC 2 F555W, F814W, and F439W ALLFRAME magnitudes calibrated the photometry to F555W, F814W, and F439W total apparent magnitudes in the WFPC 2 filter system. We next needed to transform the WFPC 2 photometry to the WFPC 1 system, for comparison to the WFC 1 ALLFRAME photometry. The WFPC 2 Status Report (Holtzman *et* al 1 994) lists the transformation to WFPC 1 system.

The status report photometric transformations were applied to *all* stars whose reported WFPC 2 ALLFRAME photometry errors were less than 0.3 magnitudes, to bring the F555W, F814W, and F439W magnitudes on to the WFPC1 system. The transformation colour terms were iterated for each star, starting with ($F555W_{WFPC2} - F814W_{WFPC2}$), or ($F439W_{WFPC2} - F555W_{WFPC2}$), as the initial approximations to the standard WFPC 1 colours. The F555W, and F814W colour terms were small, so only two or three iterations were required before the resulting WFPC 1 F555W and F814W magnitudes converged (to 0.001mag). The larger F439W colour term typically required three or four iterations for convergence.

Once *all* of these WFPC 2 stars were placed on the WFPC 1 system, wc made direct star-to-star comparisons for selected secondary standards, bet ween the WFC 1 A LLFRAME photometry and the calibrated WFPC 2 photometry. Bright, isolated stars were picked from the WFPC 2 exposures, from the list of calibrated photometry, for the WFC 1 ALLFRAME calibrating offset determination. Since one WFPC 2 F555W exposure was being used to calibrate the mean WFC 1 ALLFRAME photometry, each secondary stand ard was checked for variability in the WFC 1 observations.

For F555W, wc used 18 secondary standards in the PC chip, plus 25, 32, and 27 secondary standards in the three WF chips. The difference in the *mean* offsets for the MDS-corrected and uncorrected WFC 1 photometry was small ($\lesssim$ 0.01 mag). The mean of the four chip offsets is identical to the mean offset obtained with the MDS WFC 1 zero-points. Therefore, by using the mean calibrating offset and adding the chip-to-chip deviations from Phillips *et al.* (1994), wc found results identical to those obtained in Section A.1, as shown in Table A3 in the column titled "Mean WFPC 2". The errors listed were estimated by summing the reported MDS zero-point uncertainties in quadrature with the standard error of the mean WFPC 2-based offsets.

Inclusion of a 0,02 magnitude ramp as suggested by the WFPC 2 Status Report (correction = –0.02 mag x $y/800$), did reduce the scatter in the WFPC 2-based calibration of the WFC 1 data. This ad hoc representation of the charge transfer effect was useful in testing the robustness of the calibration. The mean zero-point, however, remained unaffected by <0,01 msg.

The WFC 1 F785LP ALLFRAME magnitudes were converted to the same system as the WFPC 2 1"814 W A LLFRAME magnitudes, using simple zero-point offsets based on differences in exposure time and instrument zero-points, We used the difference in

the WFC 1 F785LP zero-points from Phillips *et al.* (1994) and the WFPC 2 F814W zero-points from Holtzman *et al.* (1994), The error incurred by the assumption of this zero-point difference is negligible for Cepheids whose I photometry is principally derived from the F814 W observations. Since the status report 1"814 W colour term is small, the assumption insures no incursion of systematic colour effects in placing the WFC 1 F785LP magnitudes on to the WFPC1 F814W ($\approx$WFPC 2 17814W) magnitude system. The effects of this assumption are seen in the derivation of mean I photometry, discussed in Section 6, The large, mean colour term applicable for Cepheids ($\sim$ 0.11. mag, see Harris *et al.* 1991), was added to the Cepheid photometry *before* determination of mean I photometry. The full transformation of F785LP to F814W was easily derived:

$$\mathrm{F814W} = \mathrm{F785LP} + 0.1\ 124(\mathrm{V} - I) + 0.0072(V - I)^2$$

Since wc used a mean Cepheid colour, the largest incurred error in the transformation should have been about ± 0.07 mag for the single F785LP epoch of an individual Cepheid. In most cases, this error was absorbed by the F814 W data. No systematic effect is be expected in the resulting I band PI, relations.

The calibrating offsets for F814W were computed in the same manner as for F555W (additive terms for exposure time, gain setting, zero-points, image multiplication, and aperture correction), and arc listed in 'J'able A2.

The single F439W phase-point was calibrated in the same fashion as the F814 W observations. The appropriate photometric zero-point, as taken from the status report, was used (20. 117 mag $\equiv$ 1 I) N/s at gain=1 4), The aperture corrections, to convert from 1" to *2"* radius aperture magnitudes, were derived as described above.

A.3 Calibration using **Ground-Based** Secondary Standards

Our ground-based calibration data was taken at the KPNO 4m, using the Mould Cousins $BVRI$ filter set at prime focus. Seeing was about 1" - 1".2(FWHM) (see Cook *et al 1986).* These observations form the basis of an extra consistency check on the previously discussed methods. Comparison of the ground-based photometry with the HST photometry was not straightforward because crowding in the data was a severe problem, Only $\lesssim$ 10 individually resolved stars (single stars separated by roughly 12 pixels in the HST observations) were found. We therefore used the DAOPHOT/ALLSTAR package to maximize the number of usable secondary standards by taking bright, somewhat isolated stars in the HST observations, whose neighbours were unresolved from the ground. These groups were co-added to form secondary standards. If the two brightest stars in a group were separated by less than the critical separation for the resolution of two stars, $0.375 \times \mathrm{FWHM}_{\mathrm{ground}} (\approx 4.5$WFC1 pixels), then the counts from those two stars would be summed directly. Counts from stars with distances from the local "center-of-light" greater than this critical separation would' be down-weighted by a Gaussian-like kernel, with FWHM equal to the ground-based seeing (FWHM = 1 2 WFC 1 pixels, or $\sigma = \mathrm{FWHM}/2.35$). In essence, a group magnitude was defined as

$$m_{group} = -2.5 \log \sum_{i=1}^{N_{group}} 10^{0.4 m_i} \times \begin{cases} 1, & \text{if } |r| \leq 4.5 \text{ pixels;} \\ \exp\left[-\frac{(|r|-4.5)^2}{2\sigma^2} \right], & \text{if } |r| > 4.5 \text{ pixels.} \end{cases}$$

'J'bus, the HST observations were artificially convolved with a modified ground-based seeing profile (*after* determining the relative photometry for the stars in each "group"). This Gaussian-1ike kernel's fiat-top was necessary to conserve flux for unresolved pairs. The boundary between the flat-top and Gaussian wings was not smooth, but had the same limit from either side of the boundary. A potential difficulty arises because unresolved, undetected stars are smeared and artificially increase the sky level as measured from the ground-based data. Wc tested for this effect, but it proved to be small (± 0.05 mag to ± 0.1

mag) for individual secondary standards compared to the *rms* scatter (0.1 to 0.5 mag) in the ground-*HST* offsets. The typical magnitude uncertainties in the ground based photometry ranged from 0.1 mag at *V, I* = 20 to 0.3 mag at *V, I* = *24.*

The calibration derived from the ground-based KPNO data for F555W arc shown in Table A3. The offsets, and finder chart positions for individual *V* and *I* secondary standards are listed in Tables A4 and A5, along with ground-based *V* and *I* magnitudes and group sizes. The (F555W – *V)* colour term has been ignored in the determination of these offsets. This colour term, as determined by Harris *et al.* (1991), varies between zero and +0.05 mag for $0 \leq (B - V) \leq 1$.

For example, the mean $\langle B - V \rangle$ for Cepheids is 0.66, leading to an error of 0.04 mag in *V* if the mean $\langle B - V \rangle = 0$ for the secondary standards, However, the mean $\langle V - I \rangle$ of our ground-based secondary standards is $\langle V - I \rangle \approx 0.45$, corresponding to approximately $0.2 \lesssim \langle B - V \rangle \lesssim 0.3$. Thus, the additional colour term is only $\sim$ 0.02 mag, in the mean, for for stars with similar colours to Cepheids. Given the intrinsic distribution of Cepheid (*B* --V) colours, the systematic effect is negligible, Using the mean of the four chip ground-based offsets, with the chip-to-chip deviations from Phillips *et al* (1994), we derived the "Mean Ground" offsets shown in Table A3. These reflect a 0.05 mag systematic offset, in the mean, between the ground-based and 11ST-derived offsets.

For ground-based *I*, the complete Harris transformation

$$\mathrm{F814W} = I + 0.0575(V - I) - 0.0271(V - I)^2$$

was used since wc have ground-based colour information. The ground-based *I* magnitudes were first converted to F814W before direct comparison with the ALLFRAME secondary standards, processed in the same fashion as for F555W. 'The ground-based F814W ALL-FRAME calibrating offsets arc also shown in Table A3. Using the mean of the four chip

ground-based *I* offsets, with the chip-to-chip deviations from Phillips *et al* (1994), we derived the "Mean Ground" offsets shown in TaMe A3.

The *individual* CCD offsets show larger differences than expected if the random errors (listed as the offset uncertainties) dominated. A possible source of systematic difference between the ground-based and instrument calibrations may have been incomplete group membership star lists. The WFPC 2 AI, LFRAME reduction used the star list generated by the WFC 1 ALLFRAME reduction. Most of the WFC 1 observations were made in F555W, so the star list reflects colour selection, as well as poor resolution. Incompleteness in the F81 4 W data would result in improper assignment of combined ALLFRAME magnitudes to the secondary standards; these magnitudes would artificially be too faint and lead to ground-based calibrating offsets that are too small. Incompleteness at the level of several percent could easily account for this systematically missing component of ALLFRAME group fluxes. Since the list will have some arbitrary magnitude selection effects, the fainter stellar population would have been more incomplete. For example, if 50% of the faint half of the population has been left undetected, then wc would be missing, if stars were randomly distributed by luminosity in groups, about 25% of the flux in the combined A I,] FRAME secondary standards. If 20% of the faintest 20% (in a list of stars that wc *should have* detected) were left undetected, then our A LLFRAME secondary standard intensities would be deficient by 4%. in conclusion, because our WFPC 2 F814W star lists were generated by using WFC 1 F555W frames, the ground-based calibration is likely to be systematically too low.

The final comparison of the different sets of derived ALLFRAME calibrating offsets and uncertainties is shown in Table A3. Note the consistency between the three independent calibration methods, despite possible incompleteness problems.

In citing the excellent agreement between the Phillips *et al.* (1994) and WFPC 2-based calibrations, we proceeded using the Phillips *et al. (1994)* F555W calibration (identical, in the mean, to the WFPC 2-based calibration) and the WFPC 2 Status Report F814W calibration.

A.4 WFPC 2 Photometric Zero-Points

Comparison of the calibrations from the MDS photometric zero-points, the WFPC 2 secondary standards, and the ground-based secondary standards, allows us to derive an independent calibration of the WFPC 2 instrument. The agreement between the different calibrations is quite good, as evident by the mean zero-points for the three systems. Using the comparison of the MDS (Phillips *et al 1994)* and WFPC 2 calibrating offsets, and the comparison of the ground-based and WFPC 2 calibrating offsets, we derived new F555W and 1~814W zero-points for the WFPC 2 instrument,

in F555W, Holtzman *et al.* (1 994) reported a transformation zero-point of 21 .718+ 0.012 mag (Note: these reported WFPC 2 photometric zero-points are equivalent to 1 I) N/s at gain=14, as in the status report). Using the WFC 1 photometry to calibrate the WFPC 2 F555W observations, the unweighed and weighted mean WFPC 2 zero-points become 21,721 ± 0.027 mag and 21 .712+ 0,013 mag (from all 4 CCD's). Using the ground-based *V* observations, the unweighted and weighted mean WFPC 2 zero-points become 21.68 ± 0.05 mag and 21.6730.04 msg.

Holtzman *et al.* (1994) reported a transformation zero-point of 20.915 ± 0.012 mag in F814 W, The ground-based *I* observations yielded a mean photometric zero-point of 20.88 ± 0.06 mag in F814W. A weighted mean changes the zero-point to 20.854:0.08 mag.

The F555W and F814 W WFPC 2 instrument calibration results are tabulated in Table 2 in Section 5.

Table A4(a). Ground-Based V Secondary Standards For Reference Epoch CCD #1

x^1	y^1	v	σ_V	$V - \mathrm{F555W}_{\mathrm{ALLFRAME}}{}^2$	N_{group}
40.76	220.06	22.42	0.14	8.17	7
34.32	321.22	22.21	0.13	7.39	7
67.06	85.54	22.80	0.13	7.66	12
68.18	100.06	21.38	0.15	7.62	7
49.05	306.76	23.03	0.21	8.15	7
55.13	268.27	22.72	0.07	7.03	4
86.87	229.24	21.85	0.14	8.37	15
112.25	131.83	20.69	0.10	7.25	4
140.57	105.69	22.45	0.02	7.38	5
152.81	142.32	22.08	0.05	6.92	6
144.92	234.51	22.20	0.11	7.09	7
168.64	66.97	22.59	0.25	7.83	9
139.83	344.20	23.70	0.01	7.06	4
181.61	72.68	22.65	0.00	7.76	6
161.97	235.77	22.22	0.09	7.60	11
194.13	80.71	23.33	0.26	7.90	5
178.70	247.96	22.24	0.03	7.80	11
186.53	221.08	21.68	0.02	7.28	6
186.20	270.98	22.94	0.10	8.07	10
202.90	262.36	22.53	0.08	7.45	6
230.93	122.81	23.27	0.28	7.61	4
211.85	283.55	22.27	0.06	7.33	6
241.90	158.39	22.73	0.15	7.64	6
228.68	307.03	23.35	0.10	7.21	3
243.96	255.79	22.63	0.13	8.33	9
266.57	90.81	22.34	0.08	7.66	10
243.86	283.63	22.70	0.04	7.40	7
261.70	142.73	23.39	0.06	7.61	5
239.60	327.21	21.38	0.03	7.43	5
274.34	69.49	22.77	0.15	7.16	4
268.63	340.86	22.67	0.11	7.89	8
284.75	240.00	23.24	0.27	7.53	3
302.07	247.85	24.61	0.17	8.40	2
292.48	349.09	22.95	0.07	7.47	5
304.47	306.71	22.91	0.16	7.86	6
320.04	221.39	22.83	0.12	7.48	4
325.37	195.74	23.24	0.18	7.45	4
332.52	208.23	22.96	0.14	7.94	5
337.58	228.28	22.62	0.09	7.80	5
338.84	231.38	23.20	0.25	8.41	5
357.29	118.62	22.57	0.03	7.43	2
353.08	154.82	22.02	0.04	8.47	12
352.75	183.84	23.18	0.22	7.69	5
384.94	186.14	22.39	0.08	7.36	5
367.93	345.98	22.53	0.06	7.45	5

Note:
[1] Positions listed for finder chart image 2
[2] An additional $\sim$ ().02 mag is required for stars with similar colours to Cepheids (Harris *et al.* 1991).

Table Al. Calibration of WFC 1 ALLFRAME Photometry

Additive Term	Value	Correction (mag)
ALLFRAME zero-point[1]		–25.00
Exposure Time[2]	-t-2.5 log 1900	+8.20
MDS zero-point[3]		+22.90
Image multiplication[4]	+2.5 log 4	+1.50
Aperture correction		–0.02

Notes:
[1] Zero-point equivalent to magnitude of 1 DN
[2] F555 W Photometry normalized to first epoch (1900 s).
[3] Zero-point (≡ 1 DN/s) shown for WFC Chip 1 (F555W).
[4] Images initially multiplied by four and stored as short integers

Table A2. Calibration of WFPC 2 ALLFRAME Photometry

Additive Term	Value	Correction (mag)
ALLFRAME zero-point[1]		–25.000
Exposure Time[2]	+2.5 log 1200	+7.698
Status Report zero-point[3]		+21.718
Instrument gain[4]	+2.5 log 2	+0.753
Image multiplication	+2.5 log 4	+1.505
Aperture correction[6]		–0.036

Notes:
[1] Zero-point, equivalent to magnitude of 1 DN
[2] F555W exposure time was 1200 s.
[3] Zero-point (≡ 1 I) N/s at gain=14) shown for F555W. Usc 20.915 mag, 20.117 mag for F814W, F439W.
[4] Observations made with gain=7.
[5] Images initially multiplied by four and stored as short integers
[6] Aperture correction shown for PC Chip. Usc -0.031 mag for WF Chips.

Table A3. Calibration of ALLFRAME Photometry in M101

WFC 1 F555W ALLFRAME Calibrating Offsets

	MDS	WFPC 2	Mean WFPC 2	Ground	Mean Ground
Chip 1	7.58 ± 0,02	7.648 ± 0.029	7.58410.02	7.64 ± 0.06	7.54 ± 0,05
Chip 2	7.72 ± 0.04	7.698 ± 0.035	7.723:0.04	7.69 ± 0.05	7.684:0.06
Chip 3	7,72 ± 0.06	7.659 ± 0.029	7.724:0.06	7.55 ± 0.03	7.68 ± 0.08
Chip 4	7.64 ± 0.04	7.645 ± 0.035	7.6430.04	7.58 ± 0.06	7.60 ± 0.06

Notes:
Valid for F555W photometry normalized to reference exposure (1900 s).
"Mean" implies mean of the 4 Chip zero-points with chip-to-chip deviations from Phillips et al (1994).
Ground-based zero-points were derived from *V*-F555W comparison.
For the Cepheids, there is an additonal mean Cepheid colour term of 0.02 msg.

WFPC *2* F814W ALLFRAME Calibrating Offsets

	Status Report	Ground	Mean Ground
Chip 1	5.84 ± 0.01	'5.66 3:0.07	5.84 ± 0.08
Chip 2	5.84 ± 0.01	5,75 ± 0.05	5.8420.08
Chip 3	5.84 ± 0.01	6.03 ± 0.04	5.84 ± 0.08
Chip 4	5.84 ± 0.01	5.93 ± 0.05	5.844:0.08

Notes:
Valid for F814W photometry normalized to reference exposure (1200 s).
Chip-to-chip zero-point deviations have been removed by flat-fielding (Grillmair 1994).
Ground-based zero-points were derived after *I* transformed to F814W. (Harris *et al.* 1991)

Table A4(b). Ground-Based V Secondary Standards For Reference Epoch CCD #2

x^1	y^1	v	σ_V	$V - \mathrm{F555W}_{\mathrm{ALLFRAME}}{}^2$	N_{group}
234.24	783.48	21.17	0.03	**7.67**	9
743.46	714.12	23.22	0.13	**7.39**	3
525.17	668.53	22.90	0.04	**7.32**	3
233.48	630.23	22.59	0.17	**7.10**	5
504.89	655.15	23.50	0.17	**8.35**	3
497.38	632.96	23.24	0.01	**7.31**	1
226.50	**511.12**	23.30	0.02	**7.48**	2
91.27	488.72	22.86	0.17	**7.37**	4
439.04	524.82	24.33	**0.16**	**7.78**	3
697.56	544.51	23.01	0.05	**8.00**	2
203.69	447.32	23.34	0.18	**7.86**	5
430.46	437.00	22.82	0.07	**8.37**	4
561.53	440.16	23.61	0.13	**7.46**	5
401.98	409.66	22.83	0.01	**7.55**	2
295.98	394.06	22.51	0.21	**8.21**	8
343.78	377.35	22.20	0.04	**7.50**	5
280.44	351.12	22.34	0.06	**7.87**	7
158.41	329.16	21.94	0.04	**7.86**	8
193.46	310.01	23.36	0.14	**7.41**	6
233.99	289.21	22.63	0.03	**7.78**	5
133.48	255.69	22.89	0.14	**7.56**	7
191.86	251.24	22.54	0.21	**8.01**	11
365.61	239.29	23.02	0.28	**7.86**	2
138.07	201.90	22.76	0.02	**7.76**	4
37.67	188.07	22.40	0.18	**7.64**	6
147.90	**140.58**	23.08	0.01	**7.89**	4
31.30	122.03	22.63	0.17	**7.68**	5
397.67	163.32	22.13	0.02	**7.50**	1
125.33	116.92	22.70	0.20	**7.70**	6
675.15	182.73	23.45	0.03	**7.46**	2
495.78	148.13	23.66	0.22	**7.42**	3
144.82	77.83	22.75	0.29	7.63	7
29.15	59.90	21.74	0.12	7.57	5
191.61	80.02	23.78	0.17	8.07	5
49.15	44.28	22.95	0.03	7.76	5

Note:
[1] Positions listed for finder chart image 3
[2] An additional ~ 0.02 mag is required for stars with similar colours to Cepheids (Harris *et al.* **1991),**

Table A4(c). Ground-Based V Secondary Standards For Reference Epoch CCD #3

x^1	y^1	v	σ_V	V - F555W$_{ALLFRAME}$[2]	N_{group}
759.11	667.43	23.78	0.18	7.40	2
774.X3	452.99	22.42	0.09	7.65	6
739.68	604.07	23.05	0.05	7.47	2
738.45	442.45	21.60	0.05	7.60	4
773.88	138.53	22.90	0.12	7.16	2
714.45	597.87	23.01	0.03	7.37	4
737.10	400.56	23.00	0.13	7.70	3
721.51	455.41	23.17	0.14	8.12	6
701.54	430.68	22.58	0.21	7.47	5
688.11	501.60	21.17	0.07	7.97	8
714.71	233.99	23.69	0.22	7.27	3
687.30	431.41	21.30	0.14	7.54	5
681.31	380.42	22.37	0.20	7.99	10
647.12	580.39	24.10	0.03	7.09	1
677.41	316.55	22.84	0.10	7.56	4
638.00	515.80	21.44	0.15	7.42	3
657.37	241.32	22.98	0.12	8.12	3
641.36	378.05	22.65	0.08	7.58	3
624.27	517.58	23.36	0.23	7.41	4
618.87	496.49	22.57	0.09	7.54	3
616.02	473.33	23.22	0.09	7.59	5
636.38	287.20	24.17	0.07	7.52	2
618.93	406.95	23.51	0.15	7.75	3
616.90	307.23	22.02	0.02	7.42	3
593.28	405.76	23.03	0.25	7.85	5
583.56	281.97	22.93	0.15	7.43	3
564.63	404.45	23.34	0.12	8.00	3
601.05	88.68	22.52	0.10	7.49	1
560.05	378.89	21.49	0.06	7.47	3
582.88	186.87	23.08	0.23	7.86	4
471.92	729.27	23.47	0.08	7.25	2
512.69	283.57	23.29	0.18	7.77	7
473.07	531.72	22.57	0.14	7.42	4
487.65	345.93	23.08	0.06	7.68	5

Note:
[1]Positions listed for finder chart image 4
[2]An additional ~ 0.02 mag is required for stars with similar colours to Cepheids (Harris *et al.* 1991).

Table A4 (c). — Continued

x^1	y^1	v	σ_V	$V - \mathrm{F555W}_{\mathrm{ALLFRAME}}{}^2$	N_{group}
495.61	273.56	23.18	0.21	7.88	4
469.38	193.42	22.83	0.04	7.65	7
424.18	495.83	22.70	0.04	7.36	4
445.24	245.86	23.77	0.16	7.63	2
409.71	148.02	23.37	0.06	7.31	2
399.02	176.34	22.13	0.16	7.50	4
398.52	154.54	22.60	0.05	7.46	4
369.03	294.27	22.56	0.10	7.46	5
353.07	415.25	23.13	0.13	7.67	4
345.85	407.66	22.45	0.04	7.53	5
354.03	210.81	23.40	0.03	8.07	3
334.70	341.42	22.25	0.08	7.76	7
324.44	340.42	22.48	0.05	8.31	10
330.11	201.74	22.64	0.14	7.41	6
310.87	265.07	21.74	0.06	7.36	2
268.77	587.53	22.79	0.03	7.05	2
295.03	343.32	22.38	0.03	7.41	6
301.80	288.62	22.27	0.15	7.34	4
267.33	377.04	22.34	0.08	7.28	4
244.55	297.12	22,65	0.21	7.39	5
244.48	278.95	22.76	0.01	7.37	3
227.16	399.90	22.85	0.06	7.06	5
213.97	331.76	23.34	0.25	7.54	4
242.38	79.79	22.43	0.16	7.70	9
216.25	164.02	23.76	0.13	7.84	7
183.45	128.27	23.48	0.18	7.68	5
161.93	250.53	22.66	0.01	7.27	4
137.71	445.83	23.11	0.11	7.27	1
152.55	193.44	23.01	0.17	7.68	7
105.00	479.13	22.83	0.03	7.51	5
137.64	136.81	23.55	0.07	7.83	5
72.67	399.67	22.29	0.16	7.28	4
58.15	385.99	22.45	0.15	7.27	2
63.81	259.34	22.06	0.01	7.57	6

Note:
[1] Positions listed for finder chart image 4
[2] An additional ~ 0.02 mag is required for stars with similar colours to Cepheids (Harris *et al.* 1991).

Table A4(d). Ground-Based V Secondary Standards For Reference Epoch CCD #4

x^1	y^1	V	σ_V	$V - \mathrm{F555W}_{\mathrm{ALLFRAME}}{}^2$	N_{group}
74.87	45.00	23.13	0.00	7.82	5
273.02	125.06	22.84	0.25	8.16	10
149.04	120.82	22.43	0.14	7.78	6
237.01	137.97	22.27	0.02	7.73	8
136.26	162.07	23.10	0.10	8.04	8
115.59	177.09	23.08	0.01	7.49	4
129.02	203.50	22.65	0.12	7.28	9
170.68	210.28	22.90	0.16	7.19	3
779.02	357.97	22.38	0.14	7.44	4
274.89	316.54	21.32	0.02	8.33	17
260.4.5	328.76	21.49	0.02	7.90	9
294.70	344.32	22.58	0.07	7.32	10
296.49	363.84	22.17	0.05	7.27	7
386.23	386.80	23.12	0.02	7.47	7
473.33	421.66	20.41	0.24	7.71	14
151.31	391.74	23.01	0.04	7.41	3
352.15	425.83	22.46	0.05	7.46	7
410.74	444.63	22.10	0.06	7.32	5
268.42	428.79	22.73	0.10	7.20	5
657.34	499.68	21.10	0.10	7.27	2
455.20	470.74	23.37	0.16	7.68	3
351.25	460.44	19.09	0.09	7.40	9
402.80	477.45	22.14	0.19	7.83	5
335.78	469.66	22.99	0.00	7.48	4

Note:
[1]Positions listed for finder chart image 1
[2]An additional ~ 0.02 mag is required for stars with similar colours to Cepheids (Harris *et al.* 1991).

Table A5(a). Ground-Based I^1 Secondary Standards For Reference Epoch CCD #1

x^2	y^2	F814W$_{Ground}$	σ_{F814W}	F814W$_{Ground}$ -- F814W$_{ALLFRAME}$	N_{group}
57.00	337.17	20.84	0.08	5.43	7
71.18	321.20	21.18	0.07	5.49	7
91.65	89.42	20.00	0.18	5.42	14
106.98	126.89	21.27	0.22	6.02	9
109.14	136.80	21.01	0.26	5.74	7
123.30	71.88	21.29	0.22	5.50	19
123.67	132.56	21.22	0.05	5.61	10
154.52	118.58	22.11	0.16	5.39	5
163.43	246.24	21.28	0.06	5.28	7
180.18	78.46	23.31	0.20	6.10	9
206.87	89.76	22.81	0.17	5.95	5
199.37	261.21	22.07	0.12	6.64	11
207.85	284.66	21.74	0.07	5.49	10
245.32	130.90	21.75	0.05	5.61	4
232.51	292.48	20.79	0.08	5.40	6
259.35	108.11	22.41	0.26	5.39	3
257.82	166.62	22.86	0.23	5.71	6
279.79	97.07	21.41	0.17	5.52	10
277.45	149.29	23.20	0.04	5.74	7
276.39	361.72	21.99	0.22	4.83	6
287.33	302.57	21.53	0.09	5.69	5
303.60	246.38	22.90	0.22	5.64	3
314.01	353.67	21.68	0.07	4.44	5
297.89	684.66	22.73	0.14	5.41	2
338.21	225.77	22.70	0.25	5.28	4
342.25	199.49	22.22	0.12	5.61	4
356.98	234.41	22.65	0.28	6.58	5
370.90	121.78	22.19	0.15	4.99	2
370.24	187.23	22.47	0.27	5.62	5

Note:
[1] I magnitudes transformed to F814W (Harris *et* al. (1 991).
[2] Positions listed for finder chart image 2

Table A5(b). Ground-Based I[1] Secondary Standards For Reference Epoch CCD #2

x^2	y^2	$F814W_{Ground}$	σ_{F814W}	$F814W_{Ground} - F814W_{ALLFRAME}$	N_{group}
280.01	771.11	22.24	0.20	**6.56**	9
287.81	709.47	21.13	0.20	**5.93**	18
215.01	702.97	21.29	0.22	**5.81**	5
227.89	700.59	20.45	0.10	**5.22**	10
265.98	685.39	21.38	0.10	**5.80**	11
206.21	678.41	22.20	0.10	**6.07**	7
296.11	663.26	21.64	0.07	**5.74**	5
200.96	631.99	21.53	0.17	**5.44**	6
785.20	677.17	22.02	0.12	**5.47**	3
377.32	644.38	21.81	0.05	**5.56**	5
271.64	618.47	21.53	0.04	**5.54**	5
560.90	629.78	22.05	0.19	**5.50**	4
535.43	608.30	21.96	0.12	**5.34**	1
153.90	558.83	21.64	0.12	**5.63**	1
194.44	507.93	21.34	0.13	**5.21**	4
256.96	500.36	22.43	0.25	5.69	2
292.42	477.97	22.62	0.26	**6.03**	2
732.97	508.77	21.85	0.15	**5.51**	3
231.68	436.07	23.38	0.09	**6.35**	5
263.58	425.36	23.11	0.25	**6.05**	5
101.25	395.17	22.76	0.16	**5.31**	5
691.78	433.33	22.70	0.15	**4.44**	5
328.69	397.99	20.20	0.14	**5.56**	6
323.53	378.23	21.31	0.03	**6.01**	7
106.37	352.75	22.62	0.16	**5.77**	10
369.53	360.60	20.99	0.13	**5.56**	5
223.58	345.61	21.06	0.05	5.60	5
328.34	338.59	21.82	0.12	6.39	5
303.59	338.00	22.56	0.23	6.52	7
208.79	326.94	21.66	0.17	5.63	6
98.88	317.67	21.09	0.08	5.50	4
183.69	320.59	21.79	0.17	6.53	7
215.97	300.74	23.51	0.16	5.19	6
320.25	287.07	22.04	0.09	5.67	3
255.18	277.37	22.55	0.26	5.94	5
199.08	263.28	22.99	0.20	6.36	5
583.30	285.52	21.53	0.12	6.01	5
152.41	251.46	23.18	0.28	6.96	6
242.76	234.50	22.72	0.18	6.07	11
162.28	220.56	22.16	0.18	5.63	8
82.79	198.78	22.59	0.19	5.48	2
383.87	220.43	22.09	0.14	5.72	3
54.83	185.88	22.00	0.16	5.71	6
192.31	193.43	22.81	0.13	5.95	5
305.97	197.07	21.95	0.25	6.22	7
126.59	178.79	22.01	0.13	5.50	3
177.44	168.29	22.43	0.27	5.93	8
567.50	195.80	23.07	0.26	5.92	3
286.86	167.82	22.98	0.18	5.69	6
44.92	120.51	22.53	0.12	5.83	5
412.69	144.21	22.21	0.30	5.70	1
223.41	123.78	20.76	0.08	5.26	3
690.71	150.41	22.30	0.12	5.34	2
156.18	81.01	22.16	0.14	6.03	6
58.84	42.11	23.08	0.13	5.88	5

Note:
[1] I magnitudes transformed to F814W (Harris *et al.* (1991).
[2] Positions listed for finder chart image 3

Table A5(c). Ground-Based I^1 Secondary Standards For Reference Epoch CCD #3

x^2	y^2	F814W$_{Ground}$	σ_{F814W}	F814W$_{Ground}$ − F814W$_{ALLFRAME}$	N_{group}
795.13	397.31	21.64	0.16	6.68	7
762.62	328.52	20.74	0.21	6.22	7
744.54	543.34	21.84	0.21	6.02	4
758.18	346.10	23.24	0.18	7.09	3
723.07	377.04	22.05	0.15	6.35	5
715.01	448.34	21.30	0.02	6.54	9
709.26	378.17	21.40	0.13	6.39	5
700.82	327.06	22.17	0.29	6.52	10
676.34	529.27	23.06	0.07	6.14	1
694.66	264.22	21.94	0.10	6.27	6
670.58	190.54	21.67	0.22	6.11	3
660.32	327.37	22.27	0.07	6.16	3
644.28	446.62	22.64	0.06	6.37	3
632.24	257.30	21.78	0.12	6.06	3
585.23	357.42	23.03	0.21	6.18	2
508.92	686.87	20.53	0.10	5.47	2
499.32	489.43	22.54	0.14	5.64	4
506.56	303.61	23.05	0.14	6.38	5
509.08	229.93	22.67	0.12	6.14	4
479.31	151.54	21.45	0.10	6.42	7
449.59	456.20	21.59	0.05	5.86	4
403.59	718.33	21.43	0.11	5.70	4
418.29	110.21	23.48	0.28	5.97	2
408.38	137.96	21.70	0.21	5.84	4
405.87	115.89	21.80	0.19	5.97	4
383.59	257.08	22.09	0.15	6.14	5
366.38	371.65	22.31	0.19	5.93	5
355.26	198.75	22.29	0.23	6.23	5
324.73	231.23	21.47	0.11	5.73	2
313.09	310.22	22.54	0.07	6.01	6
260.61	130.23	22.45	0.05	5.82	3
237.98	328.44	19.56	0.08	5.91	11
230.70	302.70	23.69	0.30	6.13	4
247.05	49.97	21.99	0.23	5.91	7
225.29	133.22	22.38	0.29	5.97	4
190.38	100.52	22.19	0.15	6.43	5
146.68	111.91	22.37	0.26	6.22	4
78.66	364.78	22.65	0.19	6.12	2
77.86	237.79	22.06	0.13	5.95	6
62.90	449.17	21.00	0.05	6.15	5

Note:
[1] I magnitudes transformed to F814W (Harris *et al, (1 991).*
[2] Positions listed for finder chart image 4

Table A5(d). Ground-Based I^1 Secondary Standards For Reference Epoch CCD #4

x^2	y^2	$F814W_{Ground}$	σ_{F814W}	$F814W_{Ground}$ -- $F814W_{ALLFRAME}$	N_{group}
52.59	43.58	**22.40**	0.19	**5.95**	14
403.08	98.11	**22.50**	0.18	**5.47**	7
199.13	92.94	**22.24**	0.13	**6.42**	37
166.40	94.60	**22.16**	0.05	**6.18**	30
714.96	139.90	**22.10**	0.26	**5.92**	10
255.71	111.72	**21.33**	0.18	**5.98**	24
155.54	111.28	**22.06**	0.15	**6.45**	26
257.93	128.65	**22.65**	0.20	**5.97**	29
108.62	147.67	**21.08**	0.07	**5.82**	23
102.75	172.27	**21.54**	0.15	**5.74**	25
53.91	191.84	**22.10**	0.17	**6.45**	26
117.59	198.61	**22.58**	0.24	**4.98**	16
160.23	202.19	**22.55**	0.16	**5.63**	6
60.59	227.07	**22.40**	0.27	**5.97**	12
272.69	292.23	**20.40**	0.25	**6.54**	32
274.24	295.26	**21.53**	0.29	**7.56**	34
261.52	312.99	**21.73**	0.17	**6.36**	27
296.27	329.77	**22.82**	0.28	**6.71**	31
296.47	347.74	**22.38**	0.10	**5.86**	30
497.30	412.56	**21.52**	0.08	**5.72**	16
369.57	405.04	**21.93**	0.23	**6.12**	20
359.84	406.58	**22.82**	0.07	**7.12**	24
417.09	420.08	**22.38**	0.20	**5.79**	16
350.39	418.38	**23.24**	0.29	**7.47**	29
374.43	425.89	**21.27**	0.19	**6.11**	33
379.41	434.72	**21.59**	0.07	**5.96**	29
357.64	440.16	**18.56**	0.05	**5.69**	27
409.90	454.15	**20.85**	0.09	**5.93**	26
343.68	450.22	**21.51**	0.24	**6.02**	19

Note:
[1] I magnitudes transformed to F814W (Harris *et al.* (1991).
[2] Positions listed **for finder chart image 1**

Appendix B. Cepheid Photometry

F555W and F814W epoch photometry and positions for the Cepheids are listed in Tables B1 and B2, respectively. Column one contains the Julian Date of the mid-point of each *individual* exposure. Note that the cosmic-ray split pairs have not been averaged for this tabulation. Column two shows which CCD the star can be found in for a given observation. Columns three and four show the (x, y) positions for the observations, while column five shows the calibrated F555W (or 14'814W) magnitudes with their reported ALLFRAME uncertainties. Only those data included in the light-curve analysis and mean photometry derivation are listed in Tables B1 and B2. Spurious observations have been excluded.

Appendix C. Unclassified Variable Stars

Several objects, from the cross-correlation of DoPhot and ALLFRAME variable candidate lists, were clearly variable. Real-time light curve analysis and image blinking resolved any questions of variability. However, many of these objects did not have wel]-defined periods, or, even if potentially-periodic, could not be easily classified as Cepheid variables or eclipsing variables. Phase-wrapped light curves and $(V - I)$ colours for these objects were the deciding factor behind placing them into this category.

Table Cl lists the finder chart coordinates with mean F555W magnitudes, meanF814W magnitudes, and the single F439W magnitude, when applicable. These magnitudes were not transformed to BVI because, as variables, accurate mean magnitude corrections could not be derived, *and given* the uncertainties in the natures of these objects, we could not assume mean colours to assure accurate transformations.

Table B1. F555W Photometry

c 1 P=58.5				
JD	CCD	X	Y	F555W
2449049.0327	1	97.24	149.03	23.53 ± 0.12
2449049.0938	1	97.23	149.03	23.44 ± 0.10
2449057.4598	1	98.39	147.90	23.21 ± 0.10
2449064.0828	1	101.15	150.14	22.97 ± 0.38
2449064.1136	1	101.16	*150.24*	23.80 ± 0.26
2449069.2661	1	97.50	*149.94*	23.52 ± 0.10
2449069.3293	1	97.51	*149.96*	23.45 ± 0.12
2449131.6589	*2*	82.07	*133.86*	23.72 ± 0.12
2449131.7228	*2*	81.88	*133.90*	23.79 ± 0.12
2449141.6263	*2*	82.05	*134.01*	23.46 ± 0.34
2449141.6936	*2*	82.13	133.95	23.95 ± 0.12
2449146.1096	*2*	81.90	133.74	24.12 ± 0.12
2449146.1769	*2*	81.87	133.75	23.94 ± 0.22
2449156.8860	*2*	81.95	134.23	24.16 ± 0.12
2449156.9499	*2*	81.87	134.23	24.13 ± 0.17
2449160.7658	*2*	82.14	133.99	23.91 ± 0.13
2449160.8304	*2*	82.12	133.96	23.71 ± 0.12
2449163.2450	*2*	82.12	134.23	23.53 ± 0.10
2449163.3054	2	82.19	134.17	23.50 ± 0.08
2449251.6130	3	77.11	130.11	23.82 ± 0.11
2449251.6748	*3*	77.15	130.16	23.72 ± 0.12
2449295.2633	*4*	136.06	91.71	23.50 ± 0.10
2449295.3195	*4*	136.09	91.72	23.47 ± 0.13
2449307.7036	*4*	122.92	116.10	23.83 ± 0.14
2449307.7661	*4*	122.82	116.06	23.76 ± 0.12
2449429.6016	1	222.13	233.93	24.04 ± 0.09

C5 P=47.1				
JD	CCD	X	Y	F555W
2449049.0327	2	730.21	199.07	23.45 ± 0.18
2449049.0938	2	730.20	199.06	23.50 ± 0.21
2449057.4598	2	729.01	198.21	23.80 ± 0.23
2449064.0828	2	731.12	195.62	24.27 ± 0.28
2449069.2661	2	730.96	199.29	23.67 ± 0.21
2449069.3293	2	731.00	199.27	23.74 ± 0.25
2449131.6589	3	712.04	233.49	23.15 ± 0.07
2449131.7228	3	712.09	233.66	23.10 ± 0.14
2449141.6263	3	712.20	233.14	23.37 ± 0.07
2449141.6936	3	712.14	233.06	23.36 ± 0.06
2449146.1096	3	711.96	233.78	23.42 ± 0.07
2449146.1769	3	711.96	233.80	23.45 ± 0.09
2449156.8860	3	712.36	233.26	24.03 ± 0.11
2449156.9499	3	712.38	233.27	23.88 ± 0.08
2449160.7658	3	712.28	233.27	23.59 ± 0.35
2449160.8304	3	712.26	233.31	23.85 ± 0.10
2449163.2450	3	712.42	233.15	23.61 ± 0.09
2449163.3054	3	712.38	233.03	23.49 ± 0.06
2449295.2633	4	342.64	700.29	23.79 ± 0.17
2449295.3195	4	342.70	700.25	23.84 ± 0.23
2449307.7036	4	199.68	754.17	23.44 ± 0.56
2449307.7661	4	199.55	754.20	23.20 ± 0.46

Table B1. — Continued

C6 P=45.8				
JD	CCD	x	u	F555W
2449049.0327	2	199.91	263.23	23.37 ± 0.08
2449049.0938	2	199.90	263.22	23.49 ± 0.10
2449057.4598	2	198.71	262.30	23.80 ± 0.20
2449064.0828	2	200.90	259.73	23.84 ± 0.13
2449064.1136	2	200.91	259.90	23.98 ± 0.26
2449069.2661	2	200.71	263.35	23.70 ± 0.20
2449069.3293	2	200.74	263.33	23.60 ± 0.13
2449131.6.589	3	179.33	271.94	23.25 ± 0.17
2449131.7228	3	179.38	272.14	23.32 ± 0.12
2449141.6263	3	179.44	271.57	23.59 ± 0.11
2449141.6936	3	179.38	271.48	23.61 ± 0.10
2449146.1096	3	179.20	272.26	23.74 ± 0.10
2449146.1769	3	179.21	272.30	23.74 ± 0.11
2449156.8860	3	179.68	271.72	23.90 ± 0.13
2449156.9499	3	179.68	271.74	23.86 ± 0.14
2449160.7658	3	179.59	271.74	23.61 ± 0.13
2449160.8304	3	179.57	271.77	23.65 ± 0.10
2449163.2450	3	179.77	271.59	23.50 ± 0.10
2449163.3054	3	179.71	271.48	23.48 ± 0.11
2449295.2633	1	333.49	109.52	23.74 ± 0.15
2449295.3195	1	333.46	109.46	23.86 ± 0.17
2449307.7036	1	312.83	169.14	23.13 ± 0.12
2449307.7661	1	312.78	169.15	23.18 ± 0.11
2449429.6016	2	201.91	255.98	23.51 ± 0.17

C7 P=43.0				
JD	CCD	z	y	F555W
2449049.0327	2	369.09	653.48	23.55 ± 0.10
2449049.0938	2	369.07	653.51	23.67 ± 0.11
2449057.4598	2	367.85	652.58	23.75 ± 0.09
2449069.2661	2	369.84	653.61	24.06 ± 0.12
2449069.3293	2	369.84	653.61	24.13 ± 0.13
2449131.6589	3	329.05	670.05	23.61 ± 0.07
2449131.7228	3	329.10	670.25	23.76 ± 0.10
2449141.6263	3	329.17	669.73	23.82 ± 0.07
2449141.6936	3	329.11	669.65	23.87 ± 0.10
2449146.1096	3	328.95	670.40	23.99 ± 0.14
2449146.1769	3	328.94	670.44	24.0.5 ± 0.12
2449156.8860	3	329.39	669.85	24.01 ± 0.10
2449156.9499	3	329.41	669.89	23.99 ± 0.11
2449160.7658	3	329.30	669.87	23.30 ± 0.16
2449160.8304	3	329.28	669.91	23.60 ± 0.09
2449163.2450	3	329.46	669.72	23.57 ± 0.08
2449163.3054	3	329.41	669.62	23.52 ± 0.11
2449295.2633	1	712.34	300.35	23.59 ± 0.22
2449295.3195	1	712.28	300.32	23.51 ± 0.23
2449307.7036	1	644.35	433.82	23.65 ± 0.12
2449307.7661	1	644.33	433.85	23.67 ± 0.15
2449429.6016	2	376.23	654.39	23.38 ± 0.12

Table B1. —Continued

C19 P=43.0				
JD	CCD	Z	u	F555W
2449049 .032'7	4	545.49	751.72	24.02 ± 0.19
2449049.0938	4	545.46	751.68	23.86 ± 0.13
2449057.4598	4	546..58	7.52.95	23.83 ± 0.17
2449064.0828	4	544.51	75.5.52	22.94 ± 0.29
2449064.1136	4	544.58	755.61	23.13 ± 0.18
2449069.2661	4	544.60	752.00	23.16 ± 0.13
2449069.3293	4	544.58	752.00	23.17 ± 0.12
2449131.6589	1	517.28	783.30	23.65 ± 0.28
2449131.7228	1	517.23	783.08	23.71 ± 0.09
2449141.6263	1	517.47	783.35	24.14 ± 0.11
2449141.6936	1	517.53	783.46	23.72 ± 0.17
2449146.1096	1	517.30	783.14	23.49 ± 0.07
2449146.1769	1	517.29	783.11	23.44 ± 0.07
2449156.8860	1	517.28	783.23	23.21 ± 0.08
2449156.9499	1	517.30	783.17	23.23 ± 0.07
2449160.7658	1	517.36	783.4.5	23.32 ± 0.07
2449160.8304	1	517.36	783.43	23.35 ± 0.06
2449163.24.50	1	517.34	783.43	23.36 ± 0.07
2449163.30.54	1	517.36	783.52	23.61 ± 0.11

C20 P=42.5				
JD	CCD	Z	y	F555W
2449049.0327	4	137.54	199.71	23.79 ± 0.41
2449049.0938	4	137.52	199.69	24.00 ± 0.17
2449057.4598	4	138.72	200.84	24.22 ± 0.09
2449064.0828	4	136.69	203.58	24.51 ± 0.18
2449064.1136	4	136.69	203.83	24.80 ± 0.53
2449069.2661	4	136.75	200.00	24.70 ± 0.43
2449069.3293	4	136.70	200.01	24.70 ± 0.17
2449131.6589	1	148.45	205.88	23.82 ± 0.12
2449131.7228	1	148.36	205.70	23.93 ± 0.10
2449141.6263	1	148.61	205.92	24.16 ± 0.32
2449141.6936	1	148.67	206.01	24.23 ± 0.14
2449146.1096	1	148.42	205.70	24.48 ± 0.14
2449146.1769	1	148.39	205.66	24.23 ± 0.12
2449156.8860	1	148.42	205.80	24.85 ± 0.16
2449156.9499	1	148.42	205.74	24.23 ± 0.18
2449160.7658	1	148.52	206.01	24.45 ± 0.14
2449160.8304	1	148.52	205.99	24.42 ± 0.18
2449163.2450	1	148.50	206.01	24.06 ± 0.17
2449163.3054	1	148.54	206.11	24.01 ± 0.27
2449295.2633	3	204.79	66.85	23.99 ± 0.21
2449295.3195	3	204.81	66.91	24.03 ± 0.16
2449307.7036	3	190.77	104.96	24.14 ± 0.12
2449307.7661	3	190.78	104.86	24..56 ± 0.17
2449429.6016	4	201.73	223.49	24.45 ± 0.21

Table B1. — Continued

C8 P=41.0				
JD	CCD	x	y	F555W
2449049.0327	2	301.46	198.03	24.38 ± 0.12
2449049.0938	2	301.46	198.02	24.26 ± 0.13
2449057.4598	2	300.27	197.12	24.1 O* O.13
2449064.0828	2	302.44	194.56	23.33 ± 0.32
2449064.1136	2	302.45	194.71	23.49 ± 0.19
2449069.2661	2	302.26	198.18	23.50 ± 0.21
2449069.3293	2	302.29	198.16	23.63 ± 0.10
2449131.6589	3	283.95	211.71	24.06 ± 0.27
2449131.7228	3	284.00	211.91	24.21 ± 0.12
2449141.6263	3	284.07	211.34	23.8840.10
2449141.6936	3	284.01	211.26	23.82 ± 0.11
2449146.1096	3	283.83	212.02	23.67 ± 0.10
2449146.1769	3	283.83	212.06	23.59 ± 0413
2449156.8860	3	284.29	211.49	23.81 ± 0.09
2449156.9499	3	284.29	211.50	23.74 ± 0.09
2449160.7658	3	284.21	211.50	23.89 ± 0.11
2449160.8304	3	284.19	211.54	23.96 ± 0.12
2449163.2450	3	284.38	211.37	23.75 ± 0.08
2449163.3054	3	284.33	211.25	24.04 ± 0.09
2449295.2633	4	63.45	374.85	24..51 ± 0.22
2449295.3195	4	63.48	374.85	24.49 ± 0.20
2449307.7036	1	371.85	64.25	23.90 ± 0.26
2449307.7661	1	371.79	64.25	23.54 ± 0.30
2449429.6016	2	305.41	188.97	23.93 ± 0.12

C 9 P=38.0				
JD	CCD	Z	u	F555W
2449049.0327	2	337.45	56.83	23.67 ± 0.08
2449049.0938	2	337.45	56.81	23.74 ± 0.08
2449057.4598	2	336.27	55.92	23.96 ± 0.08
2449064.0828	2	338.43	53.38	22.80 ± 0.09
2449064.1136	2	338.44	53.54	22.76 ± 0.10
2449069.2661	2	338.25	56.99	23.01 ± 0.10
2449069.3293	2	338.30	.56.96	23.04 ± 0.08
2449131.6589	3	326.84	72.37	24.01 ± 0.10
2449131.7228	3	326.89	72.56	24.11 ± 0.10
2449141.6263	3	326.97	71.98	22.89 ± 0.07
2449141.6936	3	326.90	71.90	22.91 ± 0.09
2449146.1096	3	326.71	72.67	23.09 ± 0.07
2449146.1769	3	326.73	72.70	23.07 ± 0.11
2449156.8860	3	327.18	72.14	23.54 ± 0.10
2449156.9499	3	327.18	72.14	23.43 ± 0.07
2449160.7658	3	327.10	72.15	23.60 ± 0.11
2449160.8304	3	327.08	72.18	23.58 ± 0.10
2449163.2450	3	327.26	72.02	23.70 ± 0.08
2449163.3054	3	327.22	71.90	23.71 ± 0.11
2449295.2633	4	194.42	309.83	22.78 ± 0.25
2449295.3195	4	194.46	309.83	22.81 ± 0.14
2449307.7036	4	135.06	341.58	23.31 ± 0.08
2449307.7661	4	134.95	341.56	23.38 ± 0.10
2449429.6016	2	341.74	43.87	23.58 ± 0.12

Table B1. —Continued

C1O P=37.6				
JD	CCD	z	y	F555W
2449049.0327	2	346.21	738.88	23.66 ± 0.12
2449049.0938	2	346.19	738.91	23.79 ± 0.13
2449057.4598	2	344.96	737.97	23.74 ± 0.13
2449064.0828	2	347.16	735.30	23.96 ± 0.18
2449064.1136	2	347.15	735.39	23.87 ± 0.25
2449069.2661	2	346.95	739.00	24.19 ± 0.28
2449069.3293	2	346.95	739.00	24.06 ± 0.14
2449131.6589	3	302.00	7.54.27	23.79 ± 0.08
2449131.7228	3	302.05	754.47	23.81 ± 0.12
2449141.6263	3	302.11	753.96	23.94 ± 0.49
2449141.6936	3	302.06	753.88	24.1.5 ± 0.11
2449146.1096	3	301.90	754.63	24.11 ± 0.17
2449146.1769	3	301.89	7.54.67	24.18 ± 0.15
2449156.8860	3	302.34	754.08	24.51 ± 0.13
2449156.9499	3	302.36	754.12	24.5.5 ± 0.15
2449160.7658	3	302.25	754.10	24.30 ± 0.14
2449160.8304	3	302.23	754.14	23.59 ± 0.25
2449163.2450	3	302.42	753.95	23.61 ± 0.07
2449163.3054	3	302.36	753.85	23.78 ± 0.11
2449295.2633	1	749.37	380.35	24.11 ± 0.36
2449295.3195	1	749.31	380.32	24.35 ± 0.26
2449307.7036	1	664.11	519.73	24.05 ± 0.63
2449307.7661	1	664.10	519.77	24.35 ± 0.50
2449429.6016	2	353.23	741.70	23.83 ± 0.13

C21 P=33.5				
JD	CCD	z	y	F555W
2449049.0327	4	296.98	712.86	23.72 ± 0.13
2449049.0938	4	296.95	712.83	23.62 ± 0.12
2449057.4598	4	298.08	713.98	24.29 ± 0.19
2449064.0828	4	296.05	716.66	24.25 ± 0.41
2449064.1136	4	296.07	716.82	24.56 ± 0.38
2449069.2661	4	296.11	713.11	23.87 ± 0.23
2449069.3293	4	296.07	713.11	23.87 ± 0.11
2449131.6589	1	272.48	727.86	24.50 ± 0.16
2449131.7228	1	272.42	727.64	24.53 ± 0.16
2449141.6263	1	272.66	727.90	23.45 ± 0.06
2449141.6936	1	272.73	728.02	23.38 ± 0.06
2449146.1096	1	272.50	727.69	23.54 ± 0.08
2449146.1769	1	272.47	727.66	23.59 ± 0.08
2449156.8860	1	272.47	727.78	24.09 ± 0.12
2449156.9499	1	272.48	727.72	24.15 ± 0.12
2449160.7658	1	272..56	728.00	24.20 ± 0.09
2449160.8304	1	272.56	727.97	24.18 ± 0.11
2449163.2450	1	272.55	727.98	24.34 ± 0.13
2449163.3054	1	272.56	728.07	24.38 ± 0.24
244929.5.2633	3	658.01	354.75	24.27 ± 0.22
2449295.3195	3	658.01	354.79	24.41 ± 0.17
2449307.7036	3	574.84	480.12	23.32 ± 0.10
2449307.7661	3	574.85	480.04	23.36 ± 0.09
2449429.6016	4	371.69	745.66	24.37 ± 0.16

Table B1. Continued

C12 P=33.5				
JD	CCD	Z	γ	F555W
2449049.0327	3	356.29	200.10	23.16 ± 0.10
2449049.0938	3	356.32	200.07	23.13 ± 0.10
2449057.4598	3	355.33	201.07	23.41 ± 0.12
2449064 .0S28	3	352.88	198.66	23.59 ± 0.13
2449069.2661	3	356.32	198.94	24.04 ± 0.17
2449069.3293	3	356.31	198.92	24.10 ± 0.16
2449131.6589	4	343.88	235.59	23.74 ± 0.15
2449131.7228	4	344.06	23.5.50	23.76 ± 0.15
2449141.6263	4	343.92	235.79	23.52 ± 0.13
2449141.6936	4	343.83	235.86	23.44 ± 0.11
2449146.1096	4	344.00	235.54	23.02 ± 0.08
2449146.1769	4	344.02	23.5.53	23.05 ± 0.11
2449156.8860	4	344.02	235.59	23.46 ± 0.22
2449156.9499	4	344.06	23.5.58	23.53 ± 0.10
2449160.7658	4	343.92	235.71	23.71 ± 0.13
2449160.8304	4	343.91	235.69	23.69 ± 0.12
2449163.2450	4	343.95	235.70	23.67 ± 0.13
2449163.3054	4	343.84	235.74	23.62 ± 0.13
2449251.6130	1	375.4.5	221.91	22.94 ± 0.30
2449251.6748	1	375.41	221.88	23.11 ± 0.10
244929.5.2633	1	124.31	410.36	23.47 ± 0.21
2449295.3195	1	124.31	410.32	23.50 ± 0.19
2449307.7036	1	46.07	420.64	23.95 ± 0.25
2449307.7661	1	46.02	420.69	23.84 ± 0.23
2449429.6016	3	365.21	254.29	23.42 ± 0.28

C13 P=32.0				
JD	CCD	Z	*u*	F555W
2449049.0327	3	230.92	468.99	24.15 ± 0.10
2449049.0938	3	230.93	468.96	24.15 ± 0.12
2449057.4598	3	229.96	469.95	23.48 ± 0.08
2449064.0828	3	227.54	467.52	23.83 ± 0.10
2449064.1136	3	227.59	467.73	24.48 ± 0.41
2449069.2661	3	230.94	467.84	24.02 ± 0.13
2449069.3293	3	230.90	467.82	24.00 ± 0.08
2449131.6589	4	205.04	497.72	24.24 ± 0.12
2449131.7228	4	205.22	497.66	24.0640.13
2449141.6263	4	205.06	497.94	24.36 ± 0.11
2449141.6936	4	204.95	497.99	24.56 ± 0.13
2449146.1096	4	205.16	497.69	24.24 ± 0.12
2449146.1769	4	205.15	497.69	23.78 ± 0.20
2449156.8860	4	205.14	497.71	23.81 ± 0.10
2449156.9499	4	205.21	497.72	23.77 ± 0.09
2449160.7658	4	205.06	497.83	24.01 ± 0.09
2449160.8304	4	205.0.5	497.81	23.85 ± 0.20
2449163.2450	4	205.09	497.82	24.05 ± 0.12
2449163.3054	4	204.99	497.85	24.50 ± 0.24
2449251.6130	1	246.68	488.82	23.95 ± 0.09
24492.51.6748	1	246.63	488.78	23.81 ± 0.08
2449429.6016	3	238.56	530.10	24.25 i 0.14

Table B1. — Continued

C22 P=27.3				
JD	CCD	x	y	F555W
2449049.0327	4	307.15	453.01	24.31 ± 0.15
2449049.0938	4	307.13	452.98	24.19 ± 0.16
2449057.4598	4	308.29	454.14	24.53 ± 0.20
2449064.0828	4	306.24	456.85	23.77 ± 0.10
2449064.1136	4	306.27	457.02	24.00 ± 0.37
2449069.2661	4	306.31	453.29	23.94 ± 0.15
2449069.3293	4	306.27	453.29	24.08 ± 0.18
2449131.6589	1	300.18	469.65	24.44 ± 0.16
2449131.7228	1	300.11	469.4.5	24.63 ± 0.14
2449141.6263	1	300.36	469.70	23.91 ± 0.51
2449141.6936	1	300.42	469.80	24.33 ± 0.16
2449146.1096	1	300.18	469.48	23.81 ± 0.08
2449146.1769	1	300.16	469.45	23.77 ± 0.10
2449156.8860	1	300.17	469.58	24.43 ± 0.21
2449156.9499	1	300.17	469.51	24.48 ± 0.11
2449160.7658	1	300.26	469.79	24.69 ± 0.20
2449160.8304	1	300.26	469.77	24.46 ± 0.14
2449163.2450	1	300.24	469.78	24.69 ± 0.17
2449295.2633	3	497.91	1.50.30	24.06 ± 0.36
2449295.3195	3	497.92	150.3.5	24.6420.29
2449307.7036	3	460.29	247.01	23.81 ± 0.18
2449307.7661	3	460.31	246.92	23.76 ± 0.19
2449429.6016	4	378.34	479.74	24.11 ± 0.25

C23 P=25.6				
JD	CCD	X	u	F555W
2449049.0327	4	187.71	*501.00*	25.04 ± 0.18
2449049.0938	4	187.68	500.97	24.73 ± 0.18
2449057.4598	4	188.84	502.12	25.05 ± 0.21
2449064.0828	4	186.82	504.83	24.01 ± 0.13
2449064.1136	4	186.82	505.04	24.18 ± 0.31
2449069.2661	4	186.88	501.26	24.65 ± 0.23
2449131.6589	1	178.01	509.43	25.01 ± 0.11
2449131.7228	1	177.94	509.23	25.29 ± 0.22
2449146.1096	1	178.01	509.26	24.57 ± 0.17
2449146.1769	1	177.98	509.22	24.53 ± 0.13
2449156.8860	1	178.00	509.35	25.08 ± 0.19
2449156.9499	1	178.00	509.29	25.36 ± 0.21
2449160.7658	1	178.09	509.57	25.43 ± 0.23
2449160.8304	1	178.09	509.54	25.11 ± 0.16
2449163.2450	1	178.07	509.55	24.73 ± 0.17
2449163.3054	1	178.10	.509.65	24.70 ± 0.21
2449295.2633	3	437.73	263.92	24.07 ± 0.28
2449295.3195	3	437.73	263.97	24.29 ± 0.25
2449307.7036	3	378.06	345.85	24.97 ± 0.22
2449307.7661	3	378.08	345.76	25.00 ± 0.23
2449429.6016	4	257.14	530.34	24.51 ± 0.20

Table B1. — Continued

C14 P=25.0				
JD ·	CCD	X	y	F555W
2449049.0327	3	642.09	401.70	24.76 ± 0.91
2449049.0938	3	642.12	401.66	25.19 ± 0.33
2449057.4598	3	641.10	402.71	24.33 ± 0.13
2449064.0828	3	638.63	400.25	24.94 ± 0.23
2449064.1136	3	638.59	400.52	24.65 ± 0.49
2449131.6589	4	619.32	451.30	24.11 ± 0.14
2449131.7228	4	619.49	451.21	24.26 ± 0.17
2449141.6263	4	619.36	451..51	24.95 ± 0.43
2449141.6936	4	619.28	451.57	24.91 ± 0.20
2449146.1096	4	619.46	451.26	24.97 ± 0.19
2449146.1769	4	619.48	451.24	24.77 ± 0.79
2449156.8860	4	619.46	451.29	24.11 ± 0.10
2449156.9499	4	619.50	451.29	24.10 ± 0.13
2449160.7658	4	619.36	451.42	24.42 ± 0.16
2449160.8304	4	619.35	451.40	24.39 ± 0.15
2449163.2450	4	619.38	451.40	24.73 ± 0.19
2449163.3054	4	619.28	451.44	24.85 ± 0.59
2449251.6130	1	658.20	427.00	24.13 ± 0.12
2449251.6748	1	658.16	426.95	23.90 ± 0.09
2449429.6016	3	6.59.12	458.83	24.20 ± 0.14

C11 P=23.7				
JD	CCD	Z	y	F555W
2449049.0327	2	406.06	183.49	24.95 ± 0.20
2449049.0938	2	406.05	183.48	24.35 ± 0.16
2449057.4598	2	404.86	182.59	23.81 ± 0.11
2449064.0828	2	407.02	180.03	24.12 ± 0.12
2449064.1136	2	407.02	180.16	23.79 ± 0.34
2449069.2661	2	406.94	183.66	24.36 ± 0.15
2449069.3293	2	406.88	183.64	24.59 ± 0.15
2449131.6589	3	389.11	202.25	23.93 ± 0.09
2449131.7228	3	389.16	202.44	23.93 ± 0.09
2449141.6263	3	389.24	201.88	24.58 ± 0.11
2449141.6936	3	389.17	201.80	24.66 ± 0.17
2449146.1096	3	388.99	202.55	24.89 ± 0.17
2449146.1769	3	389.00	202.58	24.83 ± 0.19
2449156.8860	3	389.45	202.02	24.21 ± 0.11
2449156.9499	3	389.45	202.03	24.06 ± 0.11
2449160.7658	3	389.36	202.04	24.42 ± 0.09
2449160.8304	3	389.35	202.07	24.18 ± 0.70
2449163.2450	3	389.52	201.90	24.43 ± 0.14
2449163.3054	3	389.48	201.78	24.76 ± 0.17
2449295.2633	4	142.82	444.58	23.70 ± 0.19
2449295.3195	4	142.85	444.56	23.74 ± 0.19
2449307.7036	4	56.65	462.91	24.47 ± 0.20
2449307.7661	4	56.53	462.90	24.04 ± 0.31
2449429.6016	2	412.22	173.52	24.78 ± 0.21

Table B1. — Continued

C24 P=23.5				
JD	CCD	X	Y	F555W
2449049.0327	4	72.63	240.46	24.70 ± 0.23
2449049.0938	4	72.61	240.43	24.45 ± 0.34
2449057.4598	4	73.81	241.57	24.92 ± 0.27
2449069.2661	4	71.8.5	240.73	24.29 ± 0.20
2449069.3293	4	71.79	240.73	24.28 ± 0.17
2449131.6589	1	81.06	242.10	23.91 ± 0.11
2449131.7229	1	80.98	241.92	24.14 ± 0.14
2449141.6263	1	81.22	242.14	24.45 ± 0.19
2449141.6936	1	81.29	242.24	24.51 ± 0.17
2449146.1096	1	81.04	241.92	24.56 ± 0.15
2449146.1769	1	81.01	241.88	24.45 ± 0421
2449156.8860	1	81.04	242.02	23.79 ± 0.10
2449156.9499	1	81.03	241.95	23.78 ± 0.14
2449160.7658	1	81.14	242.23	23.97 ± 0.16
2449160.8304	1	81.14	242.21	24.16 ± 0.16
2449163.2450	1	81.12	242.23	24.46 ± 0.18
2449163.3054	1	81.15	242.32	23.79 ± 0.41
2449295.2633	3	181.5.5	139.76	24.20 ± 0.18
2449295.3195	3	181.57	139.81	24.21 ± 0.16
2449429.6016	4	136.25	266.01	24.80 ± 0.29

C15 P=23.4				
JD	CCD	X	y	F555W
2449049.0327	3	318.10	185.21	24.68 ± 0.14
2449049.0938	3	318.13	185.18	24.35 ± 0.38
2449057.4598	3	317.14	186.18	23.72 ± 0.12
2449064.0828	3	314.70	183.77	24.02 ± 0.39
2449064.1136	3	314.71	184.11	24.80 ± 0.41
2449069.2661	3	318.13	184.04	24.51 ± 0.47
2449069.3293	3	318.12	184.02	24.52 ± 0.14
2449131.6589	4	306.47	218.79	24.01 ± 0.10
2449131.7228	4	306.65	218.71	24.01 ± 0.13
2449141.6263	4	306.50	218.99	24.59 ± 0.18
2449141.6936	4	306.41	219.06	24.85 ± 0.28
2449146.1096	4	306.58	218.74	24.72 ± 0.23
2449146.1769	4	306.60	218.73	24.73 ± 0.27
2449156.8860	4	306.60	218.79	24.08 ± 0.19
2449156.9499	4	306.64	218.79	24.24 ± 0.29
2449160.7658	4	306.50	218.92	24.44 ± 0.17
2449160.8304	4	306.49	218.90	24.37 ± 0.12
2449163.2450	4	306.53	218.90	24.31 ± 0.29
2449163.3054	4	306.42	218.94	24.68 ± 0.19
2449251.6130	1	337.51	206.54	24.23 ± 0.25
2449251.6748	1	337.46	206.51	24.29 ± 0.22
2449295.2633	1	111.45	371.43	24.05 ± 0.16
2449295.3195	1	111.45	371.39	24.23 ± 0.20
2449307.7036	1	41.51	379.89	24.48 ± 0.19
2449307.7661	1	41.46	379.93	24.63 ± 0.09
2449429.6016	3	326.08	239.48	23.56 ± 0.13

Table B1. — Continued

C16 P=22.8				
JD	CCD	X	Y	F555W
2449049.0327	3	743.64	608.43	25.33 ± 0.27
2449049.0938	3	743.66	608.38	24.98 ± 0.29
2449057.4598	3	742.65	609.45	24.28 ± 0.14
2449064.0828	3	740.18	606.96	24.53 ± 0.15
2449064.1136	3	740.11	607.14	24.66 ± 0.54
2449069.2661	3	743.63	607.34	25.22 ± 0.29
2449069.3293	3	743.58	607.33	24.87 ± 0.18
2449131.6589	4	710.38	662.82	24.64 ± 0.16
2449131.7228	4	710.55	662.74	24.67 ± 0.19
2449141.6263	4	710.41	663.04	24.57 ± 0.17
2449141.6936	4	710.33	663.10	25.00 ± 0.25
2449146.1096	4	710.54	662.79	24.27 ± 0.13
2449146.1769	4	710.54	662.78	24.18 ± 0.10
2449156.8860	4	710.51	662.81	24.72 ± 0.14
2449156.9499	4	710.56	662.81	24.98 ± 0.18
2449160.7658	4	710.42	662.93	25.12 ± 0.25
2449160.8304	4	710.41	662.93	25.06 ± 0.30
2449163.2450	4	710.44	662.91	24.77 ± 0.17
2449163.3054	4	710.34	662.95	24.80 ± 0.17
2449251.6130	1	756.87	634.79	24.96 ± 0.23
2449231.6748	1	756.83	634.74	25.17$0.22

C25 P=19.4				
JD	CCD	Z	V	F555W
2449049.0938	4	304.63	501.27	24.67 ± 0.18
2449057.4598	4	305.78	502.42	24.06 ± 0.11
2449064.0828	4	303.74	505.13	24.55 ± 0.17
2449069.2661	4	303.81	501.57	24.49 ± 0.27
2449069.3293	4	303.77	501.58	24.64 ± 0.16
2449131.6589	1	294.43	517.60	23.97 ± 0.09
2449131.7228	1	294.36	517.39	24.01 ± 0.09
2449141.6263	1	294.60	517.64	24.62 ± 0.17
2449141.6936	1	294.66	517.74	24.60 ± 0.19
2449146.1096	1	294.43	517.42	24.82 ± 0.11
2449146.1769	1	294.41	517.39	24.89 ± 0.15
2449156.8860	1	294.42	517.52	24.31 ± 0.10
2449156.9499	1	294.42	517.46	24.60 ± 0.20
2449160.7658	1	294.51	517.73	24.65 ± 0.23
2449160.8304	1	294.51	517.71	24.43 ± 0.27
2449163.2450	1	294.48	517.72	24.62 ± 0.14
2449163.3054	1	294.51	517.82	24.58 ± 0.13
2449295.2633	3	527.20	188.69	24.66 ± 0.26
2449295.3195	3	527.21	188.74	25.28 ± 0.29
2449307.7036	3	481.04	290.62	23.91 ± 0.17
2449307.7661	3	481.06	290.53	23.82 ± 0.50

Table B1. — Continued

C2 P=18.2				
JD	CCD	x	Y	F555W
2449049.0327	1	217.48	344.10	24.14 ± 0.24
2449049.0938	1	217.43	344.08	24.26 ± 0.25
2449057.4598	1	218.59	342.98	24.05 ± 0.13
2449064.0828	1	221.31	345.13	24.40 ± 0.51
2449064.1136	1	221.34	345.30	24.26 ± 0.31
2449069.2661	1	217.68	344.98	23.93 ± 0.25
2449069.3293	1	217.69	345.01	23.85 ± 0.35
2449131.6X39	2	194.23	334.25	23.97 ± 0.10
2449131.7228	2	194.06	334.30	24.14 ± 0.13
2449141.6263	2	194.21	334.40	23.76 ± 0.08
2449141.6936	2	194.29	334.37	23.83 ± 0.13
2449146.1096	2	194.06	334.17	24.05 ± 0.17
2449146.1769	2	194.05	334.18	23.90 ± 0.12
2449156.8860	2	194.12	334.61	24.16 ± 0.08
2449156.9499	2	194.04	334.61	24.12 ± 0.44
2449160.7658	2	194.28	334.37	23.70 ± 0.09
2449160.8304	2	194.27	334.36	23.53 ± 0.09
2449163.2450	2	194.27	334.60	23.29 ± 0.45
2449163.3054	2	194.35	334.55	23.75 ± 0.10
2449251.6130	3	200.12	323.87	23.64 ± 0.10
2449251.6748	3	200.1.5	323.93	23.78 ± 0.13
2449295.2633	4	355.41	159.89	24.24 ± 0.20
2449295.3195	4	355.47	159.88	24.29 ± 0.24
2449307.7036	4	323.82	227.77	23.79 ± 0.19
2449307.7661	4	323.73	227.74	23.77 ± 0.19
2449429.6016	1	498.78	662.99	24.55 ± 0.14

C26 P=17.7 ‘				
JD	CCD	X	Y	F555W
2449049.0327	4	31.18	301.62	24.52 ± 0.16
2449049.0938	4	31.15	301.60	24.42 ± 0.40
2449057.4598	4	32.34	302.73	25.12 ± 0.23
2449064.0828	4	30.33	305.48	25.37 ± 0.43
2449064.1136	4	30.31	305.74	25.09 ± 0.66
2449069.2661	4	30.38	301.88	24.59 ± 0.17
2449069.3293	4	30.32	301.88	24.67 ± 0.22
2449131.6589	1	35.65	300.25	25.15 ± 0.21
2449131.7228	1	35.56	300.07	24.88 ± 0.20
2449141.6263	1	35.80	300.29	24.57 ± 0.16
2449141.6936	1	35.88	300.39	24.44 ± 0.15
2449146.1096	1	35..63	300.07	24.96 ± 0.19
2449146.1769	1	35.59	*300.03*	24.81 ± 0.17
2449156.8860	1	35.62	*300.17*	24.34 ± 0.12
2449156.9499	1	35.61	*300.10*	24.50 ± 0.19
2449160.7658	1	35.73	*300.38*	24.71 ± 0.19
2449160.8304	1	35.72	*300.36*	24.74 ± 0.19
2449163.2450	1	35.71	*300.37*	24.8.5 ± 0.18
2449163.3054	1	35.73	*300.47*	24.78 ± 0.18
2449307.7036	3	145.65	*244.95*	25.21 ± 0.30
2449307.7661	3	145.67	*244.86*	25.43 ± 0.43
2449429.6016	4	94.89	*328.98*	24.91 ± 0.13

Table B1. — Continued

C27 P=17.2				
JD	CCD	x	y	F555W
2449049.0327	4	433.81	35.42	24.36 ± 0.20
2449049.0938	4	433.81	35.40	24.39 ± 0.25
2449064.0828	4	432.94	39.32	24.21 ± 0.21
2449064.1136	4	432.99	39.51	24.19 ± 0.34
2449069.2661	4	433.03	35.78	24.62 ± 0.36
2449069.3293	4	432.99	35.79	24.38 ± 0.19
2449131.6589	1	454.55	62.15	24.14 ± 0.11
2449131.7228	1	4.54.46	61.98	24.02 ± 0.15
2449141.6263	1	454.73	62.19	24.38 ± 0.17
2449141.6936	1	454.75	62.27	24.20 ± 0.12
2449146.1096	1	454.51	61.97	23.91 ± 0.15
2449146.1769	1	454.50	61.93	23.90 ± 0.13
2449156.8860	1	454.53	62.08	24.41 ± 0.14
2449156.9499	1	454.54	62.02	24.47 ± 0.17
2449160.7658	1	454.61	62.27	23.59 ± 0.06
2449160.8304	1	454.61	62.28	23.60 ± 0.10
2449163.2450	1	454.58	62.30	24.02 ± 0.13
2449163.3054	1	454.64	62.39	23.62 ± 0.16
2449295.2633	2	295.47	331.27	24.27 ± 0.17
244929.5.3195	2	295.4.5	331.24	24.45 ± 0.24
2449307.7036	2	225.92	379.74	23.98 ± 0.31
2449307.7661	2	226.08	379.71	23.92 ± 0.25
2449429.6016	4	502.20	51.09	24.55 ± 0.22

C28 P=16.7				
JD	CCD	X	?/	F555W
2449049.0327	4	535.17	572.41	25.00 ± 0.29
2449049.0938	4	535.15	572.38	24.92 ± 0.19
2449057.4598	4	536.28	573.55	25.42 ± 0.26
2449064.0828	4	534.21	576.23	24.75 ± 0.59
2449064.1136	4	.534.28	576.35	24.95 ± 0.56
2449069.2661	4	534.30	572.71	24.97 ± 0.22
2449069.3293	4	534.28	572.72	25.20 ± 0.27
2449131.6589	1	519.13	603.97	25.08 ± 0.72
2449131.7228	1	519.07	603.75	25.08 ± 0.17
2449141.6263	1	519.33	604.01	25.39 ± 0.19
2449141.6936	1	519.37	604.11	26.21 ± 0.55
2449146.1096	1	519.14	603.80	25.26 ± 0.21
2449146.1769	1	519.13	603.77	25.45 ± 0.76
2449156.8860	1	519.13	603.89	25.37 ± 0.30
2449156.9499	1	519.15	603.84	25.24 ± 0.21
2449160.7658	1	519.21	604.11	25.81 ± 0.53
2449160.8304	1	519.21	604.09	25.34 ± 0.25
2449163.2450	1	519.18	604.10	25.15 ± 0.20
2449163.3054	1	519.22	604.19	25.48 ± 0.33
2449307.7036	3	717.56	243.72	25.94 ± 0.39
2449307.7661	3	717.57	243.63	24.92 ± 0.33
2449429.6016	4	613.13	598.65	25.14 ± 0.21

Table B1. — Continued

C3 P=16.7				
JD	CCD	x	v	F555W
2449049.0327	1	355.75	461.29	24.69 ± 0.18
2449049.0938	1	35.5.67	461.26	24.69 ± 0.15
2449057.4.598	1	356.83	460.17	25.06 ± 0.18
2449064.0828	1	359.52	462.26	24.68 ± 0.16
2449064.1136	1	359.54	462.48	24.27 ± 0.37
2449069.2661	1	355.90	462.17	2.5.06 ± 0.13
2449069.3293	1	355.92	462.19	25.00 ± 0.13
2449131.6589	*2*	327.69	457.49	24.39 ± 0.10
2449131.7228	*2*	32'7.53	457.54	24.34 ± 0.13
2449141.6263	*2*	327.67	457.64	25.08 ± 0.19
2449141.6936	*2*	327.75	457.62	25.23 ± 0.23
2449146.1096	*2*	327.53	457.43	24.20 ± 0.09
2449146.1769	2	327.54	457.45	24.26 ± 0.13
2449156.8860	2	327.58	457.83	25.27 ± 0.22
2449156.9499	*2*	327.52	457.83	*25.07 ± 0.25*
2449160.7658	*2*	327.73	457.61	*24.20 ± 0.08*
2449160.8304	*2*	327.73	457.59	24.15 ± *0.13*
2449163.24.50	*2*	327.72	457.93	*24.24 ± 0.14*
2449163.3054	2	327.81	457.78	*24.06 ± 0.25*
244929$.2633	*4*	.536.74	157.30	*23.83 ± 0.16*
2449295.3195	*4*	536.82	157.29	*24.04 ± 0.14*
2449307.7036	*4*	502.07	262.39	*24.87* ± 0.15
2449307.7661	*4*	501.99	262.37	24.82 ± 0.19

C17 P=16.5				
JD	CCD	X	y	F555W
2449049.0327	3	387.27	265.40	*25.02 ± 0.18*
2449049.0938	3	387.29	265.37	*25.50 ± 0.46*
2449057.4598	3	386.30	266.38	*24.09 ± 0.15*
2449064.0828	3	383.86	263.96	*24.50 ± 0.17*
2449064.1136	3	383.86	264.27	*24.74 ± 0.62*
2449069.2661	3	387.29	264.25	*24.44 ± 0.17*
2449069.3293	3	387.28	264.23	*24.55 ± 0.15*
2449131.6589	4	371.55	302.3.5	*25.10 ± 0.29*
2449131.7228	4	371.73	302.27	*25.17 ± 0.26*
2449141.6263	4	371.58	302.56	*24.34 ± 0.29*
2449141.6936	4	371.49	302.62	*24.45 ± 0.14*
2449146.1096	4	371.67	302.31	*24.70 ± 0.17*
2449146.1769	4	371.68	302.29	*25.06 ± 0.28*
2449156.8860	4	371.68	302.35	*24.27 ± 0.13*
2449156.9499	4	371.73	302.34	*24.34 ± 0.16*
2449160.8304	4	371.57	302.45	*24.74 ± 0.21*
2449163.2450	4	371.61	302.46	*24.88 ± 0.27*
2449163.3054	4	371.50	302.50	*25.34 ± 0.32*
2449251.6130	1	405.52	287.54	*24.63 ± 0.24*
2449251.6748	1	405.48	287.50	*24.60 ± 0.17*
2449295.2633	1	93.68	475.91	*25.20 ± 0.48*
2449295,319.5	1	93.69	475.88	*24.80 i 0.23*
2449307.7036	2	465.05	49.33	*24.88 ± 0.17*
2449307.7661	2	464.93	49.38	*24.92 ± 0.23*
2449429.6016	3	397.28	320.88	*24.87 ± 0.20*

Table B1. — Continued

C4 P=14.3				
JD	CCD	z	y	F555W
2449049.0327	1	426.18	135.88	24.41 ± 0.17
2449049.0938	1	426.16	135.89	24.58 ± 0.24
2449057.4598	1	427.30	134.79	24.10 ± 0.16
2449064.0828	1	430.00	136.98	24.57 ± 0.18
2449069.2661	1	426.43	136.85	24.53 ± 0.15
2449069.3293	1	426.44	136.86	24.12 ± 0.11
2449131.6589	2	411.80	134.92	24.28 ± 0.14
2449131.7228	2	411.62	134.95	24.13 ± 0.16
2449141.6263	2	411.79	135.07	24.30 ± 0.14
2449141.6936	2	411.89	135.00	24.34 ± 0.17
2449146.1096	2	411.67	134.81	24.25 ± 0.13
2449146.1769	2	411.63	134.81	24.01 ± 0.09
2449156.8860	2	411.68	135.28	23.85 ± 0.11
2449156.9499	2	411.62	135.26	23.99 ± 0.24
2449160.7658	2	411.89	135.07	24.17 ± 0.13
2449160.8304	2	411.86	135.03	24.04 ± 0.51
2449163.2450	2	411.85	135.29	24.41 ± 0.21
2449163.3054	2	411.93	135.23	24.24 ± 0.18
2449251.6130	3	406.20	112.74	24..53 ± 0.19
2449251.6748	3	406.24	112.77	24.88 ± 0.19
244929.5.2633	3	192.00	383.84	24.98 ± 0.39
2449295.3195	3	192.01	383.86	24.83 ± 0.27
2449307.7036	3	113.08	412.63	24.36 ± 0.18
2449307.7661	3	113.10	412.55	24.98 ± 0.32

C29 P=14.0				
JD	CCD	x	y	F555W
2449049.0327	4	61.29	181.50	24.79 ± 0.17
2449049.0938	4	61.27	181.47	25.05 ± 0.30
2449057.4598	4	62.47	182.61	26.00 ± 0.39
2449064.0828	4	60.46	185.37	25.28 ± 0.26
2449064.1136	4	60.44	185.63	25.97 ± 1.33
2449069.2661	4	60.51	181.78	25.92 ± 0.40
2449069.3293	4	60.45	181.78	25.39 ± 0.29
2449131.6589	1	73.76	182.60	24.82 ± 0.22
2449131.7228	1	73.67	182.42	24.60 ± 0.20
2449141.6936	1	73.98	182.73	25.31 ± 0.35
2449146.1096	1	73.73	182.41	24.40 ± 0.40
2449156.8860	1	73.73	182.52	25.42 ± 1.22
2449156.9499	1	73.72	182.45	24.91 ± 0.21
2449160.7658	1	73.84	182.72	25.27 ± 0.38
2449160.8304	1	73.83	182.71	25.09 ± 0.32
2449163.2450	1	73.81	182.72	25.51 ± 0.50
2449163.3054	1	73.85	182.82	25.52 ± 0.46
2449295.2633	3	134.80	102.18	25.97 ± 0.67
2449295.3195	3	134.83	102.23	25.42 ± 0.35
2449307.7036	3	115.05	125.13	25.85 ± 0.41
2449307.7661	3	115.07	125.03	25.40 ± 0.32
2449429.6016	4	123.86	206.02	24.89 ± 0.29

Table B1.— Continued

C18 P=13.0				
JD	CCD	x	y	F555W
2449049.0327	3	77.90	120.12	25.74 ± 0.49
2449049.0938	3	77.93	120.10	25.65 ± 0.41
2449057.4598	3	76.96	121.06	24.88 ± 0.31
2449064.0828	3	74.54	118.69	25.85 ± 0.44
2449069.2661	3	77.95	118.92	24.69 ± 0.19
2449069.3293	3	77.95	118.89	24.90 ± 0.18
2449131.6.589	4	69.72	141.68	25.87 ± 0.53
2449131.7228	4	69.91	141.60	25.33 ± 0.24
2449141.6263	4	69.75	141.88	25.92 ± 0.37
2449141.6936	4	69.65	141.95	25.76 ± 0.34
2449146.1096	4	69.82	141.63	24.98 ± 0.21
2449146.1769	4	69.83	141.62	24.99 ± 0.19
2449156.8860	4	69.84	141.68	25.79 ± 0.39
2449156.9499	4	69.89	141.67	25.35 ± 0.50
2449160.7658	4	69.75	141.81	25.23 ± 0.33
2449160.8304	4	69.74	141.77	25.22 ± 0.29
2449163.2450	4	69.79	141.79	25.61 ± 0.30
2449163.3054	4	69.67	141.83	25.15 ± 0.27
2449251.6130	1	98.50	138.39	24.71 ± 0.19
2449251.6748	1	98.45	138.36	24.99 ± 0.22
2449295.2633	2	131.45	47.34	25.52 ± 0.44
2449295.3195	2	131.4.5	47.31	2.5.77 ± 0.60

Table B2. F814W Photometry

C1 P=58.5

JD	CCD	x	y	F814W
2449161.1644	2	79.26	131.77	22.63 ± 0.13
2449404.6849	1	222.76	233.09	22.52 ± 0.05
2449429.5467	1	222.35	234.03	22.89 ± 0.08
2449429.5565	1	222.31	234.03	23.05 ± 0.19
2449434.5655	1	222.37	235.21	23.05 ± 0.10
2449446.4370	1	220.71	232.66	22.91 ± 0.09

C5 P=47.1

JD	CCD	X	u	F814W
2449161.1644	3	709.64	236.20	23.09 ± 0.09
2449161.2318	3	709.57	236.23	23.02 ± 0.08

C6 P=45.8

JD	CCD	Z	y	F814W
2449161.1644	3	177.36	274.66	22.87 ± 0.12
2449161.2318	3	177.37	274.60	22.72 ± 0.31
2449404.6849	2	201.79	255.52	22.37 ± 0.12
2449429..5467	2	201.97	256.02	22.77 ± 0.14
2449429.5565	2	201.94	256.25	23.38 ± 0.19
2449434.5655	2	202.47	256.04	22.62 ± 0.11
2449446.4370	2	201.39	256.85	22.30 ± 0.12

C7 P=43.0

JD	CCD	x	y	F814W
2449161.1644	3	326.96	672.45	22.88 ± 0.13
2449161.2318	3	326.95	672.39	22.90 ± 0.13
2449404.6849	2	376.01	653.64	23.08 ± 0.17
2449429.5467	2	376.20	654.15	22.62 ± 0.11
2449429.5565	2	376.18	654.42	23.06 ± 0.28
2449434.5655	2	376.70	654.20	22.61 ± 0.09
2449446.4370	2	375.68	654.89	22.91 ± 0.13

C19 P=43.0

JD	CCD	z	y	F814W
2449161.1644	1	519.51	780.12	22.4OAO.1O
2449161.2318	1	519.53	780.18	22.34 ± 0.08

C20 P=42.5

JD	CCD	X	y	F814W
2449161.1644	1	151.00	203.13	23.64 ± 0.23
2449161.2318	1	151.02	203.15	23.25 ± 1.80
2449404.6849	4	202.18	224.61	23.15 ± 0.19
2449429.5467	4	201.85	223.62	23.27 ± 0.11
2449429.5565	4	201.88	223.57	23.14 ± 0.18
2449434.5655	4	201.24	223.61	23.39 ± 0.11
2449446.4370	4	202.41	222.82	23.60 ± 0.15

Table B2. — Continued

C8 P=41.0

JD	CCD	X	y	F814W
2449161.1644	3	281.89	214.47	23.08 ± 0.14
2449161.2318	3	281.89	214.43	22.95 ± 0.28
2449404.6849	2	305.21	188.59	22.90 ± 0.11
2449429.5467	2	305.41	189.08	23.08 ± 0.09
2449429.5565	2	305.36	189.32	23.44 ± 0.23
2449434.5655	2	305.92	189.07	22.8140.09
2449446.4370	2	304.82	189.89	22.77 ± 0.12

C9 P=38.0

JD	CCD	X	y	F814W
2449161.1644	3	324.75	75.23	22.62 ± 0.12
2449161.2318	3	324.74	75.21	22.60 ± 0.48
2449404.6849	2	341.49	43.63	22.70 ± 0.10
2449429.5467	2	341.70	44.10	22.58 ± 0.19
2449429.5565	2	341.64	44.3.5	23.12 ± 0.42
2449434.5655	2	342.23	44.06	22.94 ± 0.11
2449446.4370	2	341.09	44.93	22.32 ± 0.09

C1O P=37.6

JD	CCD	X	y	F814W
2449161.1644	3	299.93	756.61	23.23 ± 0.16
2449161.2318	3	299.92	756.54	23.23 ± 0.14
2449404.6849	2	353.03	740.86	23.14 ± 0.15
2449429.5467	2	353.22	741.38	23.02 ± 0.09
2449429.5565	2	353.21	741.65	23.61 ± 0.22
2449434.5655	2	353.72	741.45	22.72 ± 0.11
2449446.4370	2	352.71	742.12	22.79 ± 0.42

C21 P=33.5

JD	CCD	X	u	F814W
2449161.1644	1	274.95	724.68	23.08 ± 0.14
2449161.2318	1	274.98	724.74	23.1OAO.12
2449404.6849	4	372.01	746.49	22.26 ± 0.16
2449429.5467	4	371.70	745.54	23.30 ± 0.08
2449429.5565	4	371.60	745.59	23.73 ± 0.28
2449434.5655	4	371.07	745.62	23.24 ± 0.11
2449446.4370	4	372.30	744.71	22.75 ± 0.12

C12 P=33.5

JD	CCD	X	y	F814W
2449161.1644	4	346.77	238.06	22.77 ± 0.16
2449161.2318	4	346.74	238.11	22.72 ± 0.11
2449404.6849	3	364.80	254.87	22.73 ± 0.19
2449429.5467	3	36.5.11	254.34	22.54 ± 0.18
2449429.5565	3	365.31	254.40	22.78 ± 0.30
2449434.5655	3	36.5.10	253.77	22.67 ± 0.21
2449446.4370	3	365.98	254.88	22.70 ± 0.19

C13 P=32.0

JD	CCD	X	u	F814W
2449161.1644	4	208.04	500.05	22.59 ± 0.09
2449161.2318	4	208.02	500.05	22.79 ± 0.14
2449404.6849	3	238.38	530.49	22.36 ± 0.13
2449429.5467	3	238.66	529.98	23.01 ± 0.13
2449429.5565	3	238.84	529.92	23.91 ± 0.48
2449434.5655	3	238.56	529.45	22.59 ± 0.13
2449446.4370	3	239.56	530.54	22.75 ± 0.09

Table B2. — Continued

C22 P=27.3				
JD	CCD	z	y	F814W
2449161.1644	1	302.61	466.70	23.17 ± 0.15
2449161.2318	1	302.62	466.74	23.19 ± 0.16
2449404.6849	4	378.68	480.73	23.34 ± 0.12
2449429.5467	4	378.35	479.76	23.36 ± 0.12
2449429.5565	4	378.33	479.76	23.82 ± 0.27
2449434.5655	4	377.75	479.79	23.45 ± 0.12
2449446.4370	4	378.93	478.93	23.13 ± 0.20

C23 P=25.6				
JD	CCD	X	u	F814W
2449161.1644	1	180.56	506.42	24.10 ± 0.25
2449161.2318	1	180.59	506.47	23.99 ± 0.21
2449404.6849	4	257.54	531.30	23.43%0.22
2449429.5467	4	257.22	530.33	23.57 ± 0.13
2449429.5565	4	257.17	530.33	23.69 ± 0.22
2449434.5655	4	256.60	530.37	23.79 ± 0.11
2449446.4370	4	257.81	529.51	23.73 ± 0.10

C14 P=25.0				
JD	CCD	x	y	F814W
2449161.1644	4	621.94	453.59	23.07 ± 0.22
2449161.2318	4	621.94	4.53.59	23.26 ± 0.18
2449404.6849	3	658.33	459.25	23.11 ± 0.17
2449429.5467	3	658.73	458.73	23.21 ± 0.18
2449429.5.565	3	658.83	458.85	23.9940.49
2449434.5655	3	658.77	458.25	23.51 ± 0.20
2449446.4370	3	659.56	459.27	23.87 ± 0.23

C11 P=23.7				
JD	CCD	z	y	F814W
2449161.1644	3	386.97	205.00	23.51 ± 0.19
2449161.2318	3	386.95	204.99	23.45 ± 0.37
2449404.6849	2	411.94	173.18	24.05 ± 0.18
2449429.5467	2	412.15	173.66	24.04 ± 0.14
2449434.5655	2	412.68	173.63	23.85 ± 0.09
2449446.4370	2	411.56	174.45	23.26 ± 0.10

C24 P=23.5				
JD	CCD	X	Y	F814W
2449161.1644	1	83.69	239.31	23.39 ± 0.16
2449161.2318	1	83.71	239.33	23.30 ± 0.16
2449404.6849	4	136.73	267.11	23.84 ± 0.26
2449429.5467	4	136.41	266.11	23.93 ± 0.20
2449429.5565	4	136.42	266.07	24.01 ± 0.34
2449434.5655	4	135.79	266.11	23.51 ± 0.20
2449446.4370	4	136.98	265.32	24.00 ± 0.24

C15 P=23.4				
JD	CCD	X	u	F814W
2449161.1644	4	309.39	221.28	23.38 ± 0.18
2449161.2318	4	309.36	221.33	23.71 ± 0.49
2449404.6849	3	325.72	240.07	22.59 ± 0.11
2449429.5467	3	326.01	239.54	22.77 ± 0.14
2449429.5565	3	326.23	239.60	23.11 ± 0.22
2449434.5655	3	325.99	238.96	22.84 ± 0.17
2449446.4370	3	326.89	240.09	23.51 ± 0.22

Table B2. — Continued

C16 P=22.8

JD	CCD	X	y	F814W
.2449161 .1644	4	712.91	664.97	23.68 ± 0.31
2449161.2318	4	712.92	664.93	23.56 ± 0.24

C25 P=19.4

JD	CCD	X	Y	F814W
2449161.1644	1	296.86	.514.60	23.40 ± 0.18
2449161.2318	1	296.88	514.64	22.78 ± 0.52
2449404.6849	4	376.82	530.04	23.12 ± 0.21
2449429.5467	4	376.50	529.07	23.36 ± 0.22
2449429.5565	4	376.46	529.08	24.23 ± 0.35
2449434.5655	4	375.89	529.11	23.50 ± 0.27
2449446.4370	4	377.08	528.24	23.27 ± 0.21

C 2 P=18.2

JD	CCD	X	Y	F814W
2449161.2318	2	191.36	332.06	23.29 ± 0.10
2449404.6849	1	499.18	661.79	23.85 ± 0.10
2449429.5467	1	498.80	662.71	23.8550.13
2449429.5565	1	498.73	662.81	23.88 ± 0.36
2449434..5655	1	498.81	663.94	23.70 ± 0.11
2449446.4370	1	497.20	661.32	23.98 ± 0.37

C26 P=17.7

JD	CCD	X	u	F814W
2449161.1644	1	38.32	297.40	23.95 ± 0.27
2449161.2318	1	38.35	297.43	23.64 ± 0.19
2449404.6849	4	95.38	330.04	23.78 ± 0.14
2449429.5467	4	95.06	329.05	24.36 ± 0.17
2449434..5655	4	94.43	329.06	24.41 ± 0.14
2449446.4370	4	9.5.64	328.26	24.11 ± 0.19

C27 P=17.2

JD	CCD	Z	y	F814W
2449161.1644	1	456,79	59.58	23.32*0.16
2449161.2318	1	456.77	59.56	23.25 ± 0.62
2449429.5467	4	502.16	51.32	23.28 ± 0.75
2449429.5565	4	502.26	51.25	24.09 ± 0.33
2449434.5655	4	501.62	51.30	24.07 ± 0.18
2449446.4370	4	.502.69	50.50	23.94 ± 0.18

C28 P=16.7

JD	CCD	Z	u	F814W
2449404.6849	4	613.34	599.58	24.04 ± 0.14
2449429.5467	4	613.00	598.62	23.95 ± 0.13
2449429.5.565	4	612.97	598.66	24.04 ± 0.32
2449434.5655	4	612.43	598.68	23.99 ± 0.11
2449446.4370	4	613.58	597.78	24.13 ± 0.14

Table B2. — Continued

C3 P=16.7				
JD	CCD	Z	Y	F814W
2449161.1644	2	324.70	455.19	23.58 ± 0.16

C17 P=16.5				
JD	CCD	X	Y	F814W
2449161.1644	4	374.40	304.77	24.14 ± 0.25
2449161.2318	4	374.38	304.81	23.76 ± 0.24
2449404.6849	3	396.84	321.42	23.45 ± 0.18
2449429.5467	3	397.16	320.89	24.11 ± 0.22
2449429.5565	3	397.34	320.95	24.39 ± 0.46
2449434.5655	3	397.14	320.34	23.60 ± 0.20
2449446.4370	3	398.03	321.43	24.05 ± 0.19

C4 P=14.3				
JD	CCD	Z	y	F814W
2449161.1644	2	408.77	132.88	23.40 ± 0.16
2449161.2318	2	408.80	132.86	23.85 ± 0.29

C29 P=14.0				
JD	CCD	X	v	F814W
2449161.1644	1	76.39	179.85	24.30 ± 0.39
2449161.2318	1	76.41	179.87	23.84 ± 0.24
2449404.6849	4	124.36	207.15	24.69 ± 0.33
2449429.5467	4	124.03	206.15	23.05 ± 0.39
2449434.56.55	4	123.41	206.14	24.98 ± 0.28
2449446.4370	4	124.59	205.36	25.07 ± 0.33

Table C1. Properties of Unclassified Variable Stars

CCD[1]	x^1	y^1	⟨F555W⟩	σ_{F555W}	⟨F814W⟩	σ_{F814W}	F439W	σ_{F439W}
1	366.4	521.7	23.67	0.07	21.12	0.12	25.76	0.62
1	81.1	98.4	24.73	0.06	23.67	0.06		
1	160.7	449,3	23.32[2]	0.07	20.99	0.06	25.04	0.24
1	430.6	790.5	24.68[3]	0.06	24,96	0.12	24.91	0.18
1	476,7	782.8	25.38[4]	0.10			26.04	0.37
2	54.8	267.1	23.54	0.03	22.03	0.06	26.58	0.71
2	252.7	300.0	23.30[5]	0.11	21,75	0.21		
2	385,0	330.6	24.52	0.05				
2	585.6	176.3	24.21[6]	0.04	23.86	0.14		
3	251.6	200.8	24.40	0.04	23.28	0.05	26.38	0.61
4	301.5	494.5	24.37	0.04	24.24	0.10		

Notes:
[1]Positions applicable for epochs shown in finder charts.
[2]Low-level variable with many discrepant points, P≈ 60 days
[3]P≈ 15.8 days, but extremely blue for Cepheid
[4]P≈ 15.4 days, also extremely blue for Cepheid
[5]Possible eclisping binary
[6]Too few observations to specify period, but definitely variable